Published in final edited form as:

Nanotechnol Rev. 2012 March ; 1(2): 111–146.

Can nanotechnology potentiate photodynamic therapy?

Ying-Ying Huang[1,2,3], **Sulbha K. Sharma**[1], **Tianhong Dai**[1,2], **Hoon Chung**[1,2], **Anastasia Yaroslavsky**[1,4], **Maria Garcia-Diaz**[1,5], **Julie Chang**[1,6], **Long Y. Chiang**[7], and **Michael R. Hamblin**[1,2,8]

Michael R. Hamblin: hamblin@helix.mgh.harvard.edu

[1]Wellman Center for Photomedicine, Massachusetts General Hospital, 40 Blossom St., Boston, MA 02114, USA

[2]Department of Dermatology, Harvard Medical School, Boston, MA, USA

[3]Aesthetic and Plastic Center, Guangxi Medical University, Nanning, China

[4]College of Engineering, Boston University, Boston, MA, USA

[5]Institut Químic de Sarrià, Universitat Ramon Llull, Barcelona 08017, Spain

[6]Department of Chemistry, Harvard University, Boston, MA, USA

[7]Department of Chemistry, University of Massachusetts, Lowell, MA, USA

[8]Harvard-MIT Division of Health Sciences and Technology, Cambridge, MA, USA

Abstract

Photodynamic therapy (PDT) uses the combination of non-toxic dyes and harmless visible light to produce reactive oxygen species that can kill cancer cells and infectious microorganisms. Due to the tendency of most photosensitizers (PS) to be poorly soluble and to form nonphotoactive aggregates, drug-delivery vehicles have become of high importance. The nanotechnology revolution has provided many examples of nanoscale drug-delivery platforms that have been applied to PDT. These include liposomes, lipoplexes, nanoemulsions, micelles, polymer nanoparticles (degradable and nondegradable), and silica nanoparticles. In some cases (fullerenes and quantum dots), the actual nanoparticle itself is the PS. Targeting ligands such as antibodies and peptides can be used to increase specificity. Gold and silver nanoparticles can provide plasmonic enhancement of PDT. Two-photon excitation or optical upconversion can be used instead of one-photon excitation to increase tissue penetration at longer wavelengths. Finally, after sections on *in vivo* studies and nanotoxicology, we attempt to answer the title question, “can nano-technology potentiate PDT?”

Keywords

dendrimer; fullerene; graphene; lipoplex; lipoprotein; liposome; magnetic nanoparticle; micelle; nanocell; nanoparticle; ORMOSIL; polymeric nanoparticle; porphysome; quantum dot; single-walled carbon nanotube; two-photon excitation; upconversion

Correspondence to: Michael R. Hamblin, hamblin@helix.mgh.harvard.edu.

1. Introduction

Photodynamic therapy (PDT) is an emerging modality for the treatment of a variety of diseases that require the killing of pathological cells (e.g., cancer cells, infectious microorganisms) or the removal of unwanted tissue (e.g., neovascularizton in the choroid, atherosclerotic plaques in the arteries). It is based on the excitation of nontoxic photosensitizers (PS) by harmless visible light leading to the production of highly toxic reactive oxygen species (ROS) that kill cells. Suitable PS have a high extinction coefficient in the far-red or near-infrared (NIR) spectral region and a high yield of the long-lived triplet electronic state (formed from the excited singlet state by intersystem crossing). The triplet PS is able to react with surrounding molecular oxygen by one of two distinct pathways. The type 1 pathway involves electron transfer to or from the triplet PS that can lead to a variety of oxygen free radicals such as superoxide, hydroxyl radicals, and hydroperoxides. The type 2 pathway relies on the fact that molecular oxygen is a triplet in its ground state and therefore has a spin-allowed interaction with PS triplet producing both species in the singlet state and singlet oxygen ($^1O_2$) is a potent oxidizing agent. Figure 1 shows a Jablonski diagram and the resulting type 1 and type 2 pathways.

For PDT to be both effective and safe, it is crucial that the PS should be delivered in therapeutic concentrations to the target cells (such as tumor cells) while simultaneously being absorbed in only small quantities by nontarget cells, thus minimizing undesirable side effects in healthy tissues. There are two main obstacles to achieving this aim: most PS have extended π-conjugation systems, making the molecules highly planar and, in addition, the molecules tend to be highly hydrophobic, and therefore, most PS form aggregates in an aqueous environment [1]. This aggregation lowers the efficiency of the PS, which must be in monomeric form to be photoactive [2]. Second, PS have generally not been found to bind or migrate preferentially to tumor cells, making it difficult to target only the diseased tissue when applying PDT [3]. Considerable efforts have therefore been directed at designing delivery systems that can incorporate PS in monomeric form without diminishing its activity and without causing any harmful effects *in vivo*.

Many of these delivery systems take the form of nanoparticles or other nanostructures. Indeed, lipid and detergent nanostructures (liposomes and micelles) were routinely used in PDT before nanotechnology became a separate and rapidly growing area of specialization. Several questions need to be answered in the design of nanoparticle delivery agents for PS. First, should the PS be noncovalently encapsulated in the nanoparticle or covalently attached to it? If the PS is only noncovalently associated, it is likely to be released more easily and therefore better taken up into cells. However, the PS may be prematurely released in the serum before the nanoparticles has had a chance to accumulate in the tumor as is hypothesized to occur *via* the enhanced permeability and retention (EPR) effect. Second, should the nanoparticles be biodegradable or not? If they are biodegradable, the material composition will be limited to lipids or certain polymers, whereas nonbiodegradable nanoparticles may remain in the body for long periods and this may lead to concerns of toxicity caused by the delivery vehicle and not the drug.

Although the majority of nanoparticles have been used as delivery vehicles for recognized PS such as tetrapyrroles, phenothiazinium dyes, or perylenequinones (see Figure 2 for representative chemical structures of PS covered in this review). However, there are some instances when the nanoparticles themselves act as the PS in the absence of preformed PS. For this to occur, the nanoparticles themselves have to be able to absorb light by virtue of possessing an extinction coefficient of appreciable size in an appropriate region of the electromagnetic spectrum and to then form an excited state that can lead to some photochemical generation of ROS. Examples of these classes of nanoparticle include fullerenes, zinc oxide (ZnO), titanium dioxide (TiO_2), and even quantum dots (QDs).

The aim of this review is therefore to give an overview of nanostructures that have been used in the PDT field and relevant examples of each class. The field has grown so rapidly in recent years that it is no longer possible to compile a comprehensive review, so we will concentrate on important and recent contributions. The readers will have to excuse the difficulties we have faced when classifying multifunctional nanoparticles. Many nanoparticles could have been covered in multiple sections (sometimes up to three or four different classifications) and there is no obvious rule for deciding between them. We will then try to critically answer our title question, “can nanotechnology potentiate PDT?”

2. Lipid-based nanoparticles

Lipids are amphiphilic molecules with both a hydrophobic and a hydrophilic part that spontaneously assemble into ordered structures in an aqueous environment, where the amphiphiles are arranged such that the hydrophobic parts cluster together and the hydrophilic parts face the water (usually on the outside). Many lipids will spontaneously form a membrane composed of a lipid bilayer, and this fact underlies one of the basic processes in the creation of life as we know it, the formation of cells. Lipid-based nanoparticles, such as liposomes, lipoplexes, and nanoemulsions have been used extensively in recent decades as drug carrier vehicles for hydrophobic PS.

2.1. Liposomes

Liposomes are nanosized artificially prepared vesicles of spherical shape made from natural phospholipids and cholesterol. Liposomes were discovered in 1961 by Alec D. Bangham who was studying phospholipids and blood clotting, and since then they have become very versatile tools in biology, biochemistry, and medicine [4]. Liposomes can be filled with drugs and used to deliver drugs for cancer and other diseases.

Liposomes have thus far been the most intensively studied carrier system for PS [5]. Their structure is composed of phospholipids with a hydrophilic head group and two hydrophobic chains, which enables them to contain both hydrophilic and hydrophobic drugs [6]. The liposome is made up of one or more concentric phospholipid bilayers, with an aqueous phase inside and between the bilayers [7]. The bilayers also often contain cholesterol, which is used to control membrane fluidity and increase stability, as well as for modulating membrane-protein interactions [3]. PS can be packaged into liposomes in two distinct manners depending on the lipophilicity and water solubility of the PS itself. First, water-soluble hydrophilic PS or even solid particles of PS are dissolved or suspended in the

aqueous interior of the liposomes (see Figure 3A). Second, hydrophobic non-water-soluble PS can be dissolved in the hydrophobic environment produced the fatty acid side-chains in the interior of the lipid bilayer (see Figure 3B). Once the PS has been packaged in the liposome, it can be delivered to cells in two main ways: the liposome can fuse with cell membranes and release its contents into the cytosol or it can be taken up by phagocytic cells and then disintegrate in the endosomes or lysosomes, again releasing the active drug into the cell [8].

Many experiments have demonstrated unequivocally that using liposomes to administer PS can substantially improve the efficacy and safety of PDT. For example, when rats whose brains were implanted with a human glioma were treated with PDT using the PS Photofrin and the uptake into the tumor tissue was significantly enhanced when the PS was delivered using liposomes [9]. Similar results have been observed with different tumor models and different PS [10]. This increased efficiency can be partly attributed to the role of liposomes in preventing aggregation of the PS. For example, when the hydrophobic PS, hypocrellin A (HA), was packaged in liposomes, it remained in monomeric form, unlike the aggregates formed when suspended in dimethyl sulfoxide-solubilized saline [11]. Liposomal HA also achieved a higher tumor-to-normal tissue ratio and higher maximal levels within the tumor cells compared with the saline suspension.

One of the most successful examples of the use of liposomal delivery vehicles has been that of Visudyne (see Figure 2A). Visudyne is a lipid-formulated composition of benzoporphyrin derivative mono acid ring A (BPD), or verteporfin, which is provided by (QLT Phototherapeutics, Vancouver, Canada); as a freeze-dried preparation composed of egg phosphatidyl glycerol and dimyristoyl phosphtidylcholine (BPD/EPG/DMPC; 1.05:3:5 w/w/w) [12]. Visudyne has been widely used in ophthalmology as a PS in combination with transpupillary red laser for destroying neovasculature in the eye secondary to disease such as wet age-related macular degeneration [13]. A second successful application of liposomes in PDT drug delivery was that of zinc(II) phthalocyanine (ZnPC; see Figure 2B). ZnPC is highly insoluble and was formulated by Ciba-Geigy Pharmaceuticals in liposomes composed of palmitoyl-oleoyl-phosphatidylcholine and di-oleoyl phosphatidylserine (ZnPC/OPOC/OOPS; 1:90:10 w/w/w) to form CGP55847 [14]. Although CGP55847 was tested in clinical trials of PDT for squamous cell carcinomas of the upper aerodigestive tract [15], it never received regulatory approval.

However, such “conventional” liposomes, with no additional features, have the drawback of a short plasma half-life, of the order of minutes [16]. This is first due to rapid lipid exchange between the liposomes and the lipoproteins, which leads to irreversible disintegration of the liposome. Second, conventional liposomes are easily opsonized by plasma proteins and are then quickly taken up by cells of the mononuclear phagocyte system, thus, they accumulate in mononuclear phagocytes in the liver, spleen, bone marrow, and blood circulation [3]. The resulting short circulation time of unmodified liposomes makes it difficult to achieve elevated tumor-to-normal tissue ratios of PS. Therefore, to make liposomes tumoritropic, they must be altered in some way. There are two main ways in which liposomes can be modified: passive and active targeting.

Passive targeting relies on the fact that if liposomes are allowed to circulate for a sufficiently long time, they will naturally preferentially accumulate in tumor tissue. This is due to the fast angiogenesis in malignant tissues, which results in enhanced vascular permeability and the lack of a functional lymphatic system in tumor tissue that impedes the return of extravasated macromolecules to the central circulation [17]. To achieve this effect, liposomes have been designed with longer circulation half-lives by making them “invisible” to lipoproteins and the mononuclear phagocyte system. Long-circulating liposomes can be created by using lipids with polyethylene glycol (PEG) headgroups; such liposomes are referred to as “sterically stabilized” or Stealth® liposomes [16, 18]. PEG is most commonly used as the polymeric steric stabilizer for liposomes, as it can be manufactured in large quantities with high purity, has low toxicity, and is nonimmunogenic and antigenic [6, 19]. One drawback of passive targeting is that Stealth® liposomes have been demonstrated to have decreased interaction with cells, suggesting that they may be less effective than conventional liposomes in transferring PS to tumor cells [3, 20]. Further studies are needed to see if this is indeed the case.

Liposomes have also been developed with a triggered release mechanism, so that the release of the PS can be tightly controlled. Various stimuli, such as heat, light, pH, and target binding have been used as the trigger [21]. Thermosensitive liposomes are constructed using temperature-sensitive lipids or coated with thermosensitive polymers that disintegrate when their temperature increases above 42°C [3, 22]. pH-sensitive liposomes are constructed by adding acid-sensitive molecules to the liposomal membrane and are designed to release their contents between pH 5 and 6.3 [23]. The basic principle underlying these mechanisms is the same: the liposomes are designed so that applying a “switch” will destabilize the phospholipid bilayer, thus increasing its permeability and releasing the PS contained within.

In active targeting, one or more molecules that have a high affinity for specific membrane markers on malignant cells are bound to the surface of the liposome, resulting in increased interaction of the liposomes with target cells [24]. The molecule can be covalently bound to the liposome, either by using a spacer molecule or by binding directly to a hydrophobic anchor in the phospholipid bilayer. In many cases, a spacer arm is used to enhance binding to the tumor cells by reducing interference from other surface molecules on the liposome that may have been added to increase the circulation half-life or to increase hydrophilicity [25]. A wide range of molecules has been used for active targeting, including glycoproteins, glycolipids, peptides, growth factors, and monoclonal antibodies (MoAbs) [3, 6, 26]. Although MoAbs are expensive, are time consuming to produce, and may result in undesirable immune reactions *in vivo*, they have the advantage of excellent specificity and significantly increase the ability of liposomes to deliver PS selectively to malignant cells [27]. Some studies have used antibody fragments (at the cost of potentially decreasing specificity) to minimize adverse immune reactions [28]. Other nonantibody ligands are often less expensive and carry a lower risk of inducing immune reactions: however, they do not have such high specificities for tumor cells, as many normal cells express the same receptors.

One application of liposomally encapsulated BPD was to destroy lymphatic vessels that might be responsible for allowing tumors to metastasize even after surgery [29]. Many

tumors produce vascular endothelial growth factor C (VEGF-C) or VEGF-D, factors that promote the formation of new lymphatic vessels (lymphangiogenesis). The newly formed lymphatic vessels enable tumor cells to travel from the primary tumor to the regional lymph nodes from whence they can spread throughout the body. Tammela et al. [29] first used the mouse ear containing tumors formed by mouse melanoma cells or human lung tumor cells after 2 weeks when the primary tumors had become established and lymphangiogenesis had been induced. Liposomal BPD accumulated specifically in the lymphatic vessels, and after illumination, they started to shrink and fragment and became leaky. When the experiment was repeated with tumors in the flanks of mice and PDT was followed by surgery, the mice had a much lower relapse rate than those that underwent surgery alone. Finally, they demonstrated PDT shutdown of lymphatic vessels in a large animal model (leg and hoof of a pig).

There have been several studies examining the use of liposomally encapsulated PS to mediate antimicrobial photodynamic inactivation (PDI) [30–33]. There is a well-known requirement for optimal antimicrobial PS to either possess one or more cationic charges on the PS itself or alternatively on the delivery vehicle in which the PS is contained [34]. Therefore, the liposomes for delivery of antimicrobial PDI are constructed to contain cationic lipids such as *N*-[1-(2,3-dioleoyloxy)propyl]-*N*,*N*,*N*-trimethylammonium chloride [33] or cationic detergents such as (1*S*,2*S*)-*N*-hexadecyl-*N*-methylprolinolinium bromide [32]. Longo et al. [35] used aluminum-chloride-phthalocyanine encapsulated in cationic liposomes to mediate PDI of oral bacteria and went on to test the antimicrobial PDT protocol in a clinical trial of 10 patients with carious lesions of the teeth.

2.2. Lipoplexes

Lipoplexes are complexes of cationic liposomes with other molecules (most commonly, negatively charged polynucleic acids), and have been most commonly used in gene therapy, for the delivery of nucleic acids such as DNAs and small interfering RNAs [36]. The cationic liposomes are created using positively charged cationic lipids (cytofectins). Recent studies have begun testing lipoplexes as a possible delivery system for negatively charged PS, and there is reason to believe that lipoplexes may improve the activity and specificity of the PS. For example, chlorin e6 (ce6) (Porphyrin Products, Inc., Logan, UT, USA) (see Figure 2C), a derivative of natural chlorophyll a, is a hydrophilic PS with seemingly limited potential, as it has low retention in tumor tissues and low potency [37]. However, when complexed with cationic liposomes, ce6 showed increased cellular uptake *in vitro* and selective targeting of tumor tissues *in vivo*, as well as increased retention within the tumor cells [38]. The use of cationic liposomes was crucial, as complexation efficiency of ce6 was higher than 90% with these liposomes, as compared with <12% for neutral and negatively charged liposomes. These findings suggest that lipoplexes would be a profitable area of research for PS delivery systems.

2.3. Nanoemulsions

Nanoemulsions are yet another proposed method for the efficient delivery of PS and are promising as a therapeutic option as they are easy to prepare and thermodynamically stable [39]. They consist of dispersions of oil and water that have dispersed phase droplets of size

20–200 nm and are often stabilized with a surfactant and co-surfactant [40]. Due to the nanosize range of the droplets, they are optically transparent and may be stored without the occurrence of sedimentation or droplet coalescence. Studies have demonstrated that nanoemulsions can enhance preferential delivery of PS to tumor sites and thus diminish the toxic side effects of PDT [41]. The application of nanoemulsions in PDT is likely to be in topical application of PS to the skin or to other mucosal surfaces. Primo et al. [42] formulated Foscan (*meta*-tetrahydroxyphenyl chlorin, *m*THPC) (Scotia Pharmaceuticals Ltd, Guilford, Surrey, UK) (see Figure 2D) in a nanoemulsion composed of soy-phosphatidylcholine Epikuron 170/Tween 80 and nonionic surfactants Poloxamer 188/ Span® 80. This formulation showed improved transdermal transport after 6 h. The same group [43] also investigated a magnetic nanoemulsion composed of biodegradable surfactants and biocompatible citrate-coated cobalt ferrite-based magnetic fluid to encapsulate ZnPC (Figure 2B) with the intention of combining PDT and magnetohyperthermia to produce synergistic cell killing.

5-Aminolevulinic acid (ALA) is not a PS itself but is a well-known precursor of the naturally formed PS, proto-porphyrin IX [PPIX; (Porphyrin Products, Inc., Logan, UT, USA) see Figure 2E] via enzymes of the heme biosynthetic cycle [44] (see Figure 4). When exogenous ALA is applied to tumors or other unwanted tissue, the feedback inhibition of the heme cycle is bypassed and excess PPIX is accumulated after a period of a few hours. As ALA is often topically applied, methods of increasing uptake and penetration through the skin have been intensively investigated [45]. For instance, Maisch et al. [46] used a nanoemulsion consisting of 30-nm particles of egg lecithin to increase ALA delivery through a full-thickness *ex vivo* skin model. Biofrontera has developed this BF-200 ALA nanoemulsion formulation in clinical trials of actinic keratoses [47].

2.4. Nanocells

Nanocells are a newly proposed technology that has been specifically designed to enhance drug delivery to solid tumors [48]. The traditional treatment method for tumors, which involves the simultaneous administration of chemotherapy and anti-angiogenesis agents, can actually inhibit the action of the chemotherapy agent. First, the action of the anti-angiogensis agent eventually decreases the blood supply to the tumor cells, making it more difficult for therapeutic concentrations of the chemotherapy drug to reach the tumor [49]. Second, the inhibited blood supply results in the accumulation of hypoxia-inducible factor 1α in the tumor, which leads to increased tumor invasiveness and resistance to chemotherapy [50]. The nanocell is designed to avoid this scenario by sophisticated packaging of the two drugs: it consists of a nuclear nanoparticle (containing the chemotherapy agent) within an extra pegylated lipid envelope (containing the anti-angiogenesis agent). When the nanocell is absorbed by the tumor, the outer envelope releases the anti-angiogenesis agent, thus shutting down the blood supply to the cancer cells. The inner nanoparticle then releases the chemotherapy agent, which can easily access the tumor cells, as the nanocell is already trapped inside the tumor. In addition to ensuring efficient delivery, this strategy results in decreased toxicity as the drugs are isolated from healthy cells. So far, this technique has only been demonstrated with chemotherapy agents, but it may be possible to design nano-cells that can carry photosynthesizers. Early studies have shown preferential uptake of nanocells

by tumors, which could be enhanced by active targeting in a similar manner to that of liposomes [40].

2.5. Porphysomes

Porphysomes are an interesting hybrid of a lipid nanoparticle and a potential PS developed by Gang Zheng's laboratory in Toronto [51, 52]. They consist of nanovesicles formed from self-assembled porphyrin bilayers that generate large, tunable extinction coefficients, structure-dependent fluorescence self-quenching and unique photothermal and photoacoustic properties. The basic building block is a conjugate between pyropheophorbide and a cationic phospholipid (Figure 5A) that spontaneously assembles into 100-nm particles composed of two high-density layers, ca. 5 nm thick in total and separated by a ~2-nm gap. Each layer is thought to correspond to a monolayer of porphyrin lipid (see Figure 5B). Because the porphyrins are packed in high density, they undergo self-quenching and at short time points can mediate photoacoustic and photothermal effects. However, at later time points, they dissociate *in vivo* and the released porphyrins can then mediate PDT.

3. Polymer-based nanoparticles

Polymeric nanoparticles have recently emerged as a new and promising tool for the delivery of drugs in PDT. Polymer-based PDT drugs offer several key advantages over molecular PDT drugs such as the ability to deliver a large amount of PS to the target area, flexibility toward surface modification for better efficiency, the ability to prevent degradation in the living biological environment, and the possibility of being loaded with multiple components such as targeting ligands and contrast agents. These advantages have a potential to improve several aspects of PDT such as tumor selectivity and hydrophobicity of the PS. The size of polymeric nanoparticles makes them an excellent tool for drug delivery. Tumor tissue has abnormally leaky blood vessels (with fenestrae up to 780 nm [53]) and nanoparticles preferentially escape from normal vasculature into the tumor, where they are subsequently retained due to poor lymphatic drainage. This effect is known as EPR [54]. A variety of polymer nanoparticles have been used to create PDT agents, and the structures are illustrated in Figure 6. These include synthetic polymers like polylactide-polyglycolide copolymers (PLGA), *N*-(2-hydroxypropyl)-methacrylamide (HPMA) copolymers, and polyacrylamide (PAA). Natural polymers composed of polysaccharides such as chitosan and alginate and proteins such as albumin and collagen have also been used. Following is a summary of recent polymeric nanoparticle applications in PDT.

3.1. Poly(D,L-lactide-co-glycolide)

PGLA (see Figure 6A) is a polymer made from a mixture of lactic acid and glycolic acid monomers that has been widely investigated for drug delivery due to its ease of formulation and biodegradability [61]. PS such porphyrins, chlorins, hypericin, and phthalocyanines (see Figure 2) have been loaded into PLGA nanoparticles and investigated for their potential in PDT. It has been reported that hypercin-loaded PLGA nanoparticles demonstrated a higher photoactivity than the free drug in NuTu-19 ovarian cancer cells [62]. The same effect was demonstrated in another study, where the efficacy of PDT with *meso*-tetra(4-hydroxyphenyl)porphyrin (*m*-THPP) (see Figure 2D with one extra double bond)-loaded

nanoparticles was compared with that seen with the free drug in EMT-6 mammary tumor cells [63]. Treatment with the 50:50 PLGA nanoparticles allowed for lower drug doses and shorter time intervals between drug administration and irradiation when compared with free *m*-THPP. ZnPc has also been loaded into PLGA nanoparticles and successfully used in PDT [55].

Several studies have been done to determine the dependence of PDT efficiency on properties of PLGA such as size and copolymer molar ratios. It has been reported in several studies that efficacy of PDT increases as the size of the nanoparticle decreases [64, 65]. When verteporfin was loaded into two PLGA nanoparticles, one 167 nm and the other 370 nm in diameter and tested on EMT-6 mammary tumor cells. It was found that the smaller nanoparticles exhibited a higher phototoxic effect than the larger ones or the free drug [64]. Another study examined three different PLGA nanoparticles with mean diameters of 117, 285, and 593 nm were loaded with *m*-THPP. The 117-nm particles demonstrated the fastest *m*-THPP release and highest rate of ROS production *in vitro* [65]. The improved performance of the smaller PLGA nanoparticles may be due to better intra-cellular uptake of the drug as well as a larger fraction of the particle that is exposed to its surroundings, which allows for a higher drug release rate [66]. It has also been found that the molar ratio of polylactide (PLA) to polyglycolide (PGA) affects the biodegradation rate [67] and the photo-toxicity of the loaded PS. When *m*-THPP was loaded into same size nanoparticles with three different molar ratios, its *in vitro* phototoxicity increased in the order of 50:50 PLGA>75:25PLGA>PLA [63]. PGA is more hydrophilic than PLA; thus, this demonstrates that the phototoxicity of the incorporated PS depends on the lipophilicity of the polymer nanoparticle [68].

3.2. Polyacrylamide

PAA (see Figure 6B) is a favorable substance for systemic administration because it is highly water-soluble, which prevents aggregation. It has been demonstrated to be nontoxic and biologically inert [69]. Another advantage of PAA nano-particles is that biodegradable cross-linkers can be introduced to make them slowly biodegradable, which improves their bioelimination *in vivo* [70]. PAA with nonbiodegradable cross-linkers has also been used successfully in PDT [71]. The polymer was shown to be an effective PDT agent when loaded with PS such as methylene blue (MB) [71, 72] and Photofrin [73]. In one study, 2- to 3-nm *meta*-tetra(hydroxyphenyl)-chlorin (*m*-THPC)-loaded PAA particles were prepared and successfully used in PDT to kill rat C6 glioma cells, proving to be as effective as the free drug [74]. The main advantage of these particles is their small size, which means $^1O_2$ should diffuse more rapidly out of them and they can be removed from the body by renal clearance. PAA-coated MB particles were also successfully used in PDT to eliminate bacterial infections [75]. The nanoparticles inhibited biofilm growth of both Gram-positive and Gram-negative strains, but killing efficiency was much higher for the Gram-positive bacteria.

3.3. *N*-(2-Hydroxypropyl)methacrylamide

HPMA (see Figure 6C) is a biocompatible copolymer that has been shown to passively accumulate in tumors and can be easily formulated to include targeting ligands [57]. HPMA

copolymer-bound drugs have been developed for the combination of PDT and chemotherapy [76]. It has been demonstrated using two different cancer models (Neuro 2A neuroblastoma [76] and human ovarian carcinoma [77]) that this novel approach is more effective than PDT or chemotherapy alone.

3.4. Dendrimers and hyperbranched polymers

Dendrimers are highly branched polymeric materials that have been used to deliver 5-ALA. ALA delivery is difficult due to its hydrophilic nature. Battah et al. [58] prepared an ALA-dendrimer, [1,3,5-Tris[*N*-(*N*-bis{*N*-[tris(5-aminolaevu-linyloxymethyl)methyl] propionamido}propionamido)car-bamido]benzene 18 trifluoroacetic acid salt (18m-ALA; see Figure 6D). An *in vitro* study demonstrated that dendrimers such as 18m-ALA could be used to carry ALA into PAM 212 murine keratinocyte and A431 human epidermoid carcinoma cell lines. It also showed that the dendrimer ALA nanoparticles are more efficient at porphyrin production than free ALA.

Li and Aida [78] have reviewed the field of dendrimeric porphyrins, phthalocyanines, and other tetrapyrroles. Kataoka's laboratory has prepared dendrimer PS based on both a Zn-porphyrin and on a Zn-phthalocyanine [79]. The porphyrin dendrimers were complexed with poly-L-lysine-PEG (PEG-PLL; see Figure 6E) block copolymers to form nanocarriers [80]. Interestingly, the larger the dendrimer (i.e., the higher the generation number), the smaller was the overall size of the nanocarrier. Dendrimeric phthalocyanines (DPc) with carboxyl groups at the periphery were complexed with PEG-PLL in a similar manner to form nanocarriers (DPc/m) with 50 nm diameter [81]. The nanoparticles were taken up into A549 human lung cancer cells, accumulated in lysosomes, and were released upon illumination. Nude mice with A549 tumors received DPc or DPc/m intravenously at a dose of 1.85 mg/kg, and after 24 h, tumor sites were irradiated with a 670-nm diode laser with a light dose of 100 J/cm^2. Mice treated with DPc/m-PDT showed a much better tumor response than those with DPc-PDT.

Li et al. [82] prepared conjugates between the PS ce6 and hyperbranched poly(ether-ester), HPEE. HPEE-ce6 nanoparticles were synthesized by carbodiimide-mediated reaction between HPEE and ce6 and characterized by ultraviolet-visible absorption spectroscopy (UV-Vis) and transmission electron microscopy. The uptake and phototoxicity of HPEE-ce6 nanoparticles toward human oral tongue cancer CAL-27 cells was detected by confocal laser scanning and MTT assay. The HPEE-ce6 nanoparticles showed significantly greater PDT effect than free ce6.

3.5. Natural polymers

Natural polymers such as proteins and polysaccharides have also been studied for potential use in PDT. Human serum albumin has been loaded with the PS pheophorbide. The nanoparticles were incubated with Jurkat cells for 24 h, and the treatment resulted in higher phototoxicity and lower dark toxicity than free pheophorbide [83]. In a study with polysaccharide nanoparticles, 5,10,15-triphenyl-20-(3-*N*-methylpyridinium-yl)porphyrin was encapsulated in marine atelocollagen/xanthan gum [84]. The incorporated PS displayed

almost four times greater phototoxicity toward HeLa cells when prepared with the nanoparticles than with phosphatidylcholinelipidic emulsion.

3.6. Chitosan

Chitosan is a β-1,4-linked polymer of glucosamine (2-amino-2-deoxy-β-D-glucose) and lesser amounts of *N*-acetylglucosamine. It is a derivative of chitin (poly-*N*-acetylglucosamine) (Figure 6F) and is the second most abundant biopolymer after cellulose. Chitosan was first discovered in 1811 by Henri Braconnot [85], a French chemist and pharmacist. Bracannot observed that a certain substance (chitin) found in mushrooms did not dissolve in sulfuric acid. Later in the century, chitin was found in crustaceans (such as crabs, lobsters, shellfish, and shrimp), the indigestible outer skeleton of insects, and the material from which the cell walls of the mycelial fungi are made. Over the last 200 years, the study and application of chitosan has taken on many different forms, but in recent years, it has been used to manufacture nanoparticles that have been investigated for improved drug delivery [86].

Reza-Saboktakin et al. [87] prepared biodegradable poly-meric nanoparticles loaded with PS *m*-THPP. *N*-Sulfonato-*N*,*O*-carboxymethylchitosan was grafted with polymethacrylic acid. The nanoparticles were loaded with *m*-THPP (10%–30% loading) and tested for PDT killing of 14C carcinoma cells. After 6 h of incubation, the phototoxicity of the nanoparticles was comparable with that of free *m*-THPP.

Lee et al. [88] prepared hydrophobically modified glycol chitosan (HGC) nanoparticles by self-assembling amphiphilic glycol chitosan-5β-cholanic acid conjugates. Ce6 was chemically conjugated to the glycol chitosan polymers, resulting in amphiphilic glycol chitosan-ce6 conjugates that formed self-assembled nanoparticles in aqueous condition. Both ce6-loaded glycol chitosan nanoparticles (HGC-ce6) and ce6-conjugated chitosan nanoparticles (GC-ce6) had similar average diameters of 300–350 nm, a similar *in vitro* $^1O_2$ generation efficacy under buffer conditions, and a rapid cellular uptake profile in the cell culture system. However, compared with GC-ce6, HGC-ce6 showed a burst of drug release *in vitro* (65% released from the particles within 6.5 h). When injected through the tail vein into nude mice bearing HT29 human colon carcinoma tumors, HGC-ce6 did not accumulate efficiently in tumor tissue, reflecting the burst in the release of the physically loaded drug, whereas GC-ce6 showed a prolonged circulation profile and a more efficient tumor accumulation. PDT (2.5 mg/kg) ce6 followed by two separate illuminations at 4 and 12 h postinjection with a red laser (671 nm, 220 mW/cm^2) for 30 min gave best tumor growth delay with GC-ce6, whereas HGC-ce6 was less effective, and free ce6 gave hardly any response.

The same group [89] prepared similar nanoparticles from glycol-chitosan with PPIX conjugated and found these amphiphilic PPIX-eGC conjugates formed a stable nano-particle structure in aqueous condition, wherein conjugated PPIX molecules formed hydrophobic inner cores and they were covered by the hydrophilic GC polymer shell. PPIX-eGCeNP showed a self-quenching effect, but after cellular uptake, the compact structure gradually decreased to generate a strong fluorescence signal and $^1O_2$ generation when irradiated. Nude mice with SCCVII squamous cell carcinomas were intravenously injected *via* a tail vein

with free PPIX or PPIX-GC-NP (20 mg/kg of PPIX). After 1 day postinjection, tumors were irradiated with a 633-nm HeNe laser, 3 mW/cm^2 for 30 min. PPIX-GC-NP gave a pronounced tumor destruction and growth delay not seen with free PPIX.

3.7. Pegylated polymers

One problem with using polymer nanoparticles for drug delivery is that they tend to be taken up by macrophages after intravenous administration [90]. To reduce this uptake, the nanoparticle can be coated with PEG, which allows for longer plasma circulation and better accumulation in tumors. In one study, it was reported that pegylation (the attachment of PEG) of PLL and ce6 conjugates increased the selectivity and improved the phototoxicity of PDT in OVCAR-5 ovarian cancer cell lines [59]. In an *in vivo* study, hexadecafluoro ZnPc was loaded into PEG coated PLA nanoparticles and tested for photodynamic activity and tumor response in EMT-6 tumor-bearing mice [91]. The results showed an improved response and longer tumor sensitivity to PDT compared with treatment with the same PS prepared in Cremophor El (CRM) emulsions. Another way to improve tumor selectivity of the polymer nanoparticle is by conjugating its surface with tumor-specific ligands for active targeting. As an example, in an *in vitro* study done with MDA-MB-435 human breast carcinoma F3-targeted PAA nanoparticles were loaded with Photofrin and iron oxide and were successfully concentrated within the nuclei of the cells [73]. Subsequent administration of light caused cell death. Active targeting is a major advantage of polymeric nanoparticles because they can be packed with multiple targeting ligands and they frequently exhibit better selectivity than targeted molecular drugs [92].

4. Micelles

Micelles are so-called colloidal dispersions (with particle size normally within the 5- to 100-nm range) of aggregates of surfactant molecules dispersed in a liquid colloid. Such colloids are spontaneously formed under certain concentration and temperature by amphiphilic or surface-active agents. These surfactant molecules consist of two clearly distinct regions with opposite affinities toward a given solvent (see Figure 7). Micelles have been widely used to carry hydrophobic drugs, which are physically entrapped in and/or covalently bound to the hydrophobic core. Micellar nanocarriers demonstrate a series of attractive properties as drug-delivery systems, such as improved bioavailability, enhanced permeability across the physiological barriers (EPR effect), and substantial beneficial changes in drug biodistribution [93, 94]. Micelles can be classified in two general groups based on the nature of the amphiphilic core: polymeric micelles, which are formed by block copolymers consisting of hydrophilic and hydrophobic monomer units, and micelles prepared from water-soluble polymers conjugated with lipids.

4.1. Polymeric micelles

Polymeric micelles represent widely used nanocarriers, comprising several possible classifications and types of polymers and copolymers. Among others, PEG-b-poly(caprolactone) (PEG-PCL) diblock copolymers seem to be successful with the delivery of photosensitizing agents. Li et al. [95] studied the formulation of hydrophobic PPIX PEG-PCL micelles and compared their PDT response with that of free PPIX. PEG-PCL micelles

have also been used for the encapsulation of phthalocyanines [96], chlorins [97, 98], and pheophorbides [99] with successful results. These findings suggest that PEG-PCL micelles have great potential as a drug-delivery system for hydrophobic photodynamic sensitizers.

The encapsulation of dendrimer PS can be also improved by means of PEG-PLL micelles [81, 100, 101].

Using another biocompatible and biodegradable block copolymer, PEG-b-poly(D,L-lactide) (PEG-PLA), Gao et al. [102] recently published the nanoscopic structure-property relationships of micelle-delivered PPIX and established a viable formulation for *in vivo* evaluation of antitumor efficacy. This group also explored the advantages of using PEG-PLA micelles for the encapsulation of mTHPC in head and neck cancer treatment [103, 104].

Pluronics (poloxamers) are commercially available water-soluble triblock copolymers of poly(ethylene oxide) and poly(propylene oxide) (PEO-PPO-PEO) and have been frequently used as a solubilization agent in drug formulations. Gallavardin et al. [105] used the pluronic nanoparticles for encapsulating two-photon chromophores. Chowdhary et al. [106] compared the pluronic P123 formulation with a lipid-based system to improve the verteporfin delivery to lipoproteins in tumor and arthritis mouse models.

Some authors reported the use of pH sensitivity of the micelle to release the PS selectively at the target site. It is known that tumors and inflamed tissues exhibit a decreased extracellular pH as well as some intracellular compartments such as lysosomes or endosomes. Low pH may change the polymer polarity and structure causing the PS deliver [107]. Following this strategy, Le Garrec et al. [108] synthesized different *N*-isopropylacrylamide (NIPAM) copolymers to prepare pH-responsive micelles encapsulating AlPc. NIPAM copolymers exhibit substantially lower cell cytotoxicity and greater activity *in vivo* than that seen with Cremophor micelle formulation. Koo et al. [109] also demonstrated an enhanced therapeutic response of PPIX-encapsulated pH-responsive micelles for cancer treatment.

4.2. PEG-lipid micelles

The structure of PEG-lipid micelles correspond to that of amphiphilic copolymers. However, the hydrophobic part is represented by a lipid instead of hydrophobic polymer block. There are several water-soluble polymers-lipid conjugates commercially available or they can be easily synthesized; however, phosphatidyl ethanolamine (PE) constituted the most used diacyl phospholipid chain. The lipid part receives the hydrophobic PS, while PEG prevents rapid uptake of the particles by RES [110]. Torchilin et al. [111–113] has extensively studied PEG-PE micelles as PS delivery systems. The use of PEG-PE micelles allowed for a 150-fold increase in the solubilization of tetraphenylporphyrin (TPP), compared with the nonformulated drug. TPP-loaded PEG-PE micelles were additionally modified with tumor-specific monoclonal 2C5 antibody (mAb 2C5), which resulted in significantly improved anticancer effect of the drug under the PDT conditions against murine Lewis lung carcinoma *in vivo* in female C57BL/6 mice. Zhang et al. [114] developed micellar PEG-DSPE formulations for increasing the solubility of lipophilic benzoporphyrins.

Cremophor EL is another easily commercially available micelle constituent. It is polyethoxylated castor oil and has been widely used for the formulation of a variety of hydrophobic drugs, also in PDT, as a simple and biocompatible solubilization system [115–119].

5. Silica-based nanoparticles

Silica is a major component of sand and glass, and it has been used in the synthesis of nanoparticles. Functional groups can also be added to the surface of silica nanoparticles (SiNPs), making them appealing for designs for different applications. Very recently, SiNPs have emerged as promising vectors for PDT applications [120]. Among the variety of nanoparticles, SiNPs have several advantages: their particle size, shape, porosity, and monodispersibility can be easily controlled during their preparation; furthermore, a variety of precursors and methods are available for their syntheses, allowing flexibility and thus numerous PDT drugs to be encapsulated. SiNPs also have advantages as drug vectors. There is no swelling or porosity change occurring with change of pH. Moreover, SiNPs are known for their compatibility in biological systems and are not subject to microbial attack. Although these SiNPs do not release the entrapped PS, their porous matrix is permeable to molecular as well as $^1O_2$. Therefore, the desired photodestructive effect of the drug will be maintained even in the encapsulated form.

There are many methods to make SiNPs, such as organically modified silicates (ORMOSIL), hollow silica, mesoporous SiNPs (MSN), and sol-gel method. The Stöber procedure, which is known to generate amorphous SiNPs of a controlled size [121], the reverse microemulsion (water-in-oil) method, and recently direct microemulsion (oil-in-water) procedure [122, 123], and the sol-gel method have all been applied to design nanoparticles for PDT applications. Both noncovalent encapsulation and covalent conjugation have been used as methods for the immobilization of the PS inside or on the surface of the SiNPs [122]. Noncovalent encapsulation is the most frequently described method, whereas covalent linkage of the PS appears to be more efficient, as no release of the PS from the nanoparticles occurs.

MB (see Figure 2I) is a heterocyclic aromatic chemical compound with photodynamic toxicity. Intravenous administration of MB is Food and Drug Administration approved for methemoglobinemia. However, clinical use of MB is limited because of the poor penetration of this drug in the cellular compartment of the tumor. Encapsulation of MB inside SiNPs is a way to vectorize it and protect it from degradation. Tang et al. [72] was the first to encapsulate MB in ORMOSIL. They compared three types sub-200-nm nanoparticles composed of PAA, sol-gel silica, and ORMOSIL, respectively. As a result, they showed that although PAA nanoparticles exhibited the most efficient delivery of $^1O_2$ and positive photodynamic effect on rat C6 glioma tumor cells, the sol-gel SiNPs had the best MB loading but the least efficient $^1O_2$ delivery.

In 2005, Roy et al. [124] established the feasibility of using ORMOSIL nanoparticles as a carrier for PS. This formulation of nanoparticles overcomes many of the limitations of “unmodified” SiNPs. The presence of both hydrophobic and hydrophilic groups on the

precursor alkoxy organosilane helps them to self-assemble as both normal micelles and reverse micelles under appropriate conditions. ORMOSIL nanoparticles are prepared from oil-in-water microemulsions, avoiding corrosive solvents such as cyclohexane and through a complex purification process. Their organic groups can be further modified for the attachment of targeting molecules and can be possibly biodegraded through the biochemical decomposition of the silicon-carbon bond. 2-Devinyl-2-(1-hexyloxyethyl) pyropheophorbide (HPPH) (see Figure 2H), an effective PS that is in phase I/II clinical trials, was encapsulated into ORMOSIL with diameter of 30 nm [125] by copolymerization mediated by controlled hydrolysis of triethoxyvinylsilane and the triethoxysilane-derivatized HPPH in micellar media (see Figure 8). *In vitro* studies demonstrated the active uptake of drug-doped nanoparticles into the cytosol of tumor cells. Significant damage to such photosensitized tumor cells was observed upon irradiation with light of wavelength 650 nm.

Following the pioneering work of Roy et al. [124] and Yan et al. [127], many other researchers encapsulated PS inside SiNPs by noncovalent methods. Different PS, such as MB [72] and PPIX [128] have been encapsulated or covalently linked to ORMOSIL particles. Higher $^1O_2$-generation quantum yield was found for the encapsulated PS than for free PS with *m*-THPC [127], HPPH [124], or HA [129].

There is a strong relationship between the sites of subcellular localization of the PS and photodamage to nearby organelles involved in cell death. Zhou et al. [129] constructed porous hollow silica nanospheres and embedded HA. Compared with free HA, the silica embedded HA showed superior light stability, higher $^1O_2$ generation, and *in vitro* experiments showed the mitochondrial membrane potential was destroyed as evidenced by rhodamine-123 staining [129].

The silicon phthalocyanine, Pc4 was encapsulated in ORMOSIL (Pc4SNP) with a size ranging from 25 to 30 nm based on hydrophobic silicon by the method modified from Roy et al. [124]. Pc4SNP not only improved the aqueous solubility, stability, and delivery of the photodynamic drug but also increased its photodynamic efficacy compared with free Pc4 molecules. Pc4SNP generated photoinduced $^1O_2$ more efficiently. They found Pc4SNP was more phototoxic to A375 or B16-F10 melanoma cells than free Pc4. The mechanism studies of Pc4SNP photodamaged melanoma cells showed an increase of intracellular protein-derived peroxides, suggesting a type 2 ($^1O_2$) mechanism for phototoxicity. More Pc4SNP than free Pc4 were localized in the mitochondria and lysosomes and cause cell death primarily by apoptosis.

Covalent coupling of the PS inside the nanoparticles offered an advantage in that this covalently linked nanofabrication meant that the PS is not released during systemic circulation. Prasad and collaborators first reported the covalent incorporation of PS molecules into ORMOSIL nanoparticles by synthesizing iodobenzyl-pyro-silane (IPS) with vinyltriethoxysilane in the nonpolar core of Tween-80/water microsmulsion. IPS is a precursor for ORMOSIL with the linked PS iodobenzylpyropheophorbide [125]. The covalently incorporated PS molecules are of an ultralow size (approx. 20 nm), which retained their spectroscopic and functional properties and could robustly generate cytotoxic $^1O_2$ molecules upon photoirradiation. The synthesized nanoparticles are highly

monodispersed and stable in aqueous suspension. Moreover, these nanoparticles are also avidly taken up by tumor cells *in vitro* and exhibit a phototoxic effect on the cultured cells proportional to the cellular uptake, thereby highlighting their potential in diagnosis and PDT of cancer.

PPIX can be considered as a natural PS because ALA is a metabolic precursor in the biosynthesis of heme, and PPIX is the immediate precursor to heme (see Figure 4). Qian et al. [130] encapsulated PPIX in ormosil nanoparticles (25 nm diameter) following Prasad's method. They showed PDT effect performed on HeLa cells, and the cell structures were destroyed by a 532-nm light source at low dose (2 mW/cm^2, 2 min). Simon et al. [131] recently published the synthesis and properties of PPIX in ORMOSIL nanoparticles prepared by Prasad's method. There is a strong relationship between the sites of subcellular localization of the PPIX and photodamage to nearby organelles involved in cell death. The intracellular accumulation of PPIX SiNPs takes place in the cytoplasm of cells. Higher ROS generation, which leads to cell destruction, was found correlated to the presence of PPIX SiNPs in both HCT 116 and HT-29 colon cancer cells [131].

MSN have been also used for various biomedical applications such as cell markers or drug and gene delivery platform. MSN are a suitable carrier for hydrophobic PS and protect the PS from degradation due to their large surface area and pore volume, as well as uniform pore size. Tu et al. [132] conjugated PPIX with MSN through covalent bonding to yield PPIX modified MSN for PDT. In *in vitro* experiments, they found that the uptake of the PPIX-modified particles by HeLa cells was quite efficient. An almost linear relationship between cellular uptake and dosage was observed. Both necrosis and apoptosis could be observed depending on the concentration and dosage- and irradiation time-dependent loss of cell viability was observed. The same group grafted a phosphorescent Pd-*meso*-tetra(4-carboxyphenyl)porphyrin (PdTPP) as the PS in prepared MSN [133].

A marked advantage of using nanoparticles is that they can be used as multifunctional platforms. A single particle platform that combines two functions has been described by Rossi and collaborators in 2007 [134]. MB as a PS was added to the silica precursor tetraorthosilicate during the growth of the silica layer and was therefore entrapped in the silica matrix. Then the magnetic cores were prepared by coprecipitation of Fe^{2+}/Fe^{3+} ions under alkaline conditions followed by stabilization with tetraethylammonium oxide. Liu et al. reported another magnetic nanocarrier using purpurin-18 as a PS for PDT [135]. They continued prepared 2,7,12,18-tetramethyl-3,8-di(1-propoxyethyl)-13,17-bis-(3-hydroxypropyl)porphyrin (PHPP) as a PS encapsulated into silica covered Fe_3O_4 magnetic nanoparticles (MNPs) [136].

6. Gold nanoparticles

Gold nanoparticles (AuNPs) have been used in two ways in PDT: first, as drug-delivery platforms in a similar manner to other inorganic nanoparticles (see Figure 9A); second, as surface plasmon-enhanced agents taking account of the nonlinear optical fields associated with very close distances to metal nanoparticles (see Figure 9B).

6.1. Standard AuNPs

The conjugation of PS molecules to AuNPs [123] and other inorganic nanoparticles [124, 137–139] represents an effective way to improve the targeting effect and efficacy for cancer treatments [66, 123, 140–145].

It is possible to modify the AuNPs either covalently or non-covalently with PS [146]. Moreover, the small size of AuNPs can be presented as a benefit, allowing them to permeate tissue and the leaky vasculature of tumors [147]. In that way, tunable AuNPs can serve as both diagnostic and therapeutic tools for cancer [148] once they are recognized for their chemical inertness and have minimum toxicity as well [149].

The AuNPs have good biocompatibility, versatile surfaces, tunable sizes, and unique optical properties [150]. When coated with PEG, which has been approved for human intravenous application, they can result in promising drug-delivery systems for cancer PDT [123] due to the stabilization by steric repulsion and inhibition of colloid aggregation in physiological conditions [151, 152].

Although PEG provides solubility in water and minimizes any protein adsorption [144], the AuNP surface provides an amphiphilic environment for lipophilic PDT drugs [123]. The PEG-AuNP drug-delivery systems for PDT in HeLa cells were previously evaluated and showed efficient drug release by membrane-mediated diffusion when the noncovalent adsorption of the PS to AuNPs was used [153].

Using the noncovalent delivery of Pc4 with PEG-gold NPs, Cheng et al. [123] observed surprisingly efficient release and penetration of the drug into the tumor *in vivo*. In addition, both the drug and the AuNPs were excreted by renal clearance and the hepatobiliary system. Another study also revealed that pegylated AuNP-Pc4 conjugates dramatically improved the delivery of the drug. In addition, the Pc4 could be well dispersed in aqueous solutions once it was formulated as an AuNP conjugate [123].

AuNP-modified porphyrin-brucine conjugates have been claimed to represent a significant improvement in PDT compared with free PS [146]. Both *para* and *meta* substitution patterns, when bound to modified AuNPs, were able to effectively reduce tumor size *in vivo*, with complete tumor regression. *In vitro*, PDT of synthesized hematoporphyrin-nanogold composites was much enhanced if compared with that of the original PS alone [145]. It was also concluded that nanocomposites with gold particles of 45 nm presented better results than the ones with 15-nm particles, which could be connected to the fact that bigger particles can transport more porphyrin molecules into malignant cells.

6.2. Plasmon-enhanced AuNPs

The phenomenon of localized surface plasmon resonance is based on the interaction of the conduction electrons of metal nanostructures with incoming light [154]. The electromagnetic waves induce an oscillation of these electrons and resonances can be observed. These resonances depend on parameters such as the kind of metal and its composition (in the case of a mixture), geometry (size, shape), and immediate environment. The last is the basis for its potential use as a sensor: for example, using an affinity layer, certain molecules bind to

the surface of such a structure, influencing, and shifting the resonance, which can be observed and used as the sensed signal for readout. Molecular plasmonics represent the field that deals with localized surface (also called particle) plasmon resonance effects in interactions with molecular components (usually bound to the surface of metal nanostructures). The observed effects can be used for novel conjugates for nano-optics (here the molecules act as a tool) as well as for biomolecular analytics aimed at molecular analytes.

A report from Fales et al. [155] in Vo-Dinh's laboratory showed that gold nanostars could be tuned for maximal absorption in the NIR spectral region and tagged with an NIR dye for surface-enhanced resonance Raman scattering. Silica coating was used to encapsulate the PS MB in a shell around the nanoparticles. Upon 785-nm excitation, surface-enhanced Raman spectroscopy (SERS) from the Raman dye was observed, whereas excitation at 633 nm showed fluorescence from MB. MB-encapsulated nanoparticles showed a significant increase in singlet-oxygen generation as compared with nanoparticles synthesized without MB. This increased singlet-oxygen generation showed a cytotoxic effect on BT549 breast cancer cells upon laser irradiation.

Khlebtsov et al. [156] prepared novel composite nanoparticles consisting of a gold-silver nanocage core and a mesoporous silica shell functionalized with the photodynamic sensitizer Yb-2,4-dimethoxyhematoporphyrin (Yb-HP). In addition to the long-wavelength plasmon resonance near 750–800 nm, the composite particles exhibited a 400-nm absorbance peak and two fluorescence peaks, near 580 and 630 nm, corresponding to bound Yb-HP. The fabricated nanocomposites generated $^1O_2$ under 630-nm excitation and produced heat under laser irradiation at the plasmon resonance wavelength (750–800 nm). In particular, they observed enhanced killing of HeLa cells incubated with nanocomposites and irradiated by 630-nm light. Furthermore, an additional advantage of fabricated conjugates was an IR-luminescence band (900–1060 nm), originating from Yb(3+) ions of bound Yb-HP and located in the long-wavelength part of the tissue transparency window. This modality was used to control the accumulation and biodistribution of composite particles in mice bearing Ehrlich carcinoma tumors in a comparative study with intravenously injected free Yb-HP molecules.

7. Semiconductor and quantum dot nanoparticles

Semiconductors are materials with conduction properties intermediate between metals and insulators. The typical structure is a crystalline lattice where the electron conduction band is <4 eV above the valence band. Electrons excited to the conduction band (either by an applied voltage or by absorption of light) leave behind electron holes, i.e., unoccupied states in the valence band. Both the conduction band electrons and the valence band holes contribute to electrical conductivity. Although hsemiconductors used in electronics are usually made from silicon doped with small amounts of other elements, other semiconductors will absorb or emit light and are composed of alloys of pairs of elements in the II–VI periodic groups (e.g., ZnO, ZnS, CdSe) or the III–V groups (GaAs, InN, InP, AlAs). These substances produce excitons on photon absorption (a bound state of an electron and hole that are attracted to each other by electrostatic force) (see Figure 10A).

7.1. Zinc oxide and titanium dioxide

Both ZnO and TiO_2 can produce ROS upon light absorption by electron transfer reactions involving oxygen and water. The active species is thought to be mainly hydroxyl radical (HO·) [157], but superoxide anion and $^1O_2$ are also produced [158, 159]. Most studies have examined excitation of these materials with UV light, but recently, attempts have been made to use visible light (often blue light) as well [160].

Zhang et al. [161] used ZnO nanorods loaded with the cytotoxic drug daunorubicin to mediate synergistic killing of human hepatocarcinoma cells. UV illumination significantly improved cytotoxicity over that seen with daunorubicin alone.

TiO_2 has been more widely studied as a PS than ZnO in a process termed “photocatalysis,” which has been proposed as an antimicrobial strategy for disinfecting wastewater [162]. However, there have also been reports of the use of photoactivated TiO_2 as an anticancer treatment. Yamaguchi et al. [163] constructed TiO_2 nanoparticles by the adsorption of chemical modified PEG on the TiO_2 surface. When C6 rat glioma cells (both as monolayers and as multicellular spheroids) were incubated with TiO_2-PEG nanoparticles followed by UV illumination, 90% of the cells were killed. Zhang and Sun [164] reported similar results by inactivating Ls-174-t human colon carcinoma cells using incubation with TiO_2 nanoparticles and ultraviolet A irradiation (UVA, 320–400 nm) but had to use much higher concentrations (200–1000 μg/ml) possibly because they did not use PEG solubilization. Wang et al. [165] showed that TiO_2-PDT could produce a therapeutic effect *in vivo* as well. They grew U87 gliomas in nude mice, injected TiO_2 nanoparticles around the subcutaneous tumor, and after 12 h exposed the tumor and irradiated it with UVA. Significant areas of tumor necrosis and extended mouse survival were obtained by PDT.

7.2. Quantum dots

QD are semiconductor crystals whose size regulates the band-gap (difference in energy between the highest valence band and the lowest conduction band). The absorption spectrum has a relatively broad peak, but the fluorescence emission is relatively narrow and tunable by size. The typical composition of the alloys in QD is chosen from cadmium selenide (CdSe), cadmium sulfide, indium arsenide, and indium phosphide (see Figure 10B). There have been scattered reports about the photoactivated generation of ROS after illumination with UV or visible light, but it is still uncertain whether they could be designed to carry out useful PDT [166]. Some workers have used QD as part of a Forster resonance energy transfer (FRET) pair to improve excitation of a standard PS. For instance, Samia et al. [167] used CdSe QD with an average diameter of 5 nm and linked to a silicon Pc PS(Pc4) through an alkyl amino group on the PS. Pc4 is a known PDT agent currently undergoing clinical trials [168]. For excitation wavelengths between 550 and 630 nm, Pc4 was directly activated. However, if wavelengths between 400 and 500 nm were used, the QD acted as a primary energy donor transferring excitation to Pc4 with a 77% FRET efficiency. In the process of investigating the two-step energy transfer mechanism in the QD/Pc4/oxygen system, they found that semiconductor QD alone could actually generate $^1O_2$ without a mediating Pc4 molecule. They measured radiative relaxation of $^1O_2$ causing emission at 1270 nm and found the $^1O_2$ quantum yield of QD to be 5%. In comparison, Pc4 alone was

reported to have a $^1O_2$ efficiency of 43% [169]. Theory predicts that the lowest excited state of CdSe QD is a triplet state, and it appears that the triplet QD can interact with $^3O_2$ to generate $^1O_2$. Moreover, the amount of defect sites on the QD surface could be controlled to some extent using additional surface passivation layers [170], which may systematically improve $^1O_2$ generation.

Generalov et al. [171] suggested that upon entry into a cell, QD are trapped and their fluorescence is quenched in endocytic vesicles such as endosomes and lysosomes. They investigated the photophysical properties of QD in liposomes as an *in vitro* vesicle model. Generation of free radicals by liposomal QD is inhibited compared with that of free QD. Nevertheless, QD fluorescence lifetime and intensity increases due to photolysis of liposomes during irradiation. In addition, protein adsorption on the QD surface and the acidic environment of vesicles also lead to quenching of QD fluorescence, which reappears during irradiation. Morosini et al. [172] used hydrophilic CdTe(S) QD conjugated to folate with different spacers (PEG or Jeffamine D-400) and examined phototoxicity against folate-receptor-positive or -negative cancer cells. They obtained evidence for foliate-receptor-mediated targeting and PDT effects using 515- or 658-nm light.

8. Fullerenes

Fullerenes are the third allotropic form of carbon material forming a family of closed-cage carbon molecules, C_n, where n=60, 70, 72, 76, 84, and even up to 100. The molecules characteristically contain 12 pentagons and a variable number of hexagons arranged in soccer ball structure (Figure 11). These nanomolecule with their unique structure have a great potential for variety of application and are being recently studied for biological activities relevant to biomedical applications. The fullerenes are seen as potential PDT agents as they possess some the characteristics that render them well suited as a photosensitive drug. Although pristine C_{60} is highly insoluble in water and biological media and thus forms nanoaggregates, which makes it photoinactive [178], fullerenes still have gained considerable attention as possible PDT mediators [179] after chemists have exploited this molecule by attaching the some hydophilic or amphiphilic functional groups [180]. This functionalization imparts a higher ability to produce $^1O_2$, hydroxyl radicals and superoxide anion thus making them potent PS (see Figure 11 for structures of some functionalized fullerenes used as PS).

Following are some of the advantages that these fullerenes possess over the traditional PS:

- They are comparatively more photostable and are less photobleached as compared with tetrapyrroles.
- Fullerenes follow both type 1 and type 2 pathways.
- They can be chemically modified easily for tuning the drug's partition coefficient for the variation of *in vivo* lipophilicity and the prediction of their distribution in a biological system.
- To enhance the overall ROS quantum yield, light harvesting antenna can be chemically attached on C_{60} [174].

- Molecular self-assembly of fullerene cages into vesicles allows multivalent drug delivery and can produce self-assembled nanoparticles that may have different tissue targeting properties.

In addition to these advantages, fullerenes demonstrate some particular disadvantages as PS for PDT. First, their extreme hydrophobicity and their innate tendency to aggregate render them even more difficult to formulate than other tetrapyrrole PS. Nevertheless, there has been many different strategies applied for drug delivery of fullerenes, e.g., liposomes [181–183], micelles [184, 185], dendrimers [186, 187], pegylation [188–191], cyclodextrin [192, 193], and self-nanoemulsifying systems [194–197]. Second, the main absorption of fullerenes is in the blue and green regions of the visible spectrum, rather than the red/NIR where light transmission through tissue is maximized. This unfavorable absorption could possibly be overcome by various strategies such as covalent attachment of light harvesting antennae to fullerenes [198–202], using optical clearing agents [203–207], or using two-photon PDT [208–212].

One potential paradox or contradiction in this field is the observation that fullerenes act as antioxidants or ROS quenchers in the absence of light [213–217] while as producers of ROS and pro-oxidants under illumination. The obvious question then arises: how then can fullerenes scavenge ROS and act as antioxidants in the dark on one hand and act as efficient producers of ROS under illumination with the correct light parameters on the other? Andrievsky et al. [218] in 2009 first proposed a way to explain this seeming contradiction. They showed that the main mechanism by which hydrated C_{60} can inactivate the highly reactive ROS, hydroxyl radical, was not by covalently scavenging the radicals but rather by action of the coat of “ordered water” that was associated with the fullerene nanoparticle [219]. They also claimed that the ordered water coat could slow down or trap the hydroxyl radicals for sufficient time for two of the radicals to react with each other, thus producing the less reactive ROS, hydrogen peroxide.

There have been many studies using fullerenes as PS to mediate PDT of both cancer cells and of pathogenic microorganisms both *in vitro* and *in vivo* [220, 221]. The first study demonstrating the phototoxic effect of fullerenes was done by Tokuyama et al. [222] using carboxylic acid-functionalized fullerenes in HeLa cells. It was shown that tris-malonic acid fullerene was more phototoxic than the dendritic derivative in killing Jurkat cells when irradiated with UVA or UVB light [223]. Burlaka et al. [224] used pristine C_{60} at 10 μM with visible light from a mercury lamp to produce some phototoxicity in Ehrlich carcinoma cells or rat thymocytes. Yang et al. [225] reported three C_{60} derivatives with two to four malonic acid groups (DMA C_{60}, TMA C60, and QMA C60) that were tested for their relative efficacy in HeLa cells, and the results showed the following order of efficacy: DMA C_{60}>TMA C_{60}>QMA C_{60}.

There have been several studies from our laboratory using a range of functionalized fullerenes [221]. We tested a group of six functionalized fullerenes that were prepared in two groups of three compounds [173, 175]. We established that the C_{60} molecule monosubstituted with a single pyrrolidinium group (BF4; Figure 11A) was an efficient PS that effectively killed a panel of mouse cancer cells at the low concentration of 2 μM on

exposure to white light. Chiang et al. [174] reported the synthesis of two new photoresponsive diphenylaminofluorene nanostructures and they investigated their intramolecular photoinduced energy and electron transfer phenomena. They demonstrated that the large light-harvesting enhancement of CPAF-OMe moiety was more efficient triplet state generator than the C_{60}>cage moiety. C_{60} (>CPAF-OMe; Figure 11B) was significantly better than C_{60} (>DPAF-OMe) at light-mediated killing of human cancer cells.

The ability of cationic fullerenes for the PDI of bacteria and other pathogens has also been demonstrated in our laboratory. We were the first to demonstrate that cationic water-soluble functionalized fullerenes, especially the tris-cationic compound (BF6; Figure 11C) were efficient antimicrobial PS and could mediate PDI of various classes of microbial cells [175]. In a study by Spesia et al. [226], it was reported that a novel fulleropyrrolidinium iodide [DT-C_{60} (2+)] produced PDI *in vitro* on *E. coli*. Lee et al. [227] showed that C_{60} derivatives were efficient in inactivating *Escherichia coli* and MS-2 bacteriophage. Recently, we have demonstrated the use of innovative cationic fullerenes as broad-spectrum light-activated antimicrobials, which was determined by quantitative structure-function relationships [228]. The most effective compound overall against the various classes of microbial cells had the hexacationic structure.

A variety of different delivery vehicles have been tested to see if the PDT efficacy of fullerenes could be improved. Ikeda et al. [229] used a series of liposomal preparations of C_{60} containing cationic or anionic lipids together. Illumination with 136-J/cm^2 350- to 500-nm light gave 85% cell killing in the case of cationic liposomes, and apoptosis was demonstrated. Akiyama et al. [185] solubilized unmodified C_{60} with high stability using various types of PEG-based block copolymer micelles, which showed cytotoxicity under photoirradiation in HeLa cells. In another study, both direct and rapid uptake (within 10 min) of fullerene into the cell membrane using an exchange reaction from a fullerene-γ-cyclodextrin complex, and the resulting photodynamic activity for a cancer cell was demonstrated [230]. Doi et al. [183] showed the PDT activity of cerasome-encapsulated C_{70} in HeLa cells was similar to that of surface cross-linked liposome C_{70}, indicating that C_{70} can act as a PS without release from cerasome membranes. Thus, from the above *in vitro* studies, it was supposed that fullerenes might be sufficiently active as PS to enable *in vivo* applications both for anticancer and for anti-infective use [231].

In 1997, Tabata et al. [191] first reported the use of fullerenes to carry out PDT of actual tumors. In this study, the fullerenes were chemically modified to make it soluble in water as well as to enlarge its molecular size by pegylating C_{60}. On intravenous injection in mice carrying a subcutaneous tumor on the back, the C_{60}-PEG conjugate demonstrated a higher accumulation and more prolonged retention in the tumor tissue than in normal tissue. The volume increase of the tumor mass was suppressed and the C_{60} conjugate exhibited a stronger suppressive effect than Photofrin. In another study, a novel PS was prepared from fullerene [C(60)] possessing magnetic resonance imaging (MRI) activity for efficient PDT of tumor. This therapeutic and diagnostic hybrid system was found to be a promising tool to enhance the PDT efficacy for tumor [190].

Chi et al. [177], in a preliminary *in vivo* study, performed PDT using hydrophilic nanospheres formed from hexa(sulfo-*n*-butyl)-C_{60} (FC_4S; Figure 11D). Intraperitoneal administration of FC_4S in mice had a slightly better inhibition effectiveness than the intravenous route.

We have recently shown [118] that intraperitoneal PDT with BF4 fullerene and white light has significant therapeutic effects in a challenging mouse model of disseminated abdominal cancer produced by engineered bioluminescent tumor cells. Intraperitoneal injection of a preparation of *N*-methylpyrrolidinium-fullerene formulated in Cremophor-EL micelles followed by white-light illumination delivered through the peritoneal wall (after creation of a skin flap) produced a statistically significant reduction in bioluminescence signal from the mouse abdomen and a survival advantage in mice. This article suggested fullerenes should continue to be explored as PS for PDT of cancer and other dreaded diseases.

In addition to *in vivo* anticancer applications, we have been able to translate the high degree of antimicrobial action of photoactivated fullerenes *in vitro* to a therapeutic effect in an *in vivo* infection model [176]. We used stable bioluminescent bacteria and a low-light imaging system to follow the progress of the infection noninvasively in real time in two potentially lethal mouse models of infected wounds. An excisional wound on the mouse back was contaminated with one of two bioluminescent Gram-negative species, *Proteus mirabilis* (2.5×10^7 cells) and *Pseudomonas aeruginosa* (5×10^6 cells). Fullerene-mediated PDT of mice infected with *P. mirabilis* led to 82% survival compared with 8% survival without treatment ($p<0.001$). PDT of mice infected with highly virulent *P. aeruginosa* did not lead to survival, but when PDT was combined with a suboptimal dose of the antibiotic tobramycin (6 mg/kg for 1 day), there was a synergistic therapeutic effect with a survival of 60% compared with a survival of 20% with tobramycin alone ($p<0.01$). The data suggested that cationic fullerenes have clinical potential as an antimicrobial PS for superficial infections where red light is not needed to penetrate tissue.

9. Carbon nanotubes and graphene

Carbon nanotubes are allotropes of carbon with a cylindrical nanostructure. Nanotubes have been constructed with length-to-diameter ratio of up to 132,000,000:1 [232] and can be several millimeters long, significantly larger than any other material. Nanotubes are categorized as single-walled nanotubes and multi-walled nanotubes. Most single-walled nanotubes have a diameter of close to 1 nm, with a tube length that can be many millions of times longer. The structure of a single-walled nanotube can be conceptualized by wrapping a one-atom-thick layer of graphite called graphene into a seamless cylinder.

Zhu et al. [233] engineered a novel molecular complex of a PS, an ssDNA aptamer, and single-walled carbon nanotubes (SWCNTs) for controllable $^1O_2$ generation (Figure 12A). It is well known that $^1O_2$ is one of the most important cytotoxic agents generated during PDT. Because the lifetime and diffusion distance of $^1O_2$ is very limited, a controllable $^1O_2$ generation (SOG) with high selectivity and localization would lead to more efficient and reliable PDT and fewer side effects. First, the aptamer was developed by an *in vitro* process known as systematic evolution of ligands by exponential enrichment. Second, a PS was

covalently attached to one end of the DNA aptamer that wrapped onto the SWCNT surface. In the absence of a target, the design becomes operational by close proximity of the PS to the SWCNT surface, which causes efficient quenching of SOG. Importantly, the conformation of the probe can be altered upon target binding. Thus, in the presence of its target, the binding between the aptamer and target molecule will disturb the DNA interaction with SWCNTs and cause the DNA to fall off the SWCNT surface, resulting in a restoration of SOG for PDT applications. $^1O_2$ can thus be regulated by target binding.

An important issue with regard to PDT agents is the delivery of these molecules into the organs/tumor tissues/tissues cells. There are many strategies for drug targeting, but a satisfactory multifunctional delivery agent is nevertheless needed. SWCNTs are one distinct possibility. Erbas et al. [234] tested the use of noncovalent functionalized SWCNTs as delivery agents for Bodipy-based potential PS in PDT. The target molecule carried a solubilizing group (PEG2000), red-absorbing chromophore (distyryl-Bodipy), intersystem-crossing promoter heavy atoms (iodines at 2 and 6 positions of the Bodipy core), and two pyrene substituents on the styryl branches of the chromophore for p-stacking interactions with the SWCNTs.

Shiraki et al. [235] developed a thermo- and light-responsive system consisting of SWCNT and helical polysaccharide modified with poly(NIPAM) side-chains through supramolecular polymer wrapping. Coagulation of the complex can be induced by the external stimuli, which leads to a catch-and-release action of a porphyrin derivative. This method, therefore, is expected to develop a novel site selective PDT technique by dual-light irradiation using visible and NIR light sources; for example, a nondisease site close to a disease site can be protected by irradiating with NIR laser through SWCNT quenching and only the disease site was selectively decomposed by visible light irradiation.

Graphene oxide (GO) consists of sheets sp2- and sp3-hybridized carbon atoms, including carboxyl, hydroxyl, and epoxide functional groups [236]. It has gained increasing attention owing to its excellent biocompatibility, well-dispersed stability in aqueous solution, and ability of the GO sheets, which have a large specific surface area, to be loaded with large amounts of hydrophobic drugs [237] such as doxo-rubicin [238]. Zhou et al. [239] loaded GO with HA (GO-HA) as shown in Figure 12B, a perylenequinonoid hydrophobic nonporphyrin PS isolated from parasitic fungi *Hypocrella bambuase* found in the People's Republic of China [240]. The optimal loading was found to be 1 mg/mg by fluores-cence and the GO-HA had a somewhat lower $^1O_2$ quantum yield compared with free HA. The stability of the GO-HA in aqueous solution was much higher than HA, and there was less dark toxicity but comparable phototoxicity toward HeLa cells. Huang et al. [241] conjugated GO with folic acid and then loaded ce6 (80% loading). These nanocarriers delivered ce6 to MGC803 folate-receptor-positive cells, and this uptake could be blocked by free folate, suggesting a receptor-mediated process. *In vitro* PDT gave significant killing. Tian et al. [242] loaded ce6 onto PEG-functionalized GO *via* π-π supra-molecular stacking. They not only studied PDT killing using a 660-nm laser but also found significant synergism when PDT was combined with the preadministered photothermal effect of exciting the GO with a 808-nm laser.

10. Miscellaneous nanoparticles

In this section, we will cover some nanoparticles that have been used for PDT and that do not conveniently fit into our other categories.

10.1. Upconverting nanoparticles

Upconversion (UC) refers to a family of nonlinear optical processes in which the sequential absorption of two or more photons leads to the emission of light at shorter wavelength than the excitation wavelength (anti-Stokes-type emission). In contrast to other emission processes based on multiphoton absorption, UC can be efficiently excited even at low excitation densities. There are three possible mechanisms for this to occur [243]: APTE effect (for the French “addition de photon par transferts d’energie”), later also named ETU for energy transfer upconversion [4, 5] excited-state absorption (ESA), and photon avalanche (PA). All three mechanisms are based on the sequential absorption of two or more photons by metastable, long-lived energy states. This sequential absorption leads to the population of a highly excited state from which UC emission occurs. In the case of ESA, the emitting species sequentially absorb at least two photons of suitable energy to reach the emitting level (Figure 13). In ETU, one photon is absorbed by the ground state but subsequent energy transfer from neighboring metastable states results in the population of a highly excited state of the emitting species (Figure 13). The most efficient UC mechanisms (even at room temperature) are present in solid-state materials doped with lanthanide ions. The most efficient UC phosphor to date, Yb^{3+}- and Er^{3+}-doped $NaYF_4$, was introduced by Menyuk et al. in 1972 [244]. The development of nanocrystal research has evoked increasing interest in the development of synthesis routes, which allow the synthesis of highly efficient, small UC particles with narrow size distribution able to form transparent solutions in a wide range of solvents. High-quality UC nanocrystals can be routinely synthesized, and their solubility, particle size, crystallographic phase, optical properties, and shape can be controlled [243]. In recent years, these particles have been discussed as promising alternatives to organic fluorophos-phors and QD in the field of medical imaging and PDT.

Chatterjee and Yong [245] designed UC NPs composed of sodium yttrium fluoride ($NaYF_4$) nanocrystals co-doped with Yb^{3+} and Er^{3+} with a polymeric coat of poly(ethylenimine) (PEI). PS ZnPC was superficially noncovalently adsorbed to the NPs. They could image cellular uptake by fluorescence imaging microscopy of PEI/$NaYF_4$:Yb^{3+}:Er^{3+} NPs, and they found significant cell death following irradiation with NIR laser light.

Ungun et al. [246] synthesized UCP nanocrystals by a high-temperature ligand exchange reaction that produced nanoparticles of approximately 160 nm in diameter with a hydrophobic trioctyl phosphene-oleic acid surface coating. The co-encapsulation of the UCP nanocrystals with the TPP PS and a PEG protective layer to form the complex functional nanoparticle UCPs was done in one step using a “flash nano-precipitation process” [247]. When these UCP-NP were excited by two 980-nm photons, they produced UC 560-nm light that excited the TPP and produced $^1O_2$ as measured by bleaching of the fluorescent dye 9,10-anthracenedipropionic acid.

Wang et al. [248] were able to show that UCP NP containing ce6 were able to kill HeLa and 4T1 cancer cells after illumination with a 980-nm laser. Furthermore, they used intratumoral injection of UCP NP into 4T1 subcutaneous tumors growing on backs of Balb/c mice followed by 980-nm laser (0.5 W/cm^2 for 30 min to give 900 J/cm^2). Tumors on 7 of 10 mice disappeared in 2 weeks after PDT and showed no tumor regrowth and survived over 60 days. Hematoxylin and eosin staining of tumor slices collected from UCNP-ce6 PDT treated mice at day 7 showed that most tumor cells were severely destroyed, in marked contrast to the control tumor slices where no obvious damage was found.

10.2. Simultaneous two-photon excitation nanoparticles

In contrast to UC, simultaneous two-photon excitation (Figure 13) requires extremely high power densities that can only be readily achieved with femtosecond lasers. Two-photon absorption (TPA) was originally proposed by Maria Göppert-Mayer in 1931 in her doctoral dissertation [208], but the first experimental verification was provided by Werner Kaiser in 1961, facilitated by the recent development of the laser, which was required for excitation because of the intrinsically low intensity of TPA. TPA is a third-order nonlinear optical process and therefore is most efficient at very high intensities.

Long-wavelength near-IR light λ>780 nm has relatively low photon energy (>1.5 eV) and is generally too low to activate most PS by one-photon excitation. Therefore, one-photon absorption fails in the phototherapeutic window 780–950 nm, where tissues have maximum transparency to light. Sensitization by simultaneous TPA [209] combines the energy of two identical photons arriving at the PS at the same time and can provide the energy of a single photon of half the wavelength, which is sufficient to excite the PS to the first excited singlet state. It was not until the 1990s that rational design principles for the construction of two-photon-absorbing molecules began to be developed, in response to a need from imaging and data storage technologies and aided by the rapid increases in computer power that allowed quantum calculations to be made. The accurate quantum mechanical analysis of two-photon absorbance is orders of magnitude more computationally intensive than that of one-photon absorbance.

Gary-Bobo et al. [249] prepared MSN containing a por-phyrin for efficient TPA-PDT. The MSN surface was post-functionalized with a mannose derivative to target lectins overexpressed by cancer cells [14]. Incubated with cancer cells, these MSNs were nontoxic under daylight illumination. TPE-PDT with these MSNs was investigated *in vitro* on human breast and colon cancer cell lines. *In vivo* experiments were also performed on athymic mice bearing xenografted tumors from colon cancer cells. They showed that the por-phyrin was covalently encapsulated inside MSNs (6850 units of PS per nanoparticle) and having a hydrodynamic diameter of 118 nm. Grafting of the mannose moiety on the surface yielded MSN-mannose. The TPA properties of PS are retained in the MSNs with 1200 Goppert-Mayer units [GM, where 1 GM=10(50) cm^4 s/photon/molecule] per PS. TPA-PDT was carried out at 760 nm using a confocal microscope equipped with a mode-locked Ti/sapphire laser generating 100-fs-wide pulses at a rate of 80 MHz. The laser beam was focused by a microscope objective lens (10×, NA 0.4). The wells were irradiated at 760 nm by three successive scans of 1-s duration each at an average power of 80 mW. The surface of the

scanned areas was 1.5×1.5 mm (mean fluence of 10.6 J/cm^2). Three cancer cells lines (MCF-7, MDA-MB-231, and HCT-116) showed TPA-PDT killing with evidence of mannose receptor targeting. TPA-PDT *in vivo*, on nude mice bearing HCT-116 xenografts used intravenous injection with MSN1-mannose (16 mg/kg). Three hours later, tumors were submitted to two-photon irradiation at 760 nm for three periods of 3 min and light was focused on three different tumor areas. Thirty days after treatment, PDT-treated tumors showed a growth delay compared with saline controls.

Grimland et al. [250] conjugated polymer nanoparticles (CP dots) that allow efficient intraparticle energy transfer from the conjugated polymer donor to a variety of acceptors. These nanoparticles formed from poly(2-fluoro-1,4-phenylene vinylene) (PFPV) were conjugated to TPP and were 50 nm diameter and formed a stable colloidal suspension in water. The TPA cross section of TPP-doped PFPV nanoparticles at an excitation wavelength of 800 nm was determined using a passively mode-locked Ti/sapphire laser (800 nm, 100 fs). The particles contained 600 molecules of PFPV and 6000 molecules of TPP. The two-photon fluorescence cross section of the TPP-doped PFPV CP dots was determined to be 5×10^5 GM. The $^1O_2$ quantum yield in aqueous solutions was determined to be 0.5 for PFPV dots doped with TPP.

10.3. Self-illuminating nanoparticles

Chen and Zhang [139] developed an innovative class of nano-particle for PDT that was termed “self-lighting. ” It relied on the combination of conventional ionizing radiation therapy with PDT. Scintillation or persistent luminescence nanoparticles with attached PS such as porphyrins were used and upon exposure to ionizing radiation such as X-rays, the nanoparticles emitted scintillation or persistent luminescence, which, in turn, activated the PS; as a consequence, $^1O_2$ was produced. Importantly, this approach could be used for deep tumor treatment as X-rays can penetrate much deeper into the tissue compared with visible light. First, absorption of the ionizing radiation (X-ray photons) creates primary electrons and holes in pairs. Next, thermalization of the low-energy secondary electrons (holes) results in a number of electron-hole pairs (excitons) with energy roughly equal to the band-gap energy Eg or electron-phonon relaxation. Energy transfer from the electron-hole pairs to the luminescence centers induces their excitation and emission from the luminescence centers occurs. High-density materials made with high-atomic-number elements will have high luminescence efficiency. Nanoparticles constructed from BaFBr/Eu^{2+} have three emission bands, peaking at around 400, 500, and 640 nm, respectively. The emission spectrum of these nanoparticles perfectly matches the absorption spectra of most porphyrins such as 5,15-diphenyl-2-3-dihydroxychlorin.

10.4. Magnetic nanoparticles

MNPs have been intensively investigated as MRI contrast agents and exhibit a unique MR contrast enhancement effect that enables noninvasive MRI of cell trafficking, gene expression, and cancer [251]. In addition, MNPs have been recognized as a promising tool for the site-specific delivery of drugs and diagnostic agents by an external magnetic field applied outside the body [252]. Figure 14 shows the general structure of a MNP with biocompatible coating and PS attached by a linker.

Huang et al. [253] coprecipitated $FeSO_4$ and $FeCl_2$ to form 10-nm MNP, functionalized them with amino groups using a silane, and conjugated ce6 using carbodiimide chemistry. Fluorescence microscopy showed uptake into human gastric cancer MGC803 cells, and phototoxicity was observed after 24-h incubation. MGC803 tumors grown in nude mice were imaged by both *in vivo* fluorescence and MRI after intravenous injection of 0.125 μmol ce6 eq/kg up to 8 h postinjection. *In vivo* PDT was carried out at 8-h time point with 632.8 nm HeNe laser, with a total light dose 5.88 J/cm^2 at an irradiance of 9.8 mW/cm^2, and significant tumor destruction was observed.

Tada et al. [254] prepared nanoparticles consisting of a silica layer over a magnetic core composed of magnetite and entrapping MB as PS. The $^1O_2$ quantum yield of MB was reduced somewhat to a level of 6%. Ding et al. [255] prepared magnetic Fe_3O_4 coated with *meso*-tetra(4-sulfonatophenyl) porphyrin dihydrochloride. They were able to perform MRI in mice with tumors and demonstrate a therapeutic effect after light delivery.

Sun et al. [256] prepared magnetic chitosan nanoparticles (MTCNPs) of 20.6-nm diameter containing a porphyrin PS called PHPP. Drug loading was 5.08% (w/w). First, the Fe_3O_4 was incubated with PHPP and then added to chitosan. Fe_3O_4 nanoparticles have extensive hydroxyl groups on the surface and thus possess negative charges. The protonation of the amine groups of chitosan allowed electrostatic interaction of cationic chitosan and negatively charged Fe_3O_4. Results showed that PHPP-MTCNPs could be used in MRI monitored PDT with excellent targeting and imaging ability. Nontoxicity and high PDT efficacy on SW480 carcinoma cells was shown *in vitro*. Two bilateral tumors were grown in nude mice and PHPP-MTCNP (1.25 μmol PHPP eq/kg) were injected intravenously. A magnetic field (1 Tesla) was placed over the left tumor that led to increased accumulation measured by MRI after 8 h. Laser illumination (650-nm, power density, 9.8 mW/cm^2; fluence, 5.88 J/cm^2) led to significant regression of the magnetically targeted tumor not seen in the contralateral tumor treated with PDT.

10.5. Lipoprotein nanoparticles

Lipoproteins are naturally occurring nanoparticles composed of specific apoproteins, phospholipids, and cholesterol on the surface that encapsulate a mixture of cholesterol esters and triglycerides in the hydrophobic core [257]. The family consists of chylomicron (75–1200 nm), very-low-density lipo-protein (30–80 nm), low-density lipoprotein (LDL, 18–25 nm), and high-density lipoprotein (HDL, 5–12 nm). Such biocompatible, lipid-protein complexes are ideal for loading and delivering cancer therapeutic and diagnostic agents. By mimicking the endogenous shape and structure of lipoproteins, the nanocarrier can remain in circulation for an extended period while largely evading the reticuloendothelial cells in the body's defenses. The small size (<30 nm) of LDL and HDL allows them to maneuver deeply into tumors. Furthermore, LDL has innate cancer-targeting potential, as LDL receptors are overexpressed on malignant cells and has been used to incorporate diverse hydrophobic molecules and deliver them to tumors.

Li et al. [258] prepared a tetra-*t*-butyl silicon phthalo-cyanine bisoleate, SiPcBOA, and efficiently incorporated it into reconstituted LDL to form r-SiPcBOA-LDL (see Figure 15). It was tested with HepG2 human hepatocarcinoma cells (which overexpress LDL receptors).

The nanoparticles had a very high payload (SiPcBOA to LDL molar ratio, 3000–35,001:1). Using electron microscopy, they found reconstituted LDL essentially retained the mean particle size of native LDL. As acetylated LDL binds to scavenger receptors of endothelial and microglial cells instead of LDLR, SiPcBOA-reconstituted acetylated LDL, r-SiPcBOA-AcLDL, was also prepared to serve as a negative control to validate the LDL receptor LDLR-targeting specificity. Confocal microscopy studies demonstrated that the internalization of r-SiPcBOA-LDL by HepG2 tumor cells was mediated by LDLR pathway. The *in vitro* PDT response of HepG2 cells to r-SiPcBOALDL was compared with SiPcBOA-free drug control using a clo-nogenic assay and indicated greatly enhanced efficacy of LDLR-targeted PDT.

Marotta et al. [259] from the same group prepared an analogous molecule, bacteriochlorin e6 bisoleate and incorporated it into reconstituted LDL to form (r-Bchl-BOA-LDL). HepG2 cells were injected into nude mice to form subcutaneous tumors. Three hours after intravenous doses of 2 μmol/kg r-Bchl-BOA-LDL, 750-nm laser illumination was delivered at fluences of 125, 150, or 175 J/cm^2 at a fluence rate of 75 mW/cm^2. The best tumor response was obtained with the 125 J/cm^2, which also gave the least phototoxicity to normal footpad.

11. Actively-targeted nanoparticles

Ideally, PDT holds the promise of dual selectivity, a preferential tumor uptake of the PS and the restricted illuminated area for an improved selectivity. However, for applications of PDT in complex anatomical sites, confined irradiation is not possible, leading to phototoxicity to normal tissues. Moreover, several cases of prolonged skin photosensitivity after sunlight exposition have been reported [260]. Targeted drug-delivery systems are one of the strategies proposed to solve these problems underlying nonspecific PS accumulation. Active targeting encompasses the strategy of coupling a specific entity to the surface of the nanoparticle, enhancing their selective interaction with target cells recognized by specific markers. Although MoAbs has received the most attention, biochemical, metabolic, and physiological alterations of tumor cells offer numerous other potent targets to exploit during the delivery of PS. Targeting nanoparticles with these specific moieties offers several advantages. The specific localization increases the efficiency and selectivity of PDT, resulting in a lower effective dose. Unlike other strategies such as ligand-PS conjugates, targeted nanoparticles can deliver thousands of molecules of PS using fewer molecules of ligands per nanoparticle, reducing considerably the cost and time-consuming synthesis of some of these targeting moieties. In addition, the presentation of multiple targeting molecules on the surface of the nanoparticle can restore multivalent binding of monovalent antibody fragments and hence increase their binding avidity for the target antigens. In this section, we will further describe some of these macromolecular moieties used to selectively address PS-containing nanoparticles to tumor tissues. Figure 16 schematically illustrates some of the targeting ligands that have been used to target PS-loaded nanoparticles.

Targeted drug delivery is a promising strategy to improve the efficacy and safety of PS. However, a potential drawback of active targeting is related to the so-called binding site barrier phenomenon. This hypothesis considers the idea that macromolecular ligands could

be prevented from penetrating tumors through their successful binding to the target receptor. Some works have reported direct experimental evidence of the binding site barrier phenomenon in various systems [261, 262].

11.1. Monoclonal antibodies

Antibody-based drug delivery is a widely studied approach to improve the selectivity of PDT. MoAbs have the advantage over most of other tumoritropics to possess a high degree of specificity. However, they have some drawbacks such the cost, the time-consuming production and the possible immune reactions that limit their extensive use and commercialization. The use of antibody fragments, such as $F_{ab}V$ and scF_v molecules, is an alternative that preserves the high degree of specificity, but the immune reactions are significantly reduced [28]. Numerous published works prove the validity of the use of MoAb in a wide range of nanoparticles for selectively targeted PDT. The high epidermal growth factor (EGF) receptor expression that frequently accompanies several tumor types makes this receptor an attractive candidate for targeting strategy. Stuchinskaya et al. [263] recently published an antibody-phthalocyanine-AuNP conjugate to selectively target breast cancer cells that overexpress the HER2 EGF receptor (EGFR). Kameyama et al. [264] used the conjugation of an anti-EGFR MoAb with a verteporfin-loaded nanoparticles. They found a threefold higher incorporation of the complex into A431 cells *in vitro*, and the tumor size *in vivo* experiments showed a significant decrease compared with tumors treated with verteporfin-nanoparticle complex without the antibody. Nevertheless, the use of MoAb for targeting therapies offers a wide range of alternatives. Rancan et al. [265] developed a fullerene hexa-adduct conjugated with the MoAb rituximab. The antibody conjugate conserved the affinity and selectivity toward CD20-positive B-lymphocytes, whereas the antibody-free complex did not show any intracellular uptake. T-43 MoAb was used to demonstrate a MoAb-dependent enhancement of the uptake by a bladder tumor cell line of a pheo-phorbide-a liposomes [266]. In a similar approach, aluminum sulfonated phthalocyanine (liposomes linked to a targeting MoAb 791T/36 showed an *in vitro* antibody-dependent cyto-toxicity on different cell lines expressing the target antigen [267]. MoAbs have also been attached to MNPs with a preliminary success [268].

11.2. Aptamers

Aptamers are small, simple, and synthetic DNA or RNA oligonucleotides and represent a nonimmunogenic alternative to binding to their target proteins specifically [269]. Their intrinsic advantages, such as reproducible synthesis, adaptability for molecular engineering, easy manipulation, and excellent stability make the design of controllable PDT feasible [270]. Zhu et al. [233] have designed a novel PDT agent using a human α-thrombin aptamer covalently linked with ce6 and then wrapping onto the surface of an SWCNT. As SWCNTs are efficient quenchers of $^1O_2$, the photodamage was only achieved when the binding of target thrombin disturbed the DNA interaction with the SWCNT and caused the aptamer to undergo spatial unquenching, restoring $^1O_2$ generation. Stephanopoulos et al. [271] used a targeted, multivalent PDT vehicle for treatment of Jurkat leukemia T cells. Bacteriophage MS2 virus capsid was internally modified with up to 180 porphyrins and the exterior with 20 copies of a Jurkat-specific aptamer. These capsids were able to target and selectively kill more that 76% of cells after illumination. Despite their advantages, fewer functional

aptamers have been identified compared with antibodies. As an attractive alternative, special attention is given to vitamins as targeting ligands for selective PDT.

11.3. Folate ligands

Folic acid, also known as vitamin B9, is essential for the proliferation and maintenance of cells. The overexpression of folate receptor (FR) on a variety of epithelial cancer cells including cancers of ovary, lung, kidney, breast, brain, and colon [272] and the high affinity of folate for its receptor has attracted wide attention as a targeting agent for tumor selectivity. Folate-decorated liposomes [273], QD-folic acid conjugates [172], pullulan/folate-PS nanogels [274], or FR-targeted solid lipid nanoparticles [275] used the specific interaction with FR to assess superior cancer cell selectivity. FR cell selectivity greatly increases phototoxicity and cellular uptake compared with nonfunctionalized drug-delivery systems. Huang et al. [241] also developed the folic acid-conjugated GO as a novel targeting drug-delivery system for PDT. It was found that ce6-loaded nanocarriers can significantly increase the accumulation in tumor cells and lead to a remarkable photodynamic efficacy on MGC803 cells upon irradiation. These findings suggest that folic acid has great potential as an effective drug-delivery system in targeting PDT.

11.4. Peptides

Small peptides that selectively recognize tumor cells represent an excellent approach for targeting therapies. Peptides are synthetic molecules consisting of several amino acids linked together and, in contrast to proteins, generally do not possess a well-defined three-dimensional structure. Their effective tissue penetration and selective binding to cancer cells make peptides ideal candidates for the delivery of therapeutic agents. Anti-angiogenesis-based research has become one of the most promising and actively explored fields. Recent studies from Qin [56] and Hah [276] have shown that the attachment of F3 peptide groups to the MB-conjugated polymeric nanoparticles results in effective and selective tumor cell killing. F3 has been shown to selectively target to tumor cells and angiogenic vasculature and to also have cell-penetrating properties. Reddy et al. [73] also used the surface-localized tumor vasculature targeting F3 peptide for a selective treatment and imaging of brain tumors. Treatment of glioma-bearing rats with targeted multifunctional polymeric nanoparticles showed a significant improvement in survival rate compared with nontargeted nanoparticles. Rozenzhak et al. [277] demonstrated that the use of a noncovalent peptide (Pep-1) facilitated the internalization of QD. Pep-1 seems to be extremely efficient in the targeting of proteins into cells independent of endocytosis. Oku and Ishii [278] used the APRPG peptide, specific for angiogenic endothelium, to modify BDP-MA-containing liposomes. This neovessel-targeted strategy results in strong tumor destruction with a low dose of the PS.

11.5. Hyaluronic acid

Hyaluronic acid is a targeting ligand that recognizes CD44, known as the hyaluronic acid receptor, which is involved in cell adhesion and is also overexpressed on many cancer cells [279]. CD44 targeting has been used to deliver many types of anticancer agents, for instance, doxorubicin or mitomycin c encapsulated within the aqueous core of the high-molecular-weight hyaluronic-modified liposomes [280]. Li et al. [281] prepared acetylated

low-molecular-weight hyaluronic acid/pheophorbide a conjugate for the preparation of nano-gels (Ac-HA-Pba). The nanogels observed were smaller than 200 nm in size, with a monodispersed size distribution. The nanogels displayed autophotoquenching qualities in water. The critical self-quenching concentration of the conjugates was found to have decreased as the content of Pba increased. Although Pba was conjugated with HA, the nanogel photoactivity, in terms of fluorescent properties, $^1O_2$ generation, and photocytotoxicity, was approximately maintained. Confocal imaging and flow cytometry analysis showed that Ac-HA-Pba nanogels were rapidly internalized into HeLa cells *via* an HA-induced endocytosis mechanism, a process that could be blocked with the application of an excess of HA polymer.

12. *In vivo* studies

Most PS molecules are hydrophobic and can aggregate easily in aqueous media, which can affect their photophysical properties (decrease of $^1O_2$ formation), chemical properties (decrease of solubility), and biological properties (biodistribution and pharmacokinetics). Moreover, some PS that were initially considered promising in *in vitro* studies have never been evaluated for clinical applications, mainly because their *in vivo* selectivity or effectiveness was not high enough due to aggregation. Nanoparticles represent emerging PS carriers that show great promise for PDT *in vivo* compared with conventional PS.

Aliphatic PLA, PGA, and their copolymer PLGA are among the most studied synthetic polymers for drug delivery *in vivo*.

Due to its well-vascularized structure, the chorioallantoic membrane (CAM) of the developing chick embryo can act as an *in vivo* model to study photodynamic activity of PS-loaded nanoparticles. Vargas et al. [282] compared the efficacy the vascular effects of *p*-THPP either as a free solution or encapsulated in polymeric nanoparticles in the CAM model. They showed that PDT-induced vascular occlusion of the PS *p*-THPP is enhanced when encapsulated into nanoparticle delivery systems. The superiority of nanoparticles over solubilized *p*-THPP might be related to the reduced diffusion of *p* -THPP nanoparticles out of the vessels. Where free *p*-THPP appeared to leak out before generating an efficient vascular occlusion, nanoparticles appeared to confer a longer residence time inside the vasculature, thus inducing an increased PDT effect [282]. Recently, they investigated the main physicochemical and photochemical properties of *m*-THPP encapsulated in PLGA nanoparticles of different sizes *via* an emulsification-diffusion technique. They reported that smallest size of nanoparticles (117 nm) exhibited the highest rate of ROS production and the fastest *m*-THPP release in the CAM model [36]. Pegaz et al. [283] compared the photodynamic activities of PS with different hydrophobicity entrapped in biodegradable nanoparticles composed of poly(D,L-lactic acid). Analysis of nanoparticles showed that the dye was more effectively entrapped in the polymeric matrix when its degree of lipophilicity increased. *Meso*-tetra-(4-carboxyphenyl)-porphyrin (TCPP) and ce6 were less hydrophobic than *m*-THPP and pheophorbidea. The nanoparticles loaded with the most lipophilic molecule (*m*-THPP) induced vascular damage in the CAM model.

Dendrimers are a new class of polymeric materials with repeatedly branched molecules, recognized as the most versatile and compositionally and structurally controlled nanoscale building blocks. Their properties are dominated by the functional groups. Casas et al. [284] demonstrated a good correlation between *in vitro* and *in vivo* properties of an ALA-dendrimer conjugate that is able to induce sustained and efficient porphyrin production. The ability of the dendrimer to enhance porphyrin synthesis was investigated in a BALB/c mouse model of subcutaneous LM3 tumors after systemic intraperitoneal administration. The ALA-dendrimer induced sustained porphyrin production for over 24 h, and background values were not reached until 48 h after administration, whereas the porphyrin kinetics from ALA exhibited an early peak between 3 and 4 h in most tissues. Integrated porphyrin accumulation from the dendrimer and ALA, at equivalent molar ratios, was comparable showing that the majority of ALA residues were liberated from the dendrimer. The porphyrin kinetics appeared to be governed by the rate of enzymatic cleavage of ALA from the dendrimer.

Reddy et al. [73] have developed a multifunctional polymeric nanoparticle consisting of a surface-localized tumor vasculature and tumor-targeting F3 peptide that encapsulated Photofrin. The rats from the Photofrin group had a median survival time of 13 days, whereas animals treated with the F3-targeted Photofrin nanoparticles had a median survival of 33 days, with three animals surviving past 60 days. Moreover, two of these three animals were found to be disease-free 6 months after treatment.

Barth et al. [285] investigated the possibility of using nanotechnology enabled PDT to treat leukemia, a form of blood cancer not generally treated with PDT. Indocyanine green (ICG), which is a highly fluorescent NIR dye that can also act as a PS, was loaded into nontoxic and nonag-gregating calcium phosphosilicate nanoparticles (CPSNP). Citrate-functionalized CPSNP were activated by 1-ethyl-3 -(3-dimethylaminopropyl)-carbodiimide and then reacted with sulfo-NHS to form a high-yield, semistable intermediate. The sulfo-NHS ester-containing CPSNP were then reacted with heterobifunctional PEG containing both amine and carboxyl functional groups. This synthetic process was repeated with the carboxyl-PEG functional terminals of the pegylated CPSNP to generate sulfo-NHS ester-containing pegylated CPSNP, which readily reacted with antibodies that recognize CD117 or CD96, surface features enhanced on leukemia stem cells. Cell-specific PDT killing was observed in *in vitro* studies with 32D-p210-GFP murine leukemia stem cells and with CD34+CD38-CD96+ cells from an acute myeloid leukemia patient. An *in vivo* study used intravenous injection of 32D-p210-GFP into C3H/HeJ mice to establish myeloid leukemia. The targeted ICG-CPSNP was intravenously injected (0.1 ml of 200 nM ICG equivalent concentration) followed within 30 min by 12.5 J/cm^2 of 810-nm laser directed to the surgically exposed spleen. When the treatment was repeated every 3 days, a 29% disease-free survival was obtained.

13. Nanotoxicology

The recent emergence of widespread biomedical and industrial applications of nanotechnology has given rise to a whole new area of nanotoxicology [286, 287]. This discipline is based on the widely held assumption that materials, which are largely harmless

on the normal macroscopic scale, can exhibit completely different biological properties on the nanoscopic scale and that undiscovered harmful effects both on people and on the environment may pose threats to health. There is even a new journal titled *Nanotoxicology*. Nanoparticles have much larger surface area to unit mass ratios, which in some cases may lead to greater proinflammatory effects (for example, in lung tissue) [288]. In addition, some nanoparticles seem to be able to translocate from their site of deposition to distant sites such as the blood and the brain [289]. Nanoparticle toxicologists study the brain, blood, liver, skin, and gut in addition to the traditional concentration on lung toxicity. Table 1 shows a selection of recent reports concerning nanotoxicology both *in vitro* and *in vivo* based on a table in a review by Meng et al. [314]. Nanotoxicity can be caused through inhalation, ingestion, skin uptake, and injection of engineered NPs. Importantly, NPS toxicity depends on multiple factors derived from both individual NPs physicochemical properties and environmental conditions: NPs size, charge, concentration, outer coating bioactivity (capping material, functional groups), and oxidative, photolytic, and mechanical stability have each been shown to be determining factors in NPs toxicity [315]. The greater surface area per mass compared with larger-sized particles of the same chemistry renders NP more active biologically. In addition, the internalization of NP was highly dependent on size, with the most efficient uptake occurring within the 25- to 50-nm size range [316]. Ultrafine particles (UFP) are defined as a size <100 nm NPs, which has most active bioactivity. This activity includes a potential for inflammatory and pro-oxidant effects but can also exhibit antioxidant activity.

It has long been known that asbestosis fibers cause asbestosis and mesothelioma when inhaled, and several authors have asked whether SWCNT (which have similar characteristics to asbestosis fibers) can have similar adverse effects [317–319]. Reports that fullerenes exhibited toxicity toward various fish [320, 321] have been discounted by other authors [322] and attributed to the presence of a tetra-hydrofuran bioproduct introduced during fullerene preparation [323].

The other important area of nanotoxicology has been that of QD. The possible use of materials such as CdSe [324] and cadmium telluride (CdTe) [325] in QD construction has led to concerns about heavy metal toxicity, which would preclude any clinical use. These studies concluded that QD could cause indirect *in vivo* genetic damage, which may be attributed to free radical-induced oxidative stress in mice.

14. Conclusion

At the end of this review, it is necessary for the authors to address the question that we originally posed, “can nano-technology potentiate PDT?” The answer in some areas is an unequivocal “yes,” but in other areas, the jury is still out. One of the areas where nanotechnology has made huge improvements is in the use of different drug-delivery vehicles for PS, particularly in the use of liposomes [326]. The enormous clinical success of Visudyne (total sales of several billion $) have made it an important member of the list of approved liposomal drugs [327]. Liposomal Visudyne has also widened the acceptance of preformulated drug-delivery vehicles in the PDT field.

In many of the articles covered in the previous sections of the present review, the authors have compared their particular nanoparticle formulated PS with the identical PS delivered in its free form. In some cases, major improvements in cell uptake, tumor localization, and PDT response were observed for the nanoparticle formulation. Some of these reports, however, use PSs that are not particularly effective in their free form so that nanoformulated preparations automatically appear better. Such criticisms could be made in the case of, for example, ce6 and PPIX. These PS are known to be only moderately effective in their free unformulated form. Other PSs, for example, Foscan (*m*-THPC) are so effective in their free state that encapsulating them into nanoparticles is likely to only reduce their effectiveness. Of course, it could then be argued that improved phar-macokinetics, better tumor targeting, or lower normal tissue phototoxicity would be a desirable consequence of reducing their overall excessive PDT activity, which could otherwise damage normal tissue.

Lessons learned from past drug-delivery problems in PDT will only underscore the necessity of using appropriate well-defined and well-characterized nanoparticle vehicles in the future. It is hoped that these nanocarriers will improve the phamacokinetics, serum stability, biodis-tribution, tumor targeting, and photophysics of many PS. The pronounced tendency of most PS to undergo self-aggregation is due to the inherent electron-delocalized planar structures needed to have a high visible absorption [328]. When this structural attribute is combined with an overall hydrophobic substitution pattern, it is not surprising that insolubility and aggregation in water is a big problem. The ability of these PS to satisfactorily dissolve in the hydrophobic domains of lipid bilayers of liposomes [3] or the interior of detergent micelles is responsible for the dramatically improved performance of PDT mediated by these delivery vehicles.

There has recently been an explosion of interest in the area of “theranostics” [329]. This area can be defined as the combination of diagnostic, imaging, and therapeutic agents on the same platform [330]. These combination agent platforms frequently take the form of multifunctional nanoparticles [331, 332]. For the detection/imaging functionality, it is possible to use one or more from the following list [333]: fluorescence imaging (based on attached fluorophores), photoacoustic imaging (based on intrinsic or attached absorbers), SERS (based on intrinsic gold or silver), MRI (based on attached paramagnetic relaxation agents), positron emission tomography (PET, based on attached PET isotopes), single-photon emission computed tomography (based on attached γ-emitting isotopes). Although the therapeutic functionality can take the form of attached cytotoxic drugs that are released from the nanoparticle [330] or therapeutic radioisotopes [334], many groups have constructed a light-activated modality into their multifunctional nanoparticle that is either photothermal or photodynamic (or even both at the same time). This property of multifunctionality is one of the areas where the concepts of nanotechnology will be critical in further progress.

The use of active targeting moieties to direct PS-loaded nanoparticles to tumors or other biological targets is another rapidly growing area where nanotechnology may provide a distinct advantage over traditional conjugation methodology. If the targeting ligand (antibody, peptide, folate, aptamer, etc.) is attached directly to the PS, the number of PS that can be delivered to each tumor cell is limited. Note that a typical number of receptors per

tumor cell is about 100,000, and the number of PS needed to kill a cancer cell could be as high as 10^7. Therefore, each receptor might need to deliver as many as 100 PS molecules, and the best method of ensuring this ratio is to attach the targeting ligand to a nanoparticle loaded with PS.

The rapid growth in nanotechnology we have seen in the last decade is only going to further continue in the coming years, and we expect that the applications of nanotechnology to potentiate PDT will also continue to grow and become ever more convincing.

Acknowledgments

Research conducted in the Hamblin Laboratory is supported by NIH (RO1 AI050875 to MRH) and US Air Force MFEL Program (FA9550-04-1-0079). T.D. was partially supported by a Bullock-Wellman Fellowship Award and an Airlift Research Foundation Extremity Trauma Research Grant (grant 109421). L.Y.C. was supported by NIH grant 1R01CA137108.

References

1. Keene JP, Kessel D, Land EJ, Redmond RW, Truscott TG. Direct detection of singlet oxygen sensitized by haematoporphyrin and related compounds. Photochem Photobiol. 1986; 43:117–120. [PubMed: 3703952]
2. Damoiseau X, Schuitmaker HJ, Lagerberg JW, Hoebeke M. Increase of the photosensitizing efficiency of the bacteriochlorin a by liposome-incorporation. J Photochem Photobiol B. 2001; 60:50–60. [PubMed: 11386681]
3. Derycke AS, de Witte PA. Liposomes for photodynamic therapy. Adv Drug Deliv Rev. 2004; 56:17–30. [PubMed: 14706443]
4. Bangham AD. A correlation between surface charge and coagulant action of phospholipids. Nature. 1961; 192:1197–1198. [PubMed: 13864660]
5. Paszko E, Ehrhardt C, Senge MO, Kelleher DP, Reynolds JV. Nanodrug applications in photodynamic therapy. Photodiagnosis Photodyn Ther. 2011; 8:14–29. [PubMed: 21333931]
6. Kozlowska D, Foran P, MacMahon P, Shelly MJ, Eustace S, O'Kennedy R. Molecular and magnetic resonance imaging: the value of immunoliposomes. Adv Drug Deliv Rev. 2009; 61:1402–1411. [PubMed: 19796661]
7. Vemuri S, Rhodes CT. Preparation and characterization of liposomes as therapeutic delivery systems: a review. Pharm Acta Helv. 1995; 70:95–111. [PubMed: 7651973]
8. Samad A, Sultana Y, Aqil M. Liposomal drug delivery systems: an update review. Curr Drug Deliv. 2007; 4:297–305. [PubMed: 17979650]
9. Jiang F, Lilge L, Grenier J, Li Y, Wilson MD, Chopp M. Photodynamic therapy of U87 human glioma in nude rat using liposome-delivered Photofrin. Lasers Surg Med. 1998; 22:74–80. [PubMed: 9484699]
10. Jiang F, Lilge L, Logie B, Li Y, Chopp M. Photodynamic therapy of 9L gliosarcoma with liposome-delivered Photofrin. Photochem Photobiol. 1997; 65:701–706. [PubMed: 9114747]
11. Wang ZJ, He YY, Huang CG, Huang JS, Huang YC, An JY, Gu Y, Jiang LJ. Pharmacokinetics, tissue distribution and photodynamic therapy efficacy of liposomal-delivered hypocrellin A, a potential photosensitizer for tumor therapy. Photochem Photobiol. 1999; 70:773–780. [PubMed: 10568169]
12. Liu, R. Methods of making liposomes containing hydro-monobenzoporphyrin photosensitizer. U S Patent. 5707608. 1998.
13. Cruess AF, Zlateva G, Pleil AM, Wirostko B. Photodynamic therapy with verteporfin in age-related macular degeneration: a systematic review of efficacy, safety, treatment modifications and pharmacoeconomic properties. Acta Ophthalmol. 2009; 87:118–132. [PubMed: 18577193]

14. Isele U, van Hoogevest P, Leuenberger H, Capraro HG, Schieweck K. Pharmaceutical development of CGP 55847: a liposomal Zn-phthalocyanine formulation using a controlled organic solvent dilution method. Proc SPIE. 1994; 2078:397.
15. Ochsner M. Light scattering of human skin: a comparison between zinc (II)-phthalocyanine and Photofrin II. J Photochem Photobiol B. 1996; 32:3–9. [PubMed: 8725049]
16. Lasic DD, Martin FJ, Gabizon A, Huang SK, Papahadjopoulos D. Sterically stabilized liposomes: a hypothesis on the molecular origin of the extended circulation times. Biochim Biophys Acta. 1991; 1070:187–192. [PubMed: 1751525]
17. Moreira JN, Gaspar R, Allen TM. Targeting Stealth liposomes in a murine model of human small cell lung cancer. Biochim Biophys Acta. 2001; 1515:167–176. [PubMed: 11718672]
18. Needham D, McIntosh TJ, Lasic DD. Repulsive interactions and mechanical stability of polymer-grafted lipid membranes. Biochim Biophys Acta. 1992; 1108:40–48. [PubMed: 1643080]
19. Torchilin VP. Recent advances with liposomes as pharmaceutical carriers. Nat Rev Drug Discov. 2005; 4:145–160. [PubMed: 15688077]
20. Gijsens A, Derycke A, Missiaen L, De Vos D, Huwyler J, Eberle A, de Witte P. Targeting of the photocytotoxic compound AlPcS4 to Hela cells by transferrin conjugated PEG-liposomes. Int J Cancer. 2002; 101:78–85. [PubMed: 12209592]
21. Zuluaga MF, Mailhos C, Robinson G, Shima DT, Gurny R, Lange N. Synergies of VEGF inhibition and photodynamic therapy in the treatment of age-related macular degeneration. Invest Ophthalmol Vis Sci. 2007; 48:1767–1772. [PubMed: 17389510]
22. Bikram M, West JL. Thermo-responsive systems for controlled drug delivery. Expert Opin Drug Deliv. 2008; 5:1077–1091. [PubMed: 18817514]
23. Powell ME, Hill SA, Saunders MI, Hoskin PJ, Chaplin DJ. Human tumor blood flow is enhanced by nicotinamide and carbogen breathing. Cancer Res. 1997; 57:5261–5264. [PubMed: 9393746]
24. Oku N, Saito N, Namba Y, Tsukada H, Dolphin D, Okada S. Application of long-circulating liposomes to cancer photodynamic therapy. Biol Pharm Bull. 1997; 20:670–673. [PubMed: 9212988]
25. Bakowsky H, Richter T, Kneuer C, Hoekstra D, Rothe U, Bendas G, Ehrhardt C, Bakowsky U. Adhesion characteristics and stability assessment of lectin-modified liposomes for site-specific drug delivery. Biochim Biophys Acta. 2008; 1778:242–249. [PubMed: 17964278]
26. Mastrobattista E, Koning GA, Storm G. Immunoliposomes for the targeted delivery of antitumor drugs. Adv Drug Deliv Rev. 1999; 40:103–127. [PubMed: 10837783]
27. Sapra P, Allen TM. Internalizing antibodies are necessary for improved therapeutic efficacy of antibody-targeted liposomal drugs. Cancer Res. 2002; 62:7190–7194. [PubMed: 12499256]
28. Allen, TM.; Lopes de Menezes, D.; Hansen, CB.; Moase, EH. Stealth® liposomes for the targeting of drugs in cancer therapy. In: Gregoriadis, G., editor. Targeting of drugs 6: strategies for stealth therapeutic systems. Vol. 300. Plenum Press; New York: p. 61-75.
29. Tammela T, Saaristo A, Holopainen T, Yla-Herttuala S, Andersson LC, Virolainen S, Immonen I, Alitalo K. Photodynamic ablation of lymphatic vessels and intralymphatic cancer cells prevents metastasis. Sci Transl Med. 2011; 3:69ra11.
30. Nisnevitch M, Nakonechny F, Nitzan Y. Photodynamic antimicrobial chemotherapy by liposome-encapsulated water-soluble photosensitizers. Bioorg Khim. 2010; 36:396–402. [PubMed: 20644595]
31. Tsai T, Yang YT, Wang TH, Chien HF, Chen CT. Improved photodynamic inactivation of gram-positive bacteria using hematoporphyrin encapsulated in liposomes and micelles. Lasers Surg Med. 2009; 41:316–322. [PubMed: 19347938]
32. Bombelli C, Bordi F, Ferro S, Giansanti L, Jori G, Mancini G, Mazzuca C, Monti D, Ricchelli F, Sennato S, Venanzi M. New cationic liposomes as vehicles of m-tetrahydroxyphenylchlorin in photodynamic therapy of infectious diseases. Mol Pharm. 2008; 5:672–679. [PubMed: 18507469]
33. Ferro S, Ricchelli F, Monti D, Mancini G, Jori G. Efficient photoinactivation of methicillin-resistant Staphylococcus aureus by a novel porphyrin incorporated into a poly-cationic liposome. Int J Biochem Cell Biol. 2007; 39:1026–1034. [PubMed: 17387034]
34. Sharma SK, Dai T, Kharkwal GB, Huang YY, Huang L, De Arce VJ, Tegos GP, Hamblin MR. Drug discovery of antimicrobial photosensitizers using animal models. Curr Pharm Des. 2011

35. Longo JP, Leal SC, Simioni AR, de Fatima Menezes Almeida-Santos M, Tedesco AC, Azevedo RB. Photodynamic therapy disinfection of carious tissue mediated by aluminum-chloride-phthalocyanine entrapped in cationic liposomes: an in vitro and clinical study. Lasers Med Sci. 201110.1007/s10103-011-0962-6
36. Zhou S, Kawakami S, Yamashita F, Hashida M. Intranasal administration of CpG DNA lipoplex prevents pulmonary metastasis in mice. Cancer Lett. 2010; 287:75–81. [PubMed: 19660857]
37. Detty MR, Gibson SL, Wagner SJ. Current clinical and preclinical photosensitizers for use in photodynamic therapy. J Med Chem. 2004; 47:3897–3915.10.1007/s10103-011-0962-6 [PubMed: 15267226]
38. Shim G, Lee S, Kim YB, Kim CW, Oh YK. Enhanced tumor localization and retention of chlorin e6 in cationic nanolipoplexes potentiate the tumor ablation effects of photodynamic therapy. Nanotechnology. 2011; 22:365101. [PubMed: 21841215]
39. Santos-Magalhaes NS, Pontes A, Pereira VM, Caetano MN. Colloidal carriers for benzathine penicillin G: nanoemulsions and nanocapsules. Int J Pharm. 2000; 208:71–80. [PubMed: 11064213]
40. Tadros T, Izquierdo P, Esquena J, Solans C. Formation and stability of nano-emulsions. Adv Colloid Interface Sci. 2004; 108–109:303–318.
41. Junping W, Takayama K, Nagai T, Maitani Y. Pharmacokinetics and antitumor effects of vincristine carried by microemulsions composed of PEG-lipid, oleic acid, vitamin E and cholesterol. Int J Pharm. 2003; 251:13–21. [PubMed: 12527171]
42. Primo FL, Bentley MV, Tedesco AC. Photophysical studies and in vitro skin permeation/retention of Foscan/nanoemulsion (NE) applicable to photodynamic therapy skin cancer treatment. J Nanosci Nanotechnol. 2008; 8:340–347. [PubMed: 18468080]
43. Primo FL, Rodrigues MM, Simioni AR, Lacava ZG, Morais PC, Tedesco AC. Photosensitizer-loaded magnetic nanoemulsion for use in synergic photodynamic and magnetohyperthermia therapies of neoplastic cells. J Nanosci Nanotechnol. 2008; 8:5873–5877. [PubMed: 19198320]
44. Krammer B, Plaetzer K. ALA and its clinical impact, from bench to bedside. Photochem Photobiol Sci. 2008; 7:283–289. [PubMed: 18389144]
45. Donnelly RF, McCarron PA, Morrow DI, Sibani SA, Woolfson AD. Photosensitiser delivery for photodynamic therapy. Part 1: topical carrier platforms. Expert Opin Drug Deliv. 2008; 5:757–766. [PubMed: 18590460]
46. Maisch T, Santarelli F, Schreml S, Babilas P, Szeimies RM. Fluorescence induction of protoporphyrin IX by a new 5-aminolevulinic acid nanoemulsion used for photodynamic therapy in a full-thickness ex vivo skin model. Exp Dermatol. 2010; 19:e302–e305. [PubMed: 19845760]
47. Szeimies RM, Radny P, Sebastian M, Borrosch F, Dirschka T, Krahn-Senftleben G, Reich K, Pabst G, Voss D, Foguet M, Gahlmann R, Lubbert H, Reinhold U. Photodynamic therapy with BF-200 ALA for the treatment of actinic keratosis: results of a prospective, randomized, double-blind, placebo-controlled phase III study. Br J Dermatol. 2010; 163:386–394. [PubMed: 20518784]
48. Sengupta S, Eavarone D, Capila I, Zhao G, Watson N, Kiziltepe T, Sasisekharan R. Temporal targeting of tumour cells and neovasculature with a nanoscale delivery system. Nature. 2005; 436:568–572. [PubMed: 16049491]
49. Kerbel RS, Kamen BA. The anti-angiogenic basis of metronomic chemotherapy. Nat Rev Cancer. 2004; 4:423–436. [PubMed: 15170445]
50. Semenza GL. Surviving ischemia: adaptive responses mediated by hypoxia-inducible factor 1. J Clin Invest. 2000; 106:809–812. [PubMed: 11018065]
51. Lovell JF, Jin CS, Huynh E, Jin H, Kim C, Rubinstein JL, Chan WC, Cao W, Wang LV, Zheng G. Porphysome nanovesicles generated by porphyrin bilayers for use as multimodal biophotonic contrast agents. Nat Mater. 2011; 10:324–332. [PubMed: 21423187]
52. de Souza N. One particle to rule them all? Nat Methods. 2011; 8:370–371. [PubMed: 21678619]
53. Gaumet M, Vargas A, Gurny R, Delie F. Nanoparticles for drug delivery: the need for precision in reporting particle size parameters. Eur J Pharm Biopharm. 2008; 69:1–9. [PubMed: 17826969]
54. Maeda H. The enhanced permeability and retention (EPR) effect in tumor vasculature: the key role of tumor-selective macromolecular drug targeting. Adv Enzyme Regul. 2001; 41:189–207. [PubMed: 11384745]

55. Fadel M, Kassab K, Fadeel DA. Zinc phthalocyanine-loaded PLGA biodegradable nanoparticles for photodynamic therapy in tumor-bearing mice. Lasers Med Sci. 2010; 25:283–292. [PubMed: 19957005]
56. Qin M, Hah HJ, Kim G, Nie G, Lee YE, Kopelman R. Methylene blue covalently loaded polyacrylamide nanoparticles for enhanced tumor-targeted photodynamic therapy. Photochem Photobiol Sci. 2011; 10:832–841. [PubMed: 21479315]
57. Kopecek J, Kopeckova P, Minko T, Lu Z. HPMA copolymer-anticancer drug conjugates: design, activity and mechanism of action. Eur J Pharm Biopharm. 2000; 50:61–81. [PubMed: 10840193]
58. Battah S, Balaratnam S, Casas A, O'Neill S, Edwards C, Batlle A, Dobbin P, MacRobert AJ. Macromolecular delivery of 5-aminolaevulinic acid for photodynamic therapy using dendrimer conjugates. Mol Cancer Ther. 2007; 6:876–885. [PubMed: 17363482]
59. Hamblin MR, Miller JL, Rizvi I, Ortel B, Maytin EV, Hasan T. Pegylation of a chlorin(e6) polymer conjugate increases tumor targeting of photosensitizer. Cancer Res. 2001; 61:7155–7162. [PubMed: 11585749]
60. Lee SJ, Park K, Oh YK, Kwon SH, Her S, Kim IS, Choi K, Kim H, Lee SG, Kim K, Kwon IC. Tumor specificity and therapeutic efficacy of photosensitizer-encapsulated glycol chitosan-based nanoparticles in tumor-bearing mice. Biomaterials. 2009; 30:2929–2939. [PubMed: 19254811]
61. Panyam J, Labhasetwar V. Biodegradable nanoparticles for drug and gene delivery to cells and tissue. Adv Drug Deliv Rev. 2003; 55:329–347. [PubMed: 12628320]
62. Zeisser-Labouebe M, Lange N, Gurny R, Delie F. Hypericin-loaded nanoparticles for the photodynamic treatment of ovarian cancer. Int J Pharm. 2006; 326:174–181. [PubMed: 16930882]
63. Konan YN, Berton M, Gurny R, Allemann E. Enhanced photodynamic activity of meso-tetra(4-hydroxyphenyl)porphyrin by incorporation into sub-200 nm nanoparticles. Eur J Pharm Sci. 2003; 18:241–249. [PubMed: 12659935]
64. Konan-Kouakou YN, Boch R, Gurny R, Allemann E. In vitro and in vivo activities of verteporfin-loaded nanoparticles. J Control Release. 2005; 103:83–91. [PubMed: 15710502]
65. Vargas A, Eid M, Fanchaouy M, Gurny R, Delie F. In vivo photodynamic activity of photosensitizer-loaded nanoparticles: formulation properties, administration parameters and biological issues involved in PDT outcome. Eur J Pharm Biopharm. 2008; 69:43–53. [PubMed: 18023564]
66. Chatterjee DK, Fong LS, Zhang Y. Nanoparticles in photodynamic therapy: an emerging paradigm. Adv Drug Deliv Rev. 2008; 60:1627–1637. [PubMed: 18930086]
67. Shive MS, Anderson JM. Biodegradation and biocompatibility of PLA and PLGA microspheres. Adv Drug Deliv Rev. 1997; 28:5–24. [PubMed: 10837562]
68. Lee YE, Kopelman R. Polymeric nanoparticles for photodynamic therapy. Methods Mol Biol. 2011; 726:151–178. [PubMed: 21424449]
69. Cosmetic Ingredient Review Expert Panel. Amended final report on the safety assessment of polyacrylamide and acrylamide residues in cosmetics. Int J Toxicol. 2005; 24(Suppl 2):21–50. [PubMed: 16154914]
70. Koo YE, Reddy GR, Bhojani M, Schneider R, Philbert MA, Rehemtulla A, Ross BD, Kopelman R. Brain cancer diagnosis and therapy with nanoplatforms. Adv Drug Deliv Rev. 2006; 58:1556–1577. [PubMed: 17107738]
71. Tang W, Xu H, Park EJ, Philbert MA, Kopelman R. Encapsulation of methylene blue in polyacrylamide nanoparticle platforms protects its photodynamic effectiveness. Biochem Biophys Res Commun. 2008; 369:579–583. [PubMed: 18298950]
72. Tang W, Xu H, Kopelman R, Philbert MA. Photodynamic characterization and in vitro application of methylene blue-containing nanoparticle platforms. Photochem Photobiol. 2005; 81:242–249. [PubMed: 15595888]
73. Reddy GR, Bhojani MS, McConville P, Moody J, Moffat BA, Hall DE, Kim G, Koo YE, Woolliscroft MJ, Sugai JV, Johnson TD, Philbert MA, Kopelman R, Rehemtulla A, Ross BD. Vascular targeted nanoparticles for imaging and treatment of brain tumors. Clin Cancer Res. 2006; 12:6677–6686. [PubMed: 17121886]

74. Gao D, Xu H, Philbert MA, Kopelman R. Ultrafine hydrogel nanoparticles: synthetic approach and therapeutic application in living cells. Angew Chem Int Ed Engl. 2007; 46:2224–2227. [PubMed: 17310481]

75. Wu J, Xu H, Tang W, Kopelman R, Philbert MA, Xi C. Eradication of bacteria in suspension and biofilms using methylene blue-loaded dynamic nanoplatforms. Antimicrob Agents Chemother. 2009; 53:3042–3048. [PubMed: 19414585]

76. Krinick NL, Sun Y, Joyner D, Spikes JD, Straight RC, Kopecek J. A polymeric drug delivery system for the simultaneous delivery of drugs activatable by enzymes and/or light. J Biomater Sci Polym Ed. 1994; 5:303–324. [PubMed: 8025029]

77. Peterson CM, Lu JM, Sun Y, Peterson CA, Shiah JG, Straight RC, Kopecek J. Combination chemotherapy and photodynamic therapy with N-(2-hydroxypropyl) methacrylamide copolymer-bound anticancer drugs inhibit human ovarian carcinoma heterotransplanted in nude mice. Cancer Res. 1996; 56:3980–3985. [PubMed: 8752167]

78. Li WS, Aida T. Dendrimer porphyrins and phthalocyanines. Chem Rev. 2009; 109:6047–6076. [PubMed: 19769361]

79. Nishiyama N, Morimoto Y, Jang WD, Kataoka K. Design and development of dendrimer photosensitizer-incorporated polymeric micelles for enhanced photodynamic therapy. Adv Drug Deliv Rev. 2009; 61:327–338. [PubMed: 19385091]

80. Li Y, Jang WD, Nishiyama N, Kishimura A, Kawauchi S, Morimoto Y, Miake S, Yamashita T, Kikuchi M, Aida T, Kataoka K. Dendrimer generation effects on photodynamic efficacy of dendrimer porphyrins and dendrimer-loaded supramolecular nanocarriers. Chem Mater. 2007; 19:5557–5562.

81. Nishiyama N, Nakagishi Y, Morimoto Y, Lai PS, Miyazaki K, Urano K, Horie S, Kumagai M, Fukushima S, Cheng Y, Jang WD, Kikuchi M, Kataoka K. Enhanced photodynamic cancer treatment by supramolecular nanocarriers charged with dendrimer phthalocyanine. J Control Release. 2009; 133:245–251. [PubMed: 19000725]

82. Li, P.; Zhou, G.; Zhu, X.; Li, G.; Yan, P.; Shen, L.; Xu, Q.; Hamblin, MR. Photodynamic therapy with hyperbranched poly(ether-ester) chlorin(e6) nanoparticles on human tongue carcinoma Cal-27 cells. Photodiagnosis Photodyn Ther. 2011. http://dx.doi.org/10.1016/j.pdpdt.2011.08.001

83. Chen K, Preuss A, Hackbarth S, Wacker M, Langer K, Roder B. Novel photosensitizer-protein nanoparticles for photodynamic therapy: photophysical characterization and in vitro investigations. J Photochem Photobiol B. 2009; 96:66–74. [PubMed: 19442534]

84. Deda DK, Uchoa AF, Carita E, Baptista MS, Toma HE, Araki K. A new micro/nanoencapsulated porphyrin formulation for PDT treatment. Int J Pharm. 2009; 376:76–83. [PubMed: 19409465]

85. Labrude P, Becq C. Pharmacist and chemist Henri Braconnot. Rev Hist Pharm (Paris). 2003; 51:61–78. [PubMed: 12894794]

86. Nagpal K, Singh SK, Mishra DN. Chitosan nanoparticles: a promising system in novel drug delivery. Chem Pharm Bull (Tokyo). 2010; 58:1423–1430. [PubMed: 21048331]

87. Reza Saboktakin M, Tabatabaie RM, Maharramov A, Ali Ramazanov M. Synthesis and in vitro studies of biodegradable modified chitosan nanoparticles for photodynamic treatment of cancer. Int J Biol Macromol. 2011; 49:1059–1065. [PubMed: 21907233]

88. Lee SJ, Koo H, Jeong H, Huh MS, Choi Y, Jeong SY, Byun Y, Choi K, Kim K, Kwon IC. Comparative study of photosensitizer loaded and conjugated glycol chitosan nanoparticles for cancer therapy. J Control Release. 2011; 152:21–29. [PubMed: 21457740]

89. Lee SJ, Koo H, Lee DE, Min S, Lee S, Chen X, Choi Y, Leary JF, Park K, Jeong SY, Kwon IC, Kim K, Choi K. Tumor-homing photosensitizer-conjugated glycol chitosan nanoparticles for synchronous photodynamic imaging and therapy based on cellular on/off system. Biomaterials. 2011; 32:4021–4029. [PubMed: 21376388]

90. Henderson BW, Bellnier DA. Tissue localization of photosensitizers and the mechanism of photodynamic tissue destruction. Ciba Found Symp. 1989; 146:112–125. discussion 125–130. [PubMed: 2697528]

91. Allemann E, Rousseau J, Brasseur N, Kudrevich SV, Lewis K, van Lier JE. Photodynamic therapy of tumours with hexadecafluoro zinc phthalocynine formulated in PEG-coated poly(lactic acid) nanoparticles. Int J Cancer. 1996; 66:821–824. [PubMed: 8647656]

92. Hong S, Leroueil PR, Majoros IJ, Orr BG, Baker JR Jr, Banaszak Holl MM. The binding avidity of a nanoparticle-based multivalent targeted drug delivery platform. Chem Biol. 2007; 14:107–115. [PubMed: 17254956]

93. Torchilin VP. Targeted polymeric micelles for delivery of poorly soluble drugs. Cell Mol Life Sci. 2004; 61:2549–2559. [PubMed: 15526161]

94. van Nostrum CF. Polymeric micelles to deliver photosensitizers for photodynamic therapy. Adv Drug Deliv Rev. 2004; 56:9–16. [PubMed: 14706442]

95. Li B, Moriyama EH, Li F, Jarvi MT, Allen C, Wilson BC. Diblock copolymer micelles deliver hydrophobic protoporphyrin IX for photodynamic therapy. Photochem Photobiol. 2007; 83:1505–1512. [PubMed: 18028227]

96. Master AM, Rodriguez ME, Kenney ME, Oleinick NL, Gupta AS. Delivery of the photosensitizer Pc 4 in PEG-PCL micelles for in vitro PDT studies. J Pharm Sci. 2010; 99:2386–2398. [PubMed: 19967780]

97. Peng CL, Shieh MJ, Tsai MH, Chang CC, Lai PS. Self-assembledstar-shapedchlorin-corepoly(epsilon-caprolactone)-poly(ethylene glycol) diblock copolymer micelles for dual chemo-photodynamic therapies. Biomaterials. 2008; 29:3599–3608. [PubMed: 18572240]

98. Hofman JW, Carstens MG, van Zeeland F, Helwig C, Flesch FM, Hennink WE, van Nostrum CF. Photocytotoxicity of mTHPC (temoporfin) loaded polymeric micelles mediated by lipase catalyzed degradation. Pharm Res. 2008; 25:2065–2073. [PubMed: 18597164]

99. Knop K, Mingotaud AF, El-Akra N, Violleau F, Souchard JP. Monomeric pheophorbide(a)-containing poly(ethyleneglycol-b-epsilon-caprolactone) micelles for photodynamic therapy. Photochem Photobiol Sci. 2009; 8:396–404. [PubMed: 19255682]

100. Sugisaki K, Usui T, Nishiyama N, Jang WD, Yanagi Y, Yamagami S, Amano S, Kataoka K. Photodynamic therapy for corneal neovascularization using polymeric micelles encapsulating dendrimer porphyrins. Invest Ophthalmol Vis Sci. 2008; 49:894–899. [PubMed: 18326709]

101. Jang WD, Nakagishi Y, Nishiyama N, Kawauchi S, Morimoto Y, Kikuchi M, Kataoka K. Polyion complex micelles for photodynamic therapy: incorporation of dendritic photosensitizer excitable at long wavelength relevant to improved tissue-penetrating property. J Control Release. 2006; 113:73–79. [PubMed: 16701915]

102. Ding H, Sumer BD, Kessinger CW, Dong Y, Huang G, Boothman DA, Gao J. Nanoscopic micelle delivery improves the photophysical properties and efficacy of photodynamic therapy of protoporphyrin IX. J Control Release. 2011; 151:271–277. [PubMed: 21232562]

103. Ding H, Mora R, Gao J, Sumer BD. Characterization and optimization of mTHPP nanoparticles for photodynamic therapy of head and neck cancer. Otolaryngol Head Neck Surg. 2011; 145:612–617. [PubMed: 21727244]

104. Cohen EM, Ding H, Kessinger CW, Khemtong C, Gao J, Sumer BD. Polymeric micelle nanoparticles for photodynamic treatment of head and neck cancer cells. Otolaryngol Head Neck Surg. 2010; 143:109–115. [PubMed: 20620628]

105. Gallavardin T, Maurin M, Marotte S, Simon T, Gabudean AM, Bretonniere Y, Lindgren M, Lerouge F, Baldeck PL, Stephan O, Leverrier Y, Marvel J, Parola S, Maury O, Andraud C. Photodynamic therapy and two-photon bio-imaging applications of hydrophobic chromophores through amphiphilic polymer delivery. Photochem Photobiol Sci. 2011; 10:1216–1225. [PubMed: 21499638]

106. Chowdhary RK, Sharif I, Chansarkar N, Dolphin D, Ratkay L, Delaney S, Meadows H. Correlation of photosensitizer delivery to lipoproteins and efficacy in tumor and arthritis mouse models; comparison of lipid-based and Pluronic P123 formulations. J Pharm Pharm Sci. 2003; 6:198–204. [PubMed: 12935430]

107. Chung JE, Yokoyama M, Yamato M, Aoyagi T, Sakurai Y, Okano T. Thermo-responsive drug delivery from polymeric micelles constructed using block copolymers of poly(N-iso-propylacrylamide) and poly(butylmethacrylate). J Control Release. 1999; 62:115–127. [PubMed: 10518643]

108. Le Garrec D, Taillefer J, Van Lier JE, Lenaerts V, Leroux JC. Optimizing pH-responsive polymeric micelles for drug delivery in a cancer photodynamic therapy model. J Drug Target. 2002; 10:429–437. [PubMed: 12442814]

109. Koo H, Lee H, Lee S, Min KH, Kim MS, Lee DS, Choi Y, Kwon IC, Kim K, Jeong SY. In vivo tumor diagnosis and photodynamic therapy via tumoral pH-responsive polymeric micelles. Chem Commun (Camb). 2010; 46:5668–5670. [PubMed: 20623050]
110. Lukyanov AN, Torchilin VP. Micelles from lipid derivatives of water-soluble polymers as delivery systems for poorly soluble drugs. Adv Drug Deliv Rev. 2004; 56:1273–1289. [PubMed: 15109769]
111. Roby A, Erdogan S, Torchilin VP. Enhanced in vivo antitumor efficacy of poorly soluble PDT agent, meso-tetraphenylporphine, in PEG-PE-based tumor-targeted immunomicelles. Cancer Biol Ther. 2007; 6:1136–1142. [PubMed: 17611407]
112. Skidan I, Dholakia P, Torchilin V. Photodynamic therapy of experimental B-16 melanoma in mice with tumor-targeted 5,10,15,20-tetraphenylporphin-loaded PEG-PE micelles. J Drug Target. 2008; 16:486–493. [PubMed: 18604661]
113. Roby A, Erdogan S, Torchilin VP. Solubilization of poorly soluble PDT agent, meso-tetraphenylporphin, in plain or immunotargeted PEG-PE micelles results in dramatically improved cancer cell killing in vitro. Eur J Pharm Biopharm. 2006; 62:235–240. [PubMed: 16326084]
114. Zhang JX, Hansen CB, Allen TM, Boey A, Boch R. Lipid-derivatized poly(ethylene glycol) micellar formulations of benzoporphyrin derivatives. J Control Release. 2003; 86:323–338. [PubMed: 12526828]
115. Xu H, Jiang XJ, Chan EY, Fong WP, Ng DK. Synthesis, photophysical properties and in vitro photodynamic activity of axially substituted subphthalocyanines. Org Biomol Chem. 2007; 5:3987–3992. [PubMed: 18043804]
116. Feofanov A, Grichine A, Karmakova T, Pljutinskaya A, Lebedeva V, Filyasova A, Yakubovskaya R, Mironov A, Egret-Charlier M, Vigny P. Near-infrared photosensitizer based on a cycloimide derivative of chlorin p6: 13,15-N-(3′-hydroxypropyl)cycloimide chlorin p6. Photochem Photobiol. 2002; 75:633–643. [PubMed: 12081326]
117. Wohrle D, Muller S, Shopova M, Mantareva V, Spassova G, Vietri F, Ricchelli F, Jori G. Effect of delivery system on the pharmacokinetic and phototherapeutic properties of bis(methyloxyethyleneoxy) silicon-phthalocyanine in tumor-bearing mice. J Photochem Photobiol B. 1999; 50:124–128. [PubMed: 10515076]
118. Mroz P, Xia Y, Asanuma D, Konopko A, Zhiyentayev T, Huang YY, Sharma SK, Dai T, Khan UJ, Wharton T, Hamblin MR. Intraperitoneal photodynamic therapy mediated by a fullerene in a mouse model of abdominal dissemination of colon adeno-carcinoma. Nanomedicine. 2011; 7:965–974. [PubMed: 21645643]
119. Woodburn K, Chang CK, Lee S, Henderson B, Kessel D. Biodistribution and PDT efficacy of a ketochlorin photosensitizer as a function of the delivery vehicle. Photochem Photobiol. 1994; 60:154–159. [PubMed: 7938213]
120. Couleaud P, Morosini V, Frochot C, Richeter S, Raehm L, Durand JO. Silica-based nanoparticles for photodynamic therapy applications. Nanoscale. 2010; 2:1083–1095. [PubMed: 20648332]
121. Walter WG, Stober A. Probe method for the microbial sampling of hospital carpets. Health Lab Sci. 1968; 5:162–170. [PubMed: 5671179]
122. Brevet D, Gary-Bobo M, Raehm L, Richeter S, Hocine O, Amro K, Loock B, Couleaud P, Frochot C, Morere A, Maillard P, Garcia M, Durand JO. Mannose-targeted mesoporous silica nanoparticles for photodynamic therapy. Chem Commun (Camb). 2009:1475–1477. [PubMed: 19277361]
123. Cheng YC, Samia A, Meyers JD, Panagopoulos I, Fei B, Burda C. Highly efficient drug delivery with gold nanoparticle vectors for in vivo photodynamic therapy of cancer. J Am Chem Soc. 2008; 130:10643–10647. [PubMed: 18642918]
124. Roy I, Ohulchanskyy TY, Pudavar HE, Bergey EJ, Oseroff AR, Morgan J, Dougherty TJ, Prasad PN. Ceramic-based nanoparticles entrapping water-insoluble photosensitizing anticancer drugs: a novel drug-carrier system for photodynamic therapy. J Am Chem Soc. 2003; 125:7860–7865. [PubMed: 12823004]

125. Ohulchanskyy TY, Roy I, Goswami LN, Chen Y, Bergey EJ, Pandey RK, Oseroff AR, Prasad PN. Organically modified silica nanoparticles with covalently incorporated photosensitizer for photodynamic therapy of cancer. Nano Lett. 2007; 7:2835–2842. [PubMed: 17718587]

126. Hocine O, Gary-Bobo M, Brevet D, Maynadier M, Fontanel S, Raehm L, Richeter S, Loock B, Couleaud P, Frochot C, Charnay C, Derrien G, Smaihi M, Sahmoune A, Morere A, Maillard P, Garcia M, Durand JO. Silicalites and mesoporous silica nanoparticles for photodynamic therapy. Int J Pharm. 2010; 402:221–230. [PubMed: 20934496]

127. Yan F, Kopelman R. The embedding of meta-tetra(hydroxyphenyl)-chlorin into silica nanoparticle platforms for photodynamic therapy and their singlet oxygen production and pH-dependent optical properties. Photochem Photobiol. 2003; 78:587–591. [PubMed: 14743867]

128. Qian HS, Guo HC, Ho PC, Mahendran R, Zhang Y. Mesoporous-silica-coated up-conversion fluorescent nanoparticles for photodynamic therapy. Small. 2009; 5:2285–2290. [PubMed: 19598161]

129. Zhou L, Ning YW, Wei SH, Feng YY, Zhou JH, Yu BY, Shen J. A nanoencapsulated hypocrellin A prepared by an improved microemulsion method for photodynamic treatment. J Mater Sci Mater Med. 2010; 21:2095–2101. [PubMed: 20364361]

130. Qian J, Gharibi A, He S. Colloidal mesoporous silica nanoparticles with protoporphyrin IX encapsulated for photodynamic therapy. J Biomed Opt. 2009; 14:014012. [PubMed: 19256700]

131. Simon V, Devaux C, Darmon A, Donnet T, Thienot E, Germain M, Honnorat J, Duval A, Pottier A, Borghi E, Levy L, Marill J. Pp IX silica nanoparticles demonstrate differential interactions with in vitro tumor cell lines and in vivo mouse models of human cancers. Photochem Photobiol. 2010; 86:213–222. [PubMed: 19769577]

132. Tu HL, Lin YS, Lin HY, Hung Y, Lo LW, Chen YF, Mou CY. In vitro studies of functionalized mesoporous silica nanoparticles for photodynamic therapy. Adv Mater. 2009; 21:172–177.

133. Cheng SH, Lee CH, Yang CS, Tseng FG, Mou CY, Lo LW. Mesoporous silica nanoparticles functionalized with an oxygen-sensing probe for cell photodynamic therapy: potential cancer theranostics. J Mater Chem. 2009; 19:1252–1257.

134. Rossi LM, Silva PR, Vono LL, Fernandes AU, Tada DB, Baptista MS. Protoporphyrin IX nanoparticle carrier: preparation, optical properties and singlet oxygen generation. Langmuir. 2008; 24:12534–12538. [PubMed: 18834155]

135. Liu F, Zhou X, Chen Z, Huang P, Wang X, Zhou Y. Preparation of purpurin-18 loaded magnetic nanocarriers in cottonseed oil for photodynamic therapy. Mater Lett. 2008; 62:2844–2847.

136. Chen ZL, Sun Y, Huang P, Yang XX, Zhou XP. Studies on Preparation of photosensitizer loaded magnetic silica nanoparticles and their anti-tumor effects for targeting photodynamic therapy. Nanoscale Res Lett. 2009; 4:400–408. [PubMed: 20596490]

137. Wieder ME, Hone DC, Cook MJ, Handsley MM, Gavrilovic J, Russell DA. Intracellular photodynamic therapy with photosensitizer-nanoparticle conjugates: cancer therapy using a ‘Trojan horse’. Photochem Photobiol Sci. 2006; 5:727–734. [PubMed: 16886087]

138. Gu H, Xu K, Yang Z, Chang CK, Xu B. Synthesis and cellular uptake of porphyrin decorated iron oxide nanoparticles – a potential candidate for bimodal anticancer therapy. Chem Commun (Camb). 2005:4270–4272. [PubMed: 16113718]

139. Chen W, Zhang J. Using nanoparticles to enable simultaneous radiation and photodynamic therapies for cancer treatment. J Nanosci Nanotechnol. 2006; 6:1159–1166. [PubMed: 16736782]

140. Elbakry A, Zaky A, Liebl R, Rachel R, Goepferich A, Breunig M. Layer-by-layer assembled gold nanoparticles for siRNA delivery. Nano Lett. 2009; 9:2059–2064. [PubMed: 19331425]

141. Jain PK, Huang X, El-Sayed IH, El-Sayed MA. Noble metals on the nanoscale: optical and photothermal properties and some applications in imaging, sensing, biology and medicine. Acc Chem Res. 2008; 41:1578–1586. [PubMed: 18447366]

142. Gao J, Gu H, Xu B. Multifunctional magnetic nanoparticles: design, synthesis and biomedical applications. Acc Chem Res. 2009; 42:1097–1107. [PubMed: 19476332]

143. Paciotti GF, Myer L, Weinreich D, Goia D, Pavel N, McLaughlin RE, Tamarkin L. Colloidal gold: a novel nanoparticle vector for tumor directed drug delivery. Drug Deliv. 2004; 11:169–183. [PubMed: 15204636]

144. Boisselier E, Astruc D. Gold nanoparticles in nanomedicine: preparations, imaging, diagnostics, therapies and toxicity. Chem Soc Rev. 2009; 38:1759–1782. [PubMed: 19587967]

145. Gamaleia NF, Shishko ED, Dolinsky GA, Shcherbakov AB, Usatenko AV, Kholin VV. Photodynamic activity of hematoporphyrin conjugates with gold nanoparticles: experiments in vitro. Exp Oncol. 2010; 32:44–47. [PubMed: 20332758]

146. Zaruba K, Kralova J, Rezanka P, Pouckova P, Veverkova L, Kral V. Modified porphyrin-brucine conjugated to gold nanoparticles and their application in photodynamic therapy. Org Biomol Chem. 2010; 8:3202–3206. [PubMed: 20485822]

147. Demberelnyamba D, Ariunaa M, Shim YK. Newly synthesized water soluble cholinium-purpurin photosensitizers and their stabilized gold nanoparticles as promising anticancer agents. Int J Mol Sci. 2008; 9:864–871. [PubMed: 19325790]

148. Loo C, Lowery A, Halas N, West J, Drezek R. Immunotargeted nanoshells for integrated cancer imaging and therapy. Nano Lett. 2005; 5:709–711. [PubMed: 15826113]

149. Connor EE, Mwamuka J, Gole A, Murphy CJ, Wyatt MD. Gold nanoparticles are taken up by human cells but do not cause acute cytotoxicity. Small. 2005; 1:325–327. [PubMed: 17193451]

150. Cheng Y, Meyers JD, Broome AM, Kenney ME, Basilion JP, Burda C. Deep penetration of a PDT drug into tumors by noncovalent drug-gold nanoparticle conjugates. J Am Chem Soc. 2011; 133:2583–2591. [PubMed: 21294543]

151. Liu Y, Shipton MK, Ryan J, Kaufman ED, Franzen S, Feldheim DL. Synthesis, stability and cellular internalization of gold nanoparticles containing mixed peptide-poly(ethylene glycol) monolayers. Anal Chem. 2007; 79:2221–2229. [PubMed: 17288407]

152. Greenwald RB, Choe YH, McGuire J, Conover CD. Effective drug delivery by PEGylated drug conjugates. Adv Drug Deliv Rev. 2003; 55:217–250. [PubMed: 12564978]

153. Cheng Y, Samia AC, Li J, Kenney ME, Resnick A, Burda C. Delivery and efficacy of a cancer drug as a function of the bond to the gold nanoparticle surface. Langmuir. 2010; 26:2248–2255. [PubMed: 19719162]

154. Csaki A, Schneider T, Wirth J, Jahr N, Steinbruck A, Stranik O, Garwe F, Muller R, Fritzsche W. Molecular plasmonics: light meets molecules at the nanoscale. Philos Transact A Math Phys Eng Sci. 2011; 369:3483–3496.

155. Fales AM, Yuan H, Vo-Dinh T. Silica-coated gold nanostars for combined surface-enhanced Raman scattering (SERS) detection and singlet-oxygen generation: a potential nanoplatform for theranostics. Langmuir. 2011; 27:12186–12190. [PubMed: 21859159]

156. Khlebtsov B, Panfilova E, Khanadeev V, Bibikova O, Terentyuk G, Ivanov A, Rumyantseva V, Shilov I, Ryabova A, Loshchenov V, Khlebtsov NG. Nanocomposites containing silica-coated gold-silver nanocages and Yb-2,4-dimethoxyhematoporphyrin: multifunctional capability of IR-luminescence detection, photosensitization and photothermolysis. ACS Nano. 2011; 5:7077–7089. [PubMed: 21838309]

157. Lipovsky A, Gedanken A, Nitzan Y, Lubart R. Enhanced inactivation of bacteria by metal-oxide nanoparticles combined with visible light irradiation. Lasers Surg Med. 2011; 43:236–240. [PubMed: 21412807]

158. Konaka R, Kasahara E, Dunlap WC, Yamamoto Y, Chien KC, Inoue M. Irradiation of titanium dioxide generates both singlet oxygen and superoxide anion. Free Radic Biol Med. 1999; 27:294–300. [PubMed: 10468201]

159. Konaka R, Kasahara E, Dunlap WC, Yamamoto Y, Chien KC, Inoue M. Ultraviolet irradiation of titanium dioxide in aqueous dispersion generates singlet oxygen. Redox Rep. 2001; 6:319–325. [PubMed: 11778850]

160. Rehman S, Ullah R, Butt AM, Gohar ND. Strategies of making TiO_2 and ZnO visible light active. J Hazard Mater. 2009; 170:560–569. [PubMed: 19540666]

161. Zhang H, Chen B, Jiang H, Wang C, Wang H, Wang X. A strategy for ZnO nanorod mediated multi-mode cancer treatment. Biomaterials. 2011; 32:1906–1914. [PubMed: 21145104]

162. Foster HA, Ditta IB, Varghese S, Steele A. Photocatalytic disinfection using titanium dioxide: spectrum and mechanism of antimicrobial activity. Appl Microbiol Biotechnol. 2011; 90:1847–1868. [PubMed: 21523480]

163. Yamaguchi S, Kobayashi H, Narita T, Kanehira K, Sonezaki S, Kubota Y, Terasaka S, Iwasaki Y. Novel photodynamic therapy using water-dispersed TiO_2-polyethylene glycol compound: evaluation of antitumor effect on glioma cells and spheroids in vitro. Photochem Photobiol. 2010; 86:964–971. [PubMed: 20492566]
164. Zhang AP, Sun YP. Photocatalytic killing effect of TiO_2 nano- particles on Ls-174-t human colon carcinoma cells. World J Gastroenterol. 2004; 10:3191–3193. [PubMed: 15457572]
165. Wang C, Cao S, Tie X, Qiu B, Wu A, Zheng Z. Induction of cytotoxicity by photoexcitation of TiO_2 can prolong survival in glioma-bearing mice. Mol Biol Rep. 2011; 38:523–530. [PubMed: 20352345]
166. Bakalova R, Ohba H, Zhelev Z, Ishikawa M, Baba Y. Quantum dots as photosensitizers? Nat Biotechnol. 2004; 22:1360–1361. [PubMed: 15529155]
167. Samia AC, Chen X, Burda C. Semiconductor quantum dots for photodynamic therapy. J Am Chem Soc. 2003; 125:15736–15737. [PubMed: 14677951]
168. Baron ED, Malbasa CL, Santo-Domingo D, Fu P, Miller JD, Hanneman KK, Hsia AH, Oleinick NL, Colussi VC, Cooper KD. Silicon phthalocyanine (Pc 4) photodynamic therapy is a safe modality for cutaneous neoplasms: results of a phase 1 clinical trial. Lasers Surg Med. 2010; 42:728–735. [PubMed: 21246576]
169. He J, Larkin HE, Li YS, Rihter D, Zaidi SI, Rodgers MA, Mukhtar H, Kenney ME, Oleinick NL. The synthesis, photophysical and photobiological properties and in vitro structure-activity relationships of a set of silicon phthalocyanine PDT photosensitizers. Photochem Photobiol. 1997; 65:581–586. [PubMed: 9077144]
170. Jose R, Zhelev Z, Nagase T, Bakalova R, Baba Y, Ishikawa M. Self-surface passivation of CdX (X=Se, Te) quantum dots. J Nanosci Nanotechnol. 2006; 6:618–623. [PubMed: 16573112]
171. Generalov R, Kavaliauskiene S, Westrom S, Chen W, Kristensen S, Juzenas P. Entrapment in phospholipid vesicles quenches photoactivity of quantum dots. Int J Nanomed. 2011; 6:1875–1888.
172. Morosini V, Bastogne T, Frochot C, Schneider R, Francois A, Guillemin F, Barberi-Heyob M. Quantum dot-folic acid conjugates as potential photosensitizers in photodynamic therapy of cancer. Photochem Photobiol Sci. 2011; 10:842–851. [PubMed: 21479314]
173. Mroz P, Pawlak A, Satti M, Lee H, Wharton T, Gali H, Sarna T, Hamblin MR. Functionalized fullerenes mediate photodynamic killing of cancer cells: type I versus type II photochemical mechanism. Free Radic Biol Med. 2007; 43:711–719. [PubMed: 17664135]
174. Chiang LY, Padmawar PA, Rogers-Haley JE, So G, Canteenwala T, Thota S, Tan LS, Pritzker K, Huang YY, Sharma SK, Kurup DB, Hamblin MR, Wilson B, Urbas A. Synthesis and characterization of highly photoresponsive fullerenyl dyads with a close chromophore antenna-C(60) contact and effective photodynamic potential. J Mater Chem. 2010; 20:5280–5293. [PubMed: 20890406]
175. Tegos GP, Demidova TN, Arcila-Lopez D, Lee H, Wharton T, Gali H, Hamblin MR. Cationic fullerenes are effective and selective antimicrobial photosensitizers. Chem Biol. 2005; 12:1127–1135. [PubMed: 16242655]
176. Lu Z, Dai T, Huang L, Kurup DB, Tegos GP, Jahnke A, Wharton T, Hamblin MR. Photodynamic therapy with a cationic functionalized fullerene rescues mice from fatal wound infections. Nanomedicine (Lond). 2010; 5:1525–1533. [PubMed: 21143031]
177. Chi Y, Canteenwala T, Chen HC, Chen BJ, Canteenwala M, Chiang LY. Hexa(sulfobutyl)fullerene-induced photodynamic effect on tumors in vivo and toxicity study in rats. Proc Electrochem Soc. 1999; 99:234–249.
178. Hotze EM, Labille J, Alvarez P, Wiesner MR. Mechanisms of photochemistry and reactive oxygen production by fullerene suspensions in water. Environ Sci Technol. 2008; 42:4175–4180. [PubMed: 18589984]
179. Duncan LK, Jinschek JR, Vikesland PJ. C60 colloid formation in aqueous systems: effects of preparation method on size, structure and surface charge. Environ Sci Technol. 2008; 42:173–178. [PubMed: 18350893]
180. Culotta L, Koshland DE Jr. Buckyballs: wide open playing field for chemists. Science. 1991; 254:1706–1709. [PubMed: 17829222]

181. Kato S, Aoshima H, Saitoh Y, Miwa N. Biological safety of liposome-fullerene consisting of hydrogenated lecithin, glycine soja sterols and fullerene-C60 upon photocytotoxicity and bacterial reverse mutagenicity. Toxicol Ind Health. 2009; 25:197–203. [PubMed: 19482914]

182. Kato S, Aoshima H, Saitoh Y, Miwa N. Fullerene-C60/lipo-some complex: defensive effects against uva-induced damages in skin structure, nucleus and collagen type I/IV fibrils and the permeability into human skin tissue. J Photochem Photobiol B. 2009; 98:99–105. [PubMed: 20036139]

183. Doi Y, Ikeda A, Akiyama M, Nagano M, Shigematsu T, Ogawa T, Takeya T, Nagasaki T. Intracellular uptake and photodynamic activity of water-soluble [60]- and [70]fullerenes incorporated in liposomes. Chemistry. 2008; 14:8892–8897. [PubMed: 18698574]

184. Yan A, Von Dem Bussche A, Kane AB, Hurt RH. Tocopheryl polyethylene glycol succinate as a safe, antioxidant surfactant for processing carbon nanotubes and fullerenes. Carbon NY. 2007; 45:2463–2470.

185. Akiyama M, Ikeda A, Shintani T, Doi Y, Kikuchi J, Ogawa T, Yogo K, Takeya T, Yamamoto N. Solubilisation of [60]fullerenes using block copolymers and evaluation of their photodynamic activities. Org Biomol Chem. 2008; 6:1015–1019. [PubMed: 18327326]

186. Kojima C, Toi Y, Harada A, Kono K. Aqueous solubilization of fullerenes using poly(amidoamine) dendrimers bearing cyclodextrin and poly(ethylene glycol). Bioconjug Chem. 2008; 19:2280–2284. [PubMed: 18844391]

187. Pan B, Cui D, Xu P, Ozkan C, Feng G, Ozkan M, Huang T, Chu B, Li Q, He R, Hu G. Synthesis and characterization of polyamidoamine dendrimer-coated multi-walled carbon nanotubes and their application in gene delivery systems. Nanotechnology. 2009; 20:125101. [PubMed: 19420458]

188. Hooper JB, Bedrov D, Smith GD. Supramolecular self-organization in PEO-modified C60 fullerene/water solutions: influence of polymer molecular weight and nanoparticle concentration. Langmuir. 2008; 24:4550–4557. [PubMed: 18402490]

189. Nitta N, Seko A, Sonoda A, Ohta S, Tanaka T, Takahashi M, Murata K, Takemura S, Sakamoto T, Tabata Y. Is the use of fullerene in photodynamic therapy effective for atherosclerosis? Cardiovasc Intervent Radiol. 2008; 31:359–366. [PubMed: 18040738]

190. Liu J, Ohta S, Sonoda A, Yamada M, Yamamoto M, Nitta N, Murata K, Tabata Y. Preparation of PEG-conjugated fullerene containing Gd3+ ions for photodynamic therapy. J Control Release. 2007; 117:104–110. [PubMed: 17156882]

191. Tabata Y, Murakami Y, Ikada Y. Photodynamic effect of polyethylene glycol-modified fullerene on tumor. Jpn J Cancer Res. 1997; 88:1108–1116. [PubMed: 9439687]

192. Filippone S, Heimann F, Rassat A. A highly water-soluble 2:1 beta-cyclodextrin-fullerene conjugate. Chem Commun (Camb). 2002:1508–1509. [PubMed: 12189867]

193. Zhao B, He YY, Bilski PJ, Chignell CF. Pristine (C60) and hydroxylated [C60(OH)24] fullerene phototoxicity towards HaCaT keratinocytes: type I vs type II mechanisms. Chem Res Toxicol. 2008; 21:1056–1063. [PubMed: 18422350]

194. Bansal T, Mustafa G, Khan ZI, Ahmad FJ, Khar RK, Talegaonkar S. Solid self-nanoemulsifying delivery systems as a platform technology for formulation of poorly soluble drugs. Crit Rev Ther Drug Carrier Syst. 2008; 25:63–116. [PubMed: 18540836]

195. Bali V, Ali M, Ali J. Novel nanoemulsion for minimizing variations in bioavailability of ezetimibe. J Drug Target. 2010; 18:506–519. [PubMed: 20067438]

196. Amani A, York P, Chrystyn H, Clark BJ. Factors affecting the stability of nanoemulsions – use of artificial neural networks. Pharm Res. 2010; 27:37–45. [PubMed: 19908130]

197. Shakeel F, Faisal MS. Nanoemulsion: a promising tool for solubility and dissolution enhancement of celecoxib. Pharm Dev Technol. 2009; 15:53–56. [PubMed: 19552546]

198. Boyd PD, Reed CA. Fullerene-porphyrin constructs. Acc Chem Res. 2005; 38:235–242. [PubMed: 15835870]

199. El-Khouly ME, Araki Y, Ito O, Gadde S, McCarty AL, Karr PA, Zandler ME, D'Souza F. Spectral, electrochemical and photophysical studies of a magnesium porphyrin-fullerene dyad. Phys Chem Chem Phys. 2005; 7:3163–3171. [PubMed: 16240027]

200. Imahori H. Porphyrin-fullerene linked systems as artificial photosynthetic mimics. Org Biomol Chem. 2004; 2:1425–1433. [PubMed: 15136797]

201. Schuster DI, Cheng P, Jarowski PD, Guldi DM, Luo C, Echegoyen L, Pyo S, Holzwarth AR, Braslavsky SE, Williams RM, Klihm G. Design, synthesis and photophysical studies of a porphyrin-fullerene dyad with parachute topology; charge recombination in the marcus inverted region. J Am Chem Soc. 2004; 126:7257–7270. [PubMed: 15186163]

202. Vail SA, Schuster DI, Guldi DM, Isosomppi M, Tkachenko N, Lemmetyinen H, Palkar A, Echegoyen L, Chen X, Zhang JZ. Energy and electron transfer in beta-alkynyl-linked porphyrin-[60]fullerene dyads. J Phys Chem B. 2006; 110:14155–14166. [PubMed: 16854114]

203. Gebhart SC, Lin WC, Mahadevan-Jansen A. In vitro determination of normal and neoplastic human brain tissue optical properties using inverse adding-doubling. Phys Med Biol. 2006; 51:2011–2027. [PubMed: 16585842]

204. Tuchin VV, Wang RK, Yeh AT. Optical clearing of tissues and cells. J Biomed Opt. 2008; 13:021101. [PubMed: 18465950]

205. Hirshburg J, Choi B, Nelson JS, Yeh AT. Correlation between collagen solubility and skin optical clearing using sugars. Lasers Surg Med. 2007; 39:140–144. [PubMed: 17311267]

206. Jiang J, Boese M, Turner P, Wang RK. Penetration kinetics of dimethyl sulphoxide and glycerol in dynamic optical clearing of porcine skin tissue in vitro studied by Fourier transform infrared spectroscopic imaging. J Biomed Opt. 2008; 13:021105. [PubMed: 18465954]

207. Kogan A, Garti N. Microemulsions as transdermal drug delivery vehicles. Adv Colloid Interface Sci. 2006; 123–126:369–385.

208. Goeppert-Mayer M. Über Elementarakte mit zwei Quantens-prüngen. Ann Phys. 1931; 9:273–295.

209. Bhawalkar JD, Kumar ND, Zhao CF, Prasad PN. Two-photon photodynamic therapy. J Clin Laser Med Surg. 1997; 15:201–204. [PubMed: 9612170]

210. Karotki A, Khurana M, Lepock JR, Wilson BC. Simultaneous two-photon excitation of Photofrin in relation to photodynamic therapy. Photochem Photobiol. 2006; 82:443–452. [PubMed: 16613497]

211. Samkoe KS, Clancy AA, Karotki A, Wilson BC, Cramb DT. Complete blood vessel occlusion in the chick chorioallantoic membrane using two-photon excitation photodynamic therapy: implications for treatment of wet age-related macular degeneration. J Biomed Opt. 2007; 12:034025. [PubMed: 17614733]

212. Samkoe KS, Cramb DT. Application of an ex ovo chicken chorioallantoic membrane model for two-photon excitation photodynamic therapy of age-related macular degeneration. J Biomed Opt. 2003; 8:410–417. [PubMed: 12880346]

213. Lens M, Medenica L, Citernesi U. Antioxidative capacity of C(60) (buckminsterfullerene) and newly synthesized fulleropyrrolidine derivatives encapsulated in liposomes. Biotechnol Appl Biochem. 2008; 51:135–140. [PubMed: 18257745]

214. Spohn P, Hirsch C, Hasler F, Bruinink A, Krug HF, Wick P. C60 fullerene: a powerful antioxidant, or a damaging agent? The importance of an in-depth material characterization prior to toxicity assays. Environ Pollut. 2009; 157:1134–1139. [PubMed: 18824284]

215. Cai X, Jia H, Liu Z, Hou B, Luo C, Feng Z, Li W, Liu J. Polyhydroxylated fullerene derivative C(60)(OH)(24) prevents mitochondrial dysfunction and oxidative damage in an MPP(+)-induced cellular model of Parkinson's disease. J Neurosci Res. 2008; 86:3622–3634. [PubMed: 18709653]

216. Gharbi N, Pressac M, Hadchouel M, Szwarc H, Wilson SR, Moussa F. 60]fullerene is a powerful antioxidant in vivo with no acute or subacute toxicity. Nano Lett. 2005; 5:2578–2585. [PubMed: 16351219]

217. Dugan LL, Gabrielsen JK, Yu SP, Lin TS, Choi DW. Buckminsterfullerenol free radical scavengers reduce excitotoxic and apoptotic death of cultured cortical neurons. Neurobiol Dis. 1996; 3:129–135. [PubMed: 9173920]

218. Andrievsky GV, Bruskov VI, Tykhomyrov AA, Gudkov SV. Peculiarities of the antioxidant and radioprotective effects of hydrated C60 fullerene nanostuctures in vitro and in vivo. Free Radic Biol Med. 2009; 47:786–793. [PubMed: 19539750]

219. Weiss DR, Raschke TM, Levitt M. How hydrophobic buck-minsterfullerene affects surrounding water structure. J Phys Chem B. 2008; 112:2981–2990. [PubMed: 18275178]
220. Mroz P, Tegos GP, Gali H, Wharton T, Sarna T, Hamblin MR. Photodynamic therapy with fullerenes. Photochem Photobiol Sci. 2007; 6:1139–1149. [PubMed: 17973044]
221. Sharma SK, Chiang LY, Hamblin MR. Photodynamic therapy with fullerenes in vivo: reality or a dream? Nanomedicine (UK). 2011; 6:1813–1825.
222. Tokuyama H, Yamago S, Nakamura E. Photoinduced biochemical activity of fullerene carboxylic acid. J Am Chem Soc. 1993; 115:7918–7919.
223. Rancan F, Rosan S, Boehm F, Cantrell A, Brellreich M, Schoenberger H, Hirsch A, Moussa F. Cytotoxicity and photo-cytotoxicity of a dendritic C(60) mono-adduct and a malonic acid C(60) tris-adduct on Jurkat cells. J Photochem Photobiol B. 2002; 67:157–162. [PubMed: 12167314]
224. Burlaka AP, Sidorik YP, Prylutska SV, Matyshevska OP, Golub OA, Prylutskyy YI, Scharff P. Catalytic system of the reactive oxygen species on the C60 fullerene basis. Exp Oncol. 2004; 26:326–327. [PubMed: 15627068]
225. Yang XL, Fan CH, Zhu HS. Photo-induced cytotoxicity of malonic acid [C(60)]fullerene derivatives and its mechanism. Toxicol In Vitro. 2002; 16:41–46. [PubMed: 11812638]
226. Spesia MB, Milanesio ME, Durantini EN. Synthesis, properties and photodynamic inactivation of Escherichia coli by novel cationic fullerene C60 derivatives. Eur J Med Chem. 2008; 43:853–861. [PubMed: 17706838]
227. Lee I, Mackeyev Y, Cho M, Li D, Kim JH, Wilson LJ, Alvarez PJ. Photochemical and antimicrobial properties of novel C60 derivatives in aqueous systems. Environ Sci Technol. 2009; 43:6604–6610. [PubMed: 19764224]
228. Huang L, Terakawa M, Zhiyentayev T, Huang YY, Sawayama Y, Jahnke A, Tegos GP, Wharton T, Hamblin MR. Innovative cationic fullerenes as broad-spectrum light-activated antimicrobials. Nanomedicine. 2009; 6:442–452. [PubMed: 19914400]
229. Ikeda A, Doi Y, Nishiguchi K, Kitamura K, Hashizume M, Kikuchi J, Yogo K, Ogawa T, Takeya T. Induction of cell death by photodynamic therapy with water-soluble lipid-membrane-incorporated [60]fullerene. Org Biomol Chem. 2007; 5:1158–1160. [PubMed: 17406710]
230. Ikeda A, Matsumoto M, Akiyama M, Kikuchi J, Ogawa T, Takeya T. Direct and short-time uptake of [70]fullerene into the cell membrane using an exchange reaction from a [70]fullerene-gamma-cyclodextrin complex and the resulting photodynamic activity. Chem Commun (Camb). 2009:1547–1549. [PubMed: 19277385]
231. Ikeda A, Nagano M, Akiyama M, Matsumoto M, Ito S, Mukai M, Hashizume M, Kikuchi J, Katagiri K, Ogawa T, Takeya T. Photodynamic activity of C70 caged within surface-cross-linked liposomes. Chem Asian J. 2009; 4:199–205. [PubMed: 18830979]
232. Wang X, Li Q, Xie J, Jin Z, Wang J, Li Y, Jiang K, Fan S. Fabrication of ultralong and electrically uniform single-walled carbon nanotubes on clean substrates. Nano Lett. 2009; 9:3137–3141. [PubMed: 19650638]
233. Zhu Z, Tang Z, Phillips JA, Yang R, Wang H, Tan W. Regulation of singlet oxygen generation using single-walled carbon nanotubes. J Am Chem Soc. 2008; 130:10856–10857. [PubMed: 18661988]
234. Erbas S, Gorgulu A, Kocakusakogullari M, Akkaya EU. Non-covalent functionalized SWNTs as delivery agents for novel Bodipy-based potential PDT sensitizers. Chem Commun (Camb). 2009:4956–4958. [PubMed: 19668814]
235. Shiraki T, Dawn A, Le TN, Tsuchiya Y, Tamaru S, Shinkai S. Heat and light dual switching of a single-walled carbon nano-tube/thermo-responsive helical polysaccharide complex: a new responsive system applicable to photodynamic therapy. Chem Commun (Camb). 2011; 47:7065–7067. [PubMed: 21623440]
236. Wang Y, Li Z, Wang J, Li J, Lin Y. Graphene and graphene oxide: biofunctionalization and applications in biotechnology. Trends Biotechnol. 2011; 29:205–212. [PubMed: 21397350]
237. Sun X, Liu Z, Welsher K, Robinson JT, Goodwin A, Zaric S, Dai H. Nano-graphene oxide for cellular imaging and drug delivery. Nano Res. 2008; 1:203–212. [PubMed: 20216934]

238. Zhang L, Xia J, Zhao Q, Liu L, Zhang Z. Functional graphene oxide as a nanocarrier for controlled loading and targeted delivery of mixed anticancer drugs. Small. 2010; 6:537–544. [PubMed: 20033930]

239. Zhou L, Wang W, Tang J, Zhou JH, Jiang HJ, Shen J. Graphene oxide noncovalent photosensitizer and its anticancer activity in vitro. Chemistry. 2011; 17:12084–12091. [PubMed: 21915922]

240. Zhenjun D, Lown JW. Hypocrellins and their use in photosensitization. Photochem Photobiol. 1990; 52:609–616. [PubMed: 2284353]

241. Huang P, Xu C, Lin J, Wang C, Wang X, Zhang C, Zhou X, Guo S, Cui D. Folic acid-conjugated graphene oxide loaded with photosensitizers for targeting photodynamic therapy. Theranostics. 2011; 1:240–250. [PubMed: 21562631]

242. Tian B, Wang C, Zhang S, Feng L, Liu Z. Photothermally enhanced photodynamic therapy delivered by nano-graphene oxide. ACS Nano. 2011; 5:7000–7009. [PubMed: 21815655]

243. Haase M, Schafer H. Upconverting nanoparticles. Angew Chem Int Ed Engl. 2011; 50:5808–5829. [PubMed: 21626614]

244. Menyuk N, Dwight K, Pierce J. NaYF4: Yb, Er – an efficient upconversion phosphor. Appl Phys Lett. 1972; 21:159–161.

245. Chatterjee DK, Yong Z. Upconverting nanoparticles as nanotransducers for photodynamic therapy in cancer cells. Nanomedicine (Lond). 2008; 3:73–82. [PubMed: 18393642]

246. Ungun B, Prud'homme RK, Budijon SJ, Shan J, Lim SF, Ju Y, Austin R. Nanofabricated upconversion nanoparticles for photodynamic therapy. Opt Express. 2009; 17:80–86. [PubMed: 19129875]

247. Johnson BK, Prud'homme RK. Flash nanoprecipitation of organic actives and block copolymers using a confined impinging jets mixer. Aust J Chem. 2003; 56:1021–1024.

248. Wang C, Tao H, Cheng L, Liu Z. Near-infrared light induced in vivo photodynamic therapy of cancer based on upconversion nanoparticles. Biomaterials. 2011; 32:6145–6154. [PubMed: 21616529]

249. Gary-Bobo M, Mir Y, Rouxel C, Brevet D, Basile I, Maynadier M, Vaillant O, Mongin O, Blanchard-Desce M, Morere A, Garcia M, Durand JO, Raehm L. Mannose-functionalized mesoporous silica nanoparticles for efficient two-photon photodynamic therapy of solid tumors. Angew Chem Int Ed Engl. 2011; 50:11425–11429. [PubMed: 21976357]

250. Grimland JL, Wu C, Ramoutar RR, Brumaghim JL, McNeill J. Photosensitizer-doped conjugated polymer nanoparticles with high cross-sections for one- and two-photon excitation. Nanoscale. 2011; 3:1451–1455. [PubMed: 21293789]

251. Tassa C, Shaw SY, Weissleder R. Dextran-coated iron oxide nanoparticles: a versatile platform for targeted molecular imaging, molecular diagnostics and therapy. Acc Chem Res. 2011; 44:842–852. [PubMed: 21661727]

252. McCarthy JR, Kelly KA, Sun EY, Weissleder R. Targeted delivery of multifunctional magnetic nanoparticles. Nanomedicine (Lond). 2007; 2:153–167. [PubMed: 17716118]

253. Huang P, Li Z, Lin J, Yang D, Gao G, Xu C, Bao L, Zhang C, Wang K, Song H, Hu H, Cui D. Photosensitizer-conjugated magnetic nanoparticles for in vivo simultaneous magnetofluorescent imaging and targeting therapy. Biomaterials. 2011; 32:3447–3458. [PubMed: 21303717]

254. Tada DB, Vono LL, Duarte EL, Itri R, Kiyohara PK, Baptista MS, Rossi LM. Methylene blue-containing silica-coated magnetic particles: a potential magnetic carrier for photodynamic therapy. Langmuir. 2007; 23:8194–8199. [PubMed: 17590032]

255. Ding J, Zhao J, Cheng K, Liu G, Xiu D. In vivo photodynamic therapy and magnetic resonance imaging of cancer by TSPP-coated Fe3O4 nanoconjugates. J Biomed Nanotechnol. 2010; 6:683–686. [PubMed: 21361133]

256. Sun Y, Chen ZL, Yang XX, Huang P, Zhou XP, Du XX. Magnetic chitosan nanoparticles as a drug delivery system for targeting photodynamic therapy. Nanotechnology. 2009; 20:135102. [PubMed: 19420486]

257. Ng KK, Lovell JF, Zheng G. Lipoprotein-inspired nano-particles for cancer theranostics. Acc Chem Res. 2011; 44:1105–1113. [PubMed: 21557543]

258. Li H, Marotta DE, Kim S, Busch TM, Wileyto EP, Zheng G. High payload delivery of optical imaging and photodynamic therapy agents to tumors using phthalocyanine-reconstituted low-density lipoprotein nanoparticles. J Biomed Opt. 2005; 10:41203. [PubMed: 16178627]

259. Marotta DE, Cao W, Wileyto EP, Li H, Corbin I, Rickter E, Glickson JD, Chance B, Zheng G, Busch TM. Evaluation of bacteriochlorophyll-reconstituted low-density lipoprotein nanoparticles for photodynamic therapy efficacy in vivo. Nanomedicine. 2011; 6:475–487. [PubMed: 21542686]

260. Brown SB, Brown EA, Walker I. The present and future role of photodynamic therapy in cancer treatment. Lancet Oncol. 2004; 5:497–508. [PubMed: 15288239]

261. Weinstein JN, van Osdol W. Early intervention in cancer using monoclonal antibodies and other biological ligands: micro-pharmacology and the “binding site barrier”. Cancer Res. 1992; 52:2747s–2751s. [PubMed: 1563006]

262. Adams GP, Schier R, McCall AM, Simmons HH, Horak EM, Alpaugh RK, Marks JD, Weiner LM. High affinity restricts the localization and tumor penetration of single-chain fv antibody molecules. Cancer Res. 2001; 61:4750–4755. [PubMed: 11406547]

263. Stuchinskaya T, Moreno M, Cook MJ, Edwards DR, Russell DA. Targeted photodynamic therapy of breast cancer cells using antibody-phthalocyanine-gold nanoparticle conjugates. Photochem Photobiol Sci. 2011; 10:822–831. [PubMed: 21455532]

264. Kameyama N, Matsuda S, Itano O, Ito A, Konno T, Arai T, Ishihara K, Ueda M, Kitagawa Y. Photodynamic therapy using an anti-EGF receptor antibody complexed with verte-porfin nanoparticles: a proof of concept study. Cancer Biother Radiopharm. 2011; 26:697–704. [PubMed: 21861705]

265. Rancan F, Helmreich M, Molich A, Ermilov EA, Jux N, Roder B, Hirsch A, Bohm F. Synthesis and in vitro testing of a pyropheophorbide-a-fullerene hexakis adduct immunoconjugate for photodynamic therapy. Bioconjug Chem. 2007; 18:1078–1086. [PubMed: 17550226]

266. Bergstrom LC, Vucenik I, Hagen IK, Chernomorsky SA, Poretz RD. In-vitro photocytotoxicity of lysosomotropic immunoliposomes containing pheophorbide a with human bladder carcinoma cells. J Photochem Photobiol B. 1994; 24:17–23. [PubMed: 8057202]

267. Morgan J, Gray AG, Huehns ER. Specific targeting and toxicity of sulphonated aluminium phthalocyanine photosensitised liposomes directed to cells by monoclonal antibody in vitro. Br J Cancer. 1989; 59:366–370. [PubMed: 2930700]

268. Xu J, Sun Y, Huang J, Chen C, Liu G, Jiang Y, Zhao Y, Jiang Z. Photokilling cancer cells using highly cell-specific antibody-TiO(2) bioconjugates and electroporation. Bioelectrochemistry. 2007; 71:217–222. [PubMed: 17643355]

269. Nimjee SM, Rusconi CP, Sullenger BA. Aptamers: an emerging class of therapeutics. Annu Rev Med. 2005; 56:555–583. [PubMed: 15660527]

270. Lee JH, Yigit MV, Mazumdar D, Lu Y. Molecular diagnostic and drug delivery agents based on aptamer-nanomaterial conjugates. Adv Drug Deliv Rev. 2010; 62:592–605. [PubMed: 20338204]

271. Stephanopoulos N, Tong GJ, Hsiao SC, Francis MB. Dual-surface modified virus capsids for targeted delivery of photodynamic agents to cancer cells. ACS Nano. 2010; 4:6014–6020. [PubMed: 20863095]

272. Parker N, Turk MJ, Westrick E, Lewis JD, Low PS, Leamon CP. Folate receptor expression in carcinomas and normal tissues determined by a quantitative radioligand binding assay. Anal Biochem. 2005; 338:284–293. [PubMed: 15745749]

273. Garcia-Diaz M, Nonell S, Villanueva A, Stockert JC, Canete M, Casado A, Mora M, Sagrista ML. Do folate-receptor targeted liposomal photosensitizers enhance photodynamic therapy selectivity? Biochim Biophys Acta. 2011; 1808:1063–1071. [PubMed: 21215723]

274. Bae BC, Na K. Self-quenching polysaccharide-based nanogels of pullulan/folate-photosensitizer conjugates for photodynamic therapy. Biomaterials. 2010; 31:6325–6335. [PubMed: 20493523]

275. Stevens PJ, Sekido M, Lee RJ. Synthesis and evaluation of a hematoporphyrin derivative in a folate receptor-targeted solid-lipid nanoparticle formulation. Anticancer Res. 2004; 24:161–165. [PubMed: 15015592]

276. Hah HJ, Kim G, Lee YE, Orringer DA, Sagher O, Philbert MA, Kopelman R. Methylene blue-conjugated hydrogel nanoparticles and tumor-cell targeted photodynamic therapy. Macromol Biosci. 2011; 11:90–99. [PubMed: 20976722]

277. Rozenzhak SM, Kadakia MP, Caserta TM, Westbrook TR, Stone MO, Naik RR. Cellular internalization and targeting of semiconductor quantum dots. Chem Commun (Camb). 2005:2217–2219. [PubMed: 15856101]

278. Oku N, Ishii T. Antiangiogenic photodynamic therapy with targeted liposomes. Methods Enzymol. 2009; 465:313–330. [PubMed: 19913174]

279. Rudzki Z, Jothy S. CD44 and the adhesion of neoplastic cells. Mol Pathol. 1997; 50:57–71. [PubMed: 9231152]

280. Platt VM, Szoka FC Jr. Anticancer therapeutics: targeting macromolecules and nanocarriers to hyaluronan or CD44, a hyaluronan receptor. Mol Pharm. 2008; 5:474–486. [PubMed: 18547053]

281. Li F, Bae BC, Na K. Acetylated hyaluronic acid/photosensitizer conjugate for the preparation of nanogels with controllable phototoxicity: synthesis, characterization, autophotoquenching properties and in vitro phototoxicity against HeLa cells. Bioconjug Chem. 2010; 21:1312–1320. [PubMed: 20586473]

282. Vargas A, Pegaz B, Debefve E, Konan-Kouakou Y, Lange N, Ballini JP, van den Bergh H, Gurny R, Delie F. Improved photodynamic activity of porphyrin loaded into nanoparticles: an in vivo evaluation using chick embryos. Int J Pharm. 2004; 286:131–145. [PubMed: 15501010]

283. Pegaz B, Debefve E, Borle F, Ballini JP, van den Bergh H, Kouakou-Konan YN. Encapsulation of porphyrins and chlorins in biodegradable nanoparticles: the effect of dye lipophilicity on the extravasation and the photothrombic activity. A comparative study. J Photochem Photobiol B. 2005; 80:19–27. [PubMed: 15963434]

284. Casas A, Battah S, Di Venosa G, Dobbin P, Rodriguez L, Fukuda H, Batlle A, MacRobert AJ. Sustained and efficient porphyrin generation in vivo using dendrimer conjugates of 5-ALA for photodynamic therapy. J Control Release. 2009; 135:136–143. [PubMed: 19168101]

285. Barth BM, Altinoğlu EI, Shanmugavelandy SS, Kaiser JM, Crespo-Gonzalez D, DiVittore NA, McGovern C, Goff TM, Keasey NR, Adair JH, Loughran TP Jr, Claxton DF, Kester M. Targeted indocyanine-green-loaded calcium phosphosilicate nanoparticles for in vivo photodynamic therapy of leukemia. ACS Nano. 2011; 5:5325–5337. [PubMed: 21675727]

286. Oberdorster G, Maynard A, Donaldson K, Castranova V, Fitzpatrick J, Ausman K, Carter J, Karn B, Kreyling W, Lai D, Olin S, Monteiro-Riviere N, Warheit D, Yang H. Principles for characterizing the potential human health effects from exposure to nanomaterials: elements of a screening strategy. Part Fibre Toxicol. 2005; 2:8. [PubMed: 16209704]

287. Oberdorster G. Safety assessment for nanotechnology and nanomedicine: concepts of nanotoxicology. J Intern Med. 2010; 267:89–105. [PubMed: 20059646]

288. Fubini B, Fenoglio I, Tomatis M, Turci F. Effect of chemical composition and state of the surface on the toxic response to high aspect ratio nanomaterials. Nanomedicine (Lond). 2011; 6:899–920. [PubMed: 21793679]

289. Oberdorster G, Elder A, Rinderknecht A. Nanoparticles and the brain: cause for concern? J Nanosci Nanotechnol. 2009; 9:4996–5007. [PubMed: 19928180]

290. Xia T, Kovochich M, Liong M, Zink JI, Nel AE. Cationic polystyrene nanosphere toxicity depends on cell-specific endocytic and mitochondrial injury pathways. ACS Nano. 2008; 2:85–96. [PubMed: 19206551]

291. Liu J, Hopfinger AJ. Identification of possible sources of nanotoxicity from carbon nanotubes inserted into membrane bilayers using membrane interaction quantitative structure –activity relationship analysis. Chem Res Toxicol. 2008; 21:459–466. [PubMed: 18189365]

292. Linse S, Cabaleiro-Lago C, Xue WF, Lynch I, Lindman S, Thulin E, Radford SE, Dawson KA. Nucleation of protein fibrillation by nanoparticles. Proc Natl Acad Sci USA. 2007; 104:8691–8696. [PubMed: 17485668]

293. Pan BF, Gao F, Gu HC. Dendrimer modified magnetite nanoparticles for protein immobilization. J Colloid Interface Sci. 2005; 284:1–6. [PubMed: 15752777]

294. AshaRani PV, Low Kah Mun G, Hande MP, Valiyaveettil S. Cytotoxicity and genotoxicity of silver nanoparticles in human cells. ACS Nano. 2009; 3:279–290. [PubMed: 19236062]

295. Li N, Xia T, Nel AE. The role of oxidative stress in ambient particulate matter-induced lung diseases and its implications in the toxicity of engineered nanoparticles. Free Radic Biol Med. 2008; 44:1689–1699. [PubMed: 18313407]

296. Tang M, Wang M, Xing T, Zeng J, Wang H, Ruan DY. Mechanisms of unmodified CdSe quantum dot-induced elevation of cytoplasmic calcium levels in primary cultures of rat hippocampal neurons. Biomaterials. 2008; 29:4383–4391. [PubMed: 18752844]

297. Li N, Hao M, Phalen RF, Hinds WC, Nel AE. Particulate air pollutants and asthma. A paradigm for the role of oxidative stress in PM-induced adverse health effects. Clin Immunol. 2003; 109:250–265. [PubMed: 14697739]

298. Poland CA, Duffin R, Kinloch I, Maynard A, Wallace WA, Seaton A, Stone V, Brown S, Macnee W, Donaldson K. Carbon nanotubes introduced into the abdominal cavity of mice show asbestos-like pathogenicity in a pilot study. Nat Nanotechnol. 2008; 3:423–428. [PubMed: 18654567]

299. Xia T, Kovochich M, Liong M, Madler L, Gilbert B, Shi H, Yeh JI, Zink JI, Nel AE. Comparison of the mechanism of toxicity of zinc oxide and cerium oxide nanoparticles based on dissolution and oxidative stress properties. ACS Nano. 2008; 2:2121–2134. [PubMed: 19206459]

300. Shvedova AA, Kisin ER, Mercer R, Murray AR, Johnson VJ, Potapovich AI, Tyurina YY, Gorelik O, Arepalli S, Schwegler-Berry D, Hubbs AF, Antonini J, Evans DE, Ku BK, Ramsey D, Maynard A, Kagan VE, Castranova V, Baron P. Unusual inflammatory and fibrogenic pulmonary responses to single-walled carbon nanotubes in mice. Am J Physiol Lung Cell Mol Physiol. 2005; 289:L698–L708. [PubMed: 15951334]

301. Chen Z, Meng H, Xing G, Yuan H, Zhao F, Liu R, Chang X, Gao X, Wang T, Jia G, Ye C, Chai Z, Zhao Y. Age-related differences in pulmonary and cardiovascular responses to SiO_2 nanoparticle inhalation: nanotoxicity has susceptible population. Environ Sci Technol. 2008; 42:8985–8992. [PubMed: 19192829]

302. Berry JP, Arnoux B, Stanislas G, Galle P, Chretien J. A micro-analytic study of particles transport across the alveoli: role of blood platelets. Biomedicine. 1977; 27:354–357. [PubMed: 606312]

303. Li SQ, Zhu RR, Zhu H, Xue M, Sun XY, Yao SD, Wang SL. Nanotoxicity of TiO(2) nanoparticles to erythrocyte in vitro. Food Chem Toxicol. 2008; 46:3626–3631. [PubMed: 18840495]

304. Park EJ, Bae E, Yi J, Kim Y, Choi K, Lee SH, Yoon J, Lee BC, Park K. Repeated-dose toxicity and inflammatory responses in mice by oral administration of silver nanoparticles. Environ Toxicol Pharmacol. 2010; 30:162–168. [PubMed: 21787647]

305. Yu T, Malugin A, Ghandehari H. Impact of silica nanoparticle design on cellular toxicity and hemolytic activity. ACS Nano. 2011; 5:5717–5728. [PubMed: 21630682]

306. Grassian VH, O'Shaughnessy PT, Adamcakova-Dodd A, Pettibone JM, Thorne PS. Inhalation exposure study of titanium dioxide nanoparticles with a primary particle size of 2 to 5 nm. Environ Health Perspect. 2007; 115:397–402. [PubMed: 17431489]

307. Geys J, Nemmar A, Verbeken E, Smolders E, Ratoi M, Hoylaerts MF, Nemery B, Hoet PH. Acute toxicity and pro-thrombotic effects of quantum dots: impact of surface charge. Environ Health Perspect. 2008; 116:1607–1613. [PubMed: 19079709]

308. Oberdorster G, Sharp Z, Atudorei V, Elder A, Gelein R, Kreyling W, Cox C. Translocation of inhaled ultrafine particles to the brain. Inhal Toxicol. 2004; 16:437–445. [PubMed: 15204759]

309. Long TC, Tajuba J, Sama P, Saleh N, Swartz C, Parker J, Hester S, Lowry GV, Veronesi B. Nanosize titanium dioxide stimulates reactive oxygen species in brain microglia and damages neurons in vitro. Environ Health Perspect. 2007; 115:1631–1637. [PubMed: 18007996]

310. Ballou B, Lagerholm BC, Ernst LA, Bruchez MP, Waggoner AS. Noninvasive imaging of quantum dots in mice. Bioconjug Chem. 2004; 15:79–86. [PubMed: 14733586]

311. Oberdorster G, Sharp Z, Atudorei V, Elder A, Gelein R, Lunts A, Kreyling W, Cox C. Extrapulmonary translocation of ultrafine carbon particles following whole-body inhalation exposure of rats. J Toxicol Environ Health A. 2002; 65:1531–1543. [PubMed: 12396867]

312. Chen YS, Hung YC, Liau I, Huang GS. Assessment of the in vivo toxicity of gold nanoparticles. Nanoscale Res Lett. 2009; 4:858–864. [PubMed: 20596373]

313. Hanley C, Thurber A, Hanna C, Punnoose A, Zhang J, Wingett DG. The influences of cell type and ZnO nanoparticle size on immune cell cytotoxicity and cytokine induction. Nanoscale Res Lett. 2009; 4:1409–1420. [PubMed: 20652105]

314. Meng H, Xia T, George S, Nel AE. A predictive toxicological paradigm for the safety assessment of nanomaterials. ACS Nano. 2009; 3:1620–1627. [PubMed: 21452863]

315. Krug HF, Wick P. Nanotoxicology: an interdisciplinary challenge. Angew Chem Int Ed Engl. 2011; 50:1260–1278. [PubMed: 21290492]

316. Jiang W, Kim BY, Rutka JT, Chan WC. Nanoparticle-mediated cellular response is size-dependent. Nat Nanotechnol. 2008; 3:145–150. [PubMed: 18654486]

317. Palomaki J, Valimaki E, Sund J, Vippola M, Clausen PA, Jensen KA, Savolainen K, Matikainen S, Alenius H. Long, needle-like carbon nanotubes and asbestos activate the NLRP3 inflammasome through a similar mechanism. ACS Nano. 2011; 5:6861–6870. [PubMed: 21800904]

318. Stella GM. Carbon nanotubes and pleural damage: perspectives of nanosafety in the light of asbestos experience. Biointerphases. 2011; 6:P1–17. [PubMed: 21721837]

319. Murphy FA, Poland CA, Duffin R, Al-Jamal KT, Ali-Boucetta H, Nunes A, Byrne F, Prina-Mello A, Volkov Y, Li S, Mather SJ, Bianco A, Prato M, Macnee W, Wallace WA, Kostarelos K, Donaldson K. Length-dependent retention of carbon nanotubes in the pleural space of mice initiates sustained inflammation and progressive fibrosis on the parietal pleura. Am J Pathol. 2011; 178:2587–2600. [PubMed: 21641383]

320. Fraser TW, Reinardy HC, Shaw BJ, Henry TB, Handy RD. Dietary toxicity of single-walled carbon nanotubes and fullerenes (C60) in rainbow trout (Oncorhynchus mykiss). Nanotoxicology. 2011; 5:98–108. [PubMed: 21417691]

321. Jovanovic B, Anastasova L, Rowe EW, Palic D. Hydroxylated fullerenes inhibit neutrophil function in fathead minnow (Pimephales promelas Rafinesque, 1820). Aquat Toxicol. 2011; 101:474–482. [PubMed: 21122929]

322. Henry TB, Petersen EJ, Compton RN. Aqueous fullerene aggregates (nC60) generate minimal reactive oxygen species and are of low toxicity in fish: a revision of previous reports. Curr Opin Biotechnol. 2011; 22:533–537. [PubMed: 21719272]

323. Kovochich M, Espinasse B, Auffan M, Hotze EM, Wessel L, Xia T, Nel AE, Wiesner MR. Comparative toxicity of C60 aggregates toward mammalian cells: role of tetrahydrofuran (THF) decomposition. Environ Sci Technol. 2009; 43:6378–6384. [PubMed: 19746740]

324. Khalil WK, Girgis E, Emam AN, Mohamed MB, Rao KV. Genotoxicity evaluation of nanomaterials: DNA damage, micronuclei and 8-hydroxy-2-deoxyguanosine induced by magnetic doped CdSe quantum dots in male mice. Chem Res Toxicol. 2011; 24:640–650. [PubMed: 21425850]

325. Tino A, Ambrosone A, Mattera L, Marchesano V, Susha A, Rogach A, Tortiglione C. A new in vivo model system to assess the toxicity of semiconductor nanocrystals. Int J Biomater. 201110.1155/2011/792854

326. Bechet D, Couleaud P, Frochot C, Viriot ML, Guillemin F, Barberi-Heyob M. Nanoparticles as vehicles for delivery of photodynamic therapy agents. Trends Biotechnol. 2008; 26:612–621. [PubMed: 18804298]

327. Zhang L, Gu FX, Chan JM, Wang AZ, Langer RS, Farokhzad OC. Nanoparticles in medicine: therapeutic applications and developments. Clin Pharmacol Ther. 2008; 83:761–769. [PubMed: 17957183]

328. Uchoa AF, de Oliveira KT, Baptista MS, Bortoluzzi AJ, Iamamoto Y, Serra OA. Chlorin photosensitizers sterically designed to prevent self-aggregation. J Org Chem. 2011; 76:8824–8832. [PubMed: 21932835]

329. Lee DY, Li KC. Molecular theranostics: a primer for the imaging professional. AJR Am J Roentgenol. 2011; 197:318–324. [PubMed: 21785076]

330. Janib SM, Moses AS, MacKay JA. Imaging and drug delivery using theranostic nanoparticles. Adv Drug Deliv Rev. 2010; 62:1052–1063. [PubMed: 20709124]

331. Fernandez-Fernandez A, Manchanda R, McGoron AJ. Theranostic applications of nanomaterials in cancer: drug delivery, image-guided therapy and multifunctional platforms. Appl Biochem Biotechnol. 2011; 165:1628–1651. [PubMed: 21947761]

332. Hahn MA, Singh AK, Sharma P, Brown SC, Moudgil BM. Nanoparticles as contrast agents for in-vivo bioimaging: current status and future perspectives. Anal Bioanal Chem. 2011; 399:3–27. [PubMed: 20924568]

333. Cheon J, Lee JH. Synergistically integrated nanoparticles as multimodal probes for nanobiotechnology. Acc Chem Res. 2008; 41:1630–1640. [PubMed: 18698851]

334. Grimm J, Scheinberg DA. Will nanotechnology influence targeted cancer therapy? Semin Radiat Oncol. 2011; 21:80–87. [PubMed: 21356476]

Biographies

Ying-Ying Huang, MD, has been a postdoctoral fellow in Dr. Hamblin's laboratory for 4 years. Her research interests lie in Quantitative structure–activity relationship of photosensitizers in photodynamic therapy and cellular response and mechanism of low level light therapy. She has published over 20 peer review articles.

Michael R. Hamblin, PhD, is a principal investigator at the Wellman Center for Photomedicine at Massachusetts General Hospital and an associate Professor of Dermatology at Harvard Medical School and Harvard-MIT Division of Health Science and Technology. His research interests lie in the areas of photodynamic therapy and low-level light therapy. He has published more than 160 peer-reviewed articles.

Long Y. Chiang, PhD, is Professor of Chemistry at the University of Massachusetts Lowell and has collaborated with Dr. Hamblin for 4 years.

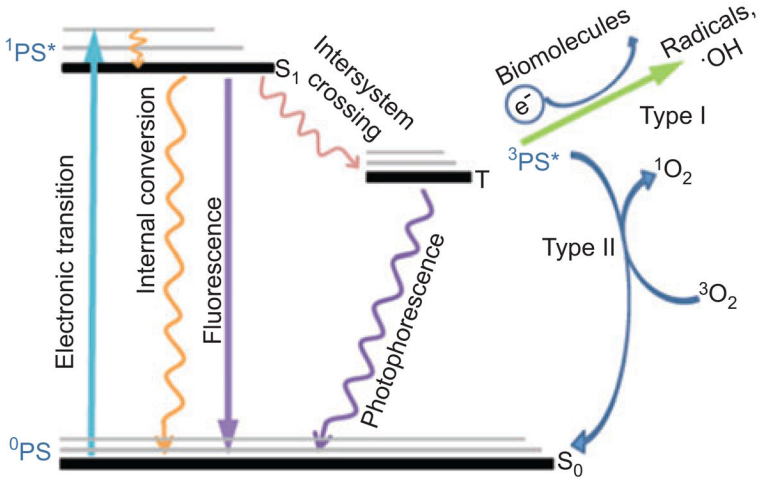

Figure 1.

Jablonski diagram.

Initial absorption of a photon by the ground state of the singlet PS gives rise to the short-lived excited singlet state. This can lose energy by fluorescence, internal conversion to heat, or by intersystem crossing to the long-lived triplet state. PS triplet states are efficiently quenched by energy transfer to molecular oxygen (a triplet state) to give type 2 (singlet oxygen) or by electron transfer to oxygen or to biomolecules to give type 1 ROS (superoxide and hydroxyl radical).

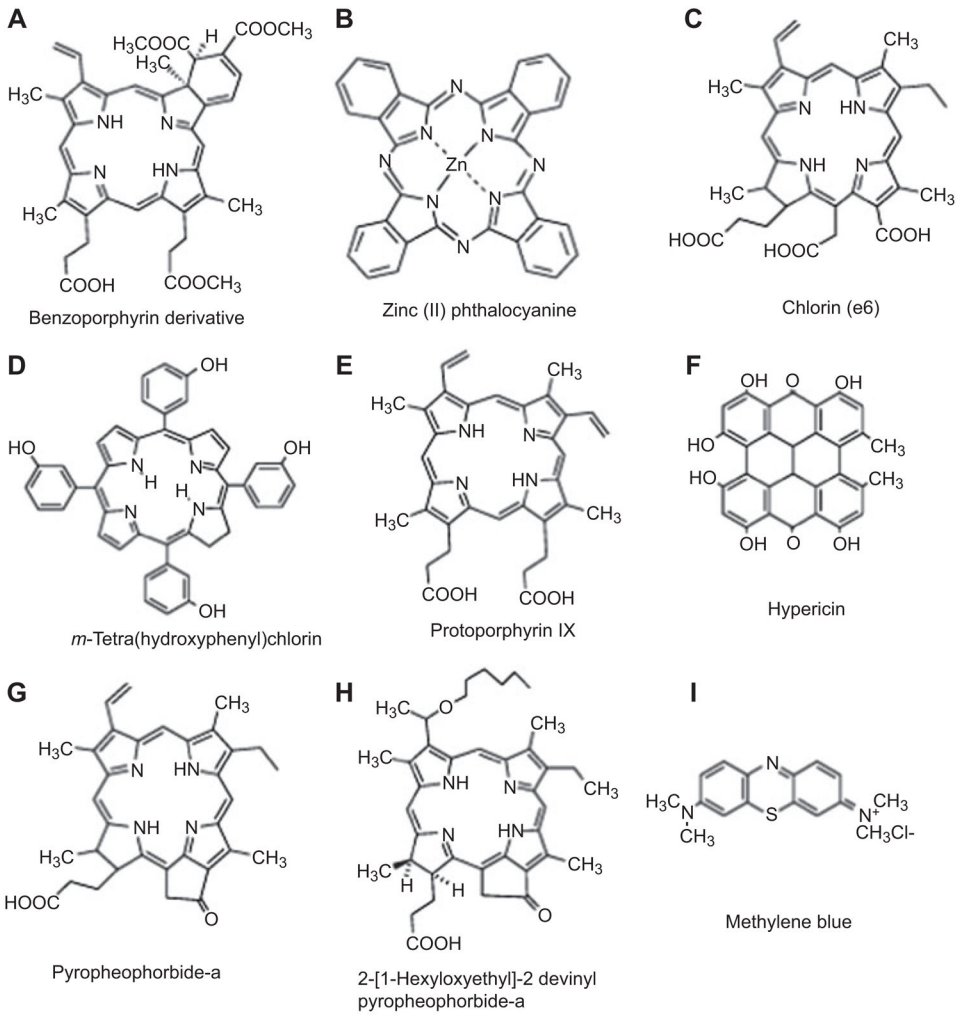

Figure 2.

Representative chemical structures of PS that have been used in combination with nanoparticles.

(A) BPD, (B) ZnPC, (C) ce6, (D) *m*-THPC, (E), PPIX, (F) hypericin, (G) pyropheophorbide a (Ppa), (H) HPPH, and (I) MB.

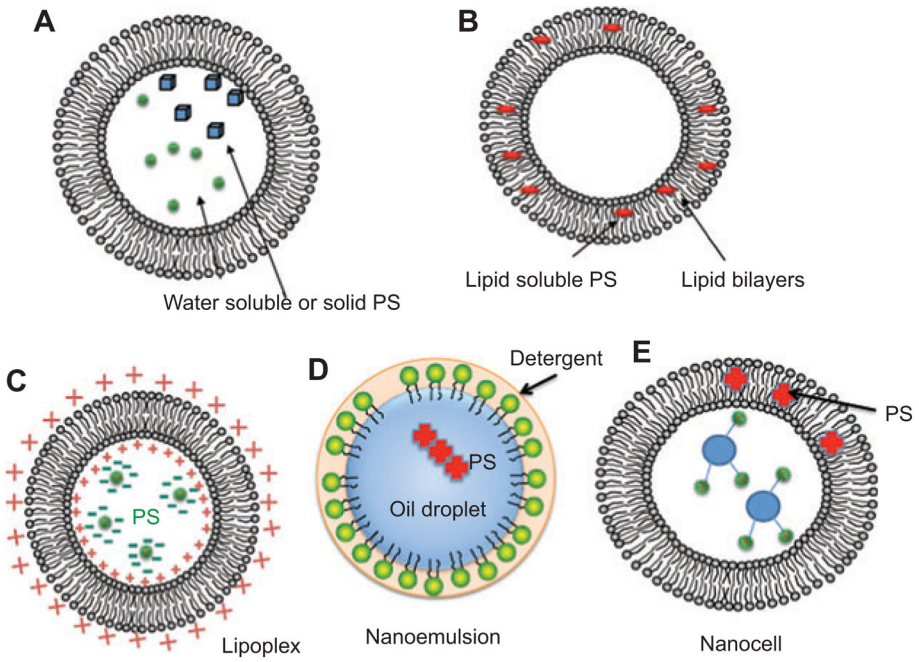

Figure 3.

Lipid nanoparticles.

(A) Liposomes containing water-soluble PS in aqueous interior. (B) Liposomes containing lipid soluble PS in hydrophobic region of lipid bilayer. (C) Lipoplex formed from cationic lipids encapsulating anionic PS. (D) Nanoemulsion formed from nanometer-sized oil droplets with dissolved hydrophobic PS coated by neutral detergent. (E) Nanocell formed from a liposome with hydrophobic PS encapsulating additional targeting molecules such as antibodies in interior.

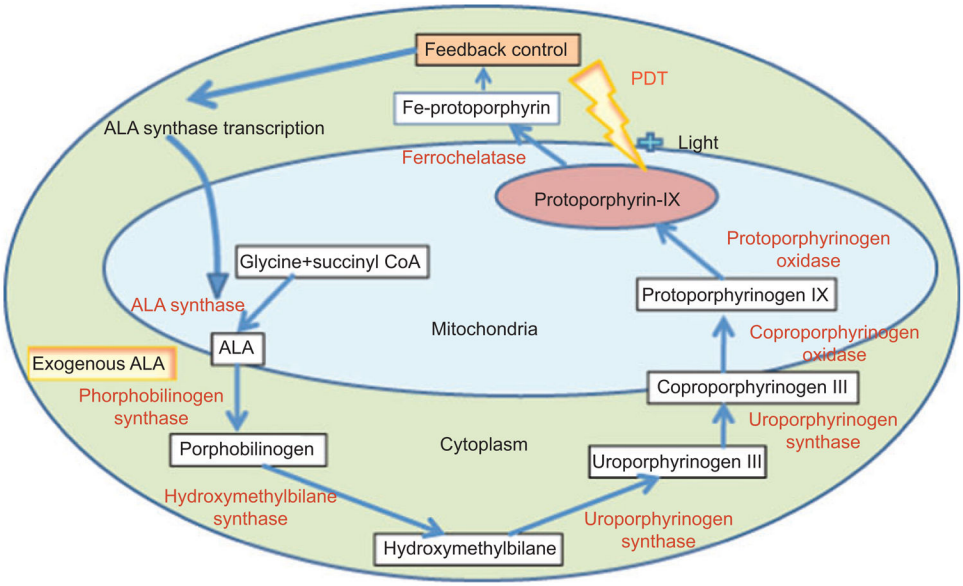

Figure 4.

Heme biosynthesis cycle.

Exogenous ALA is added that bypasses feedback control inhibition of ALA synthase. Because the rate-limiting step is the introduction of iron into PPIX by ferrochelatase to form heme, the levels of PPIX build up and allow effective PDT to be carried out.

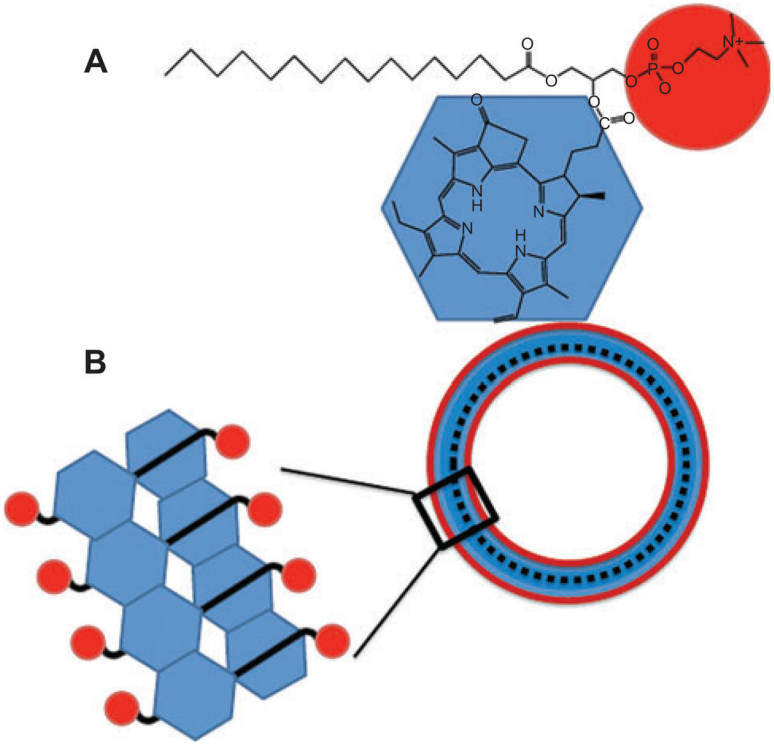

Figure 5.
Porphysomes.
As described by Lovell [51], lysophosphatidylcholine pyropheophorbide a (A) spontaneously assembles into nanovesicles designated “porphysomes” (B).

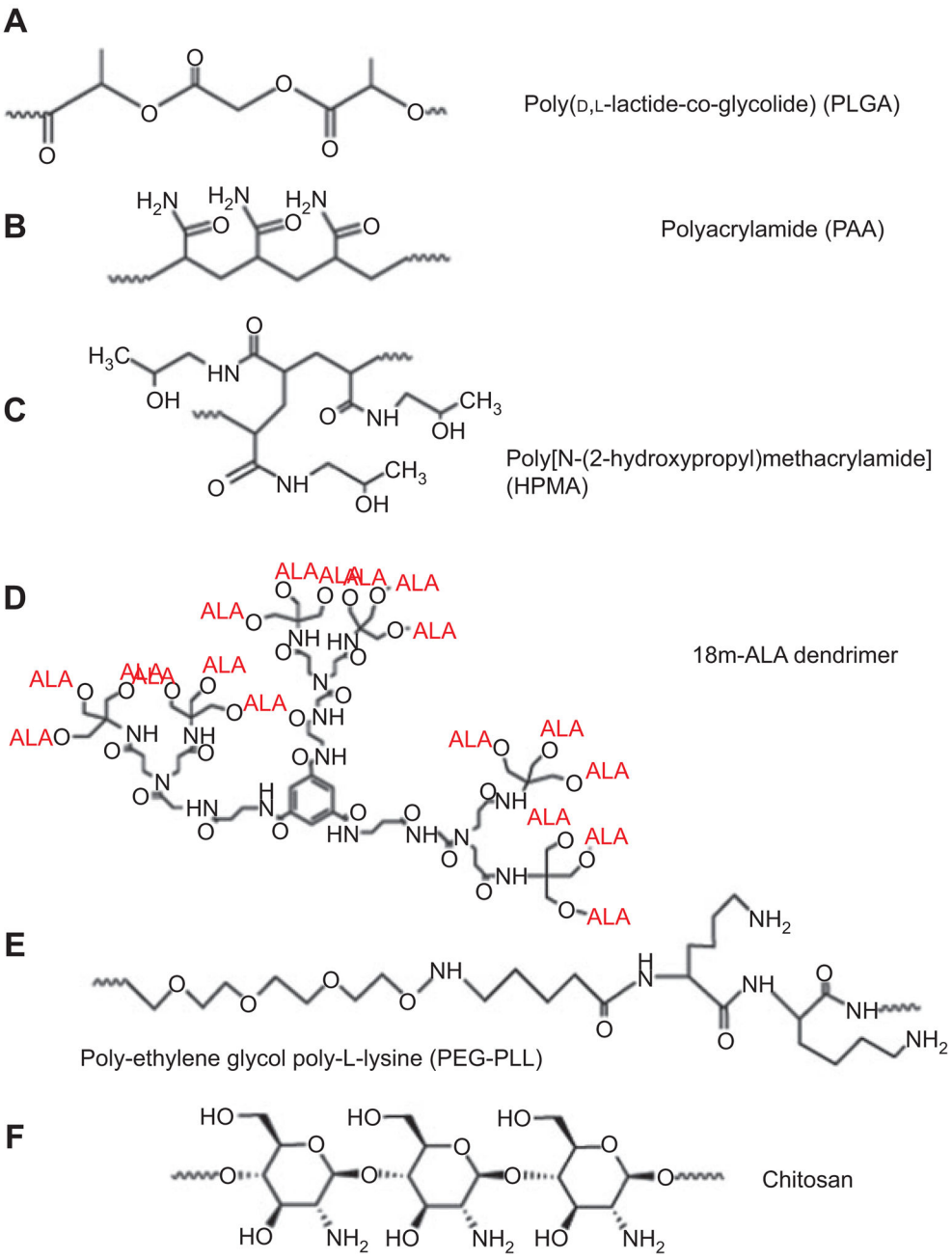

Figure 6.

Chemical structures of polymers used to prepare nanoparticles.

(A) PLGA [55], (B) PAA [56], (C) HPMA [57], (D) 18m-ALA-dendrimer [58], (E) PEG-PLL [59], and (F) chitosan [60].

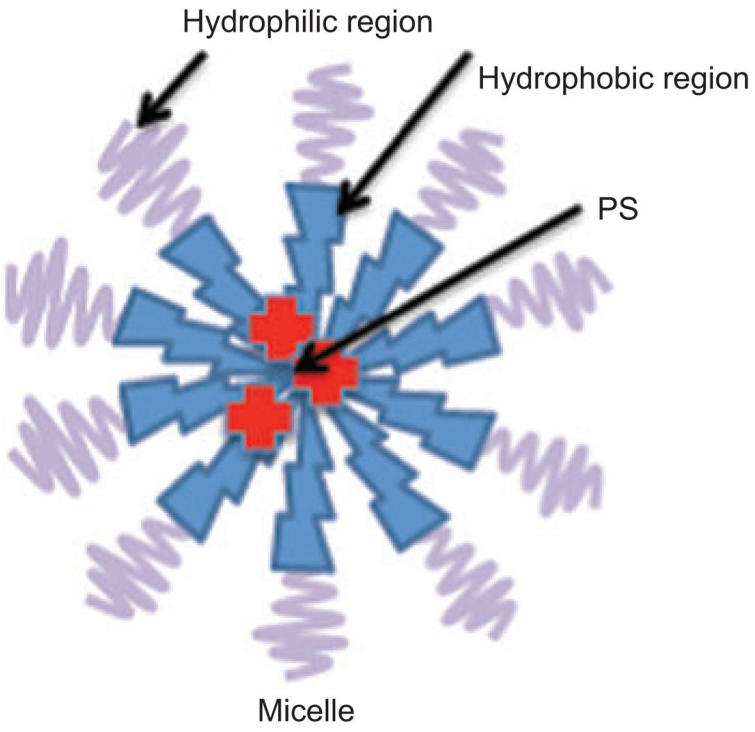

Figure 7.
Micelle structure.
Detergents with hydrophilic and hydrophobic blocks spontaneously assemble into micelles with hydrophobic interiors that dissolve lipophilic PS.

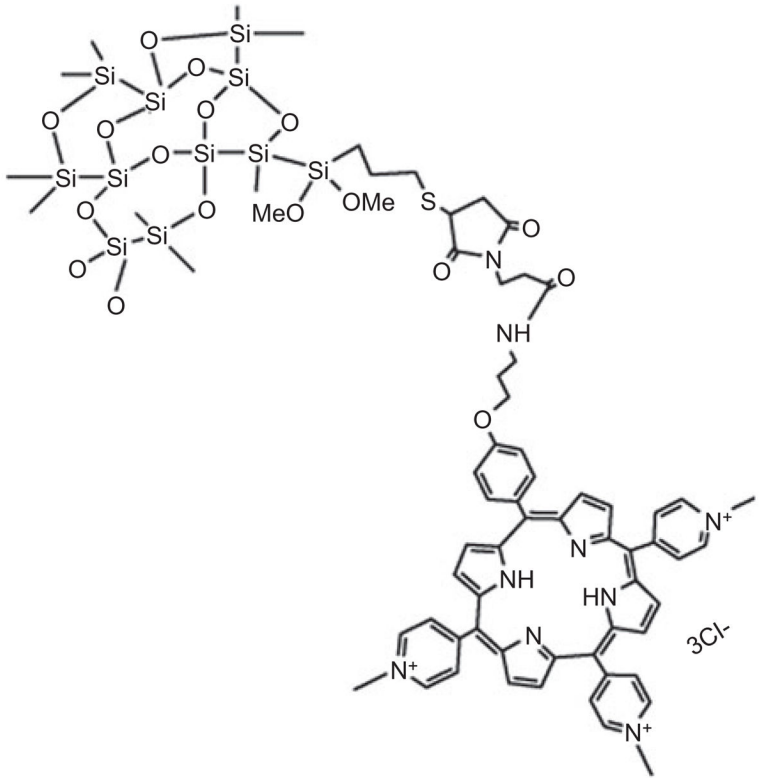

Figure 8.

ORMOSIL nanoparticle bound to porphyrin.

As described by Hocine et al. [126], a trimethoxysilane functionalized tris-cationic porphyrin was prepared and copolymerized intro a SiNP.

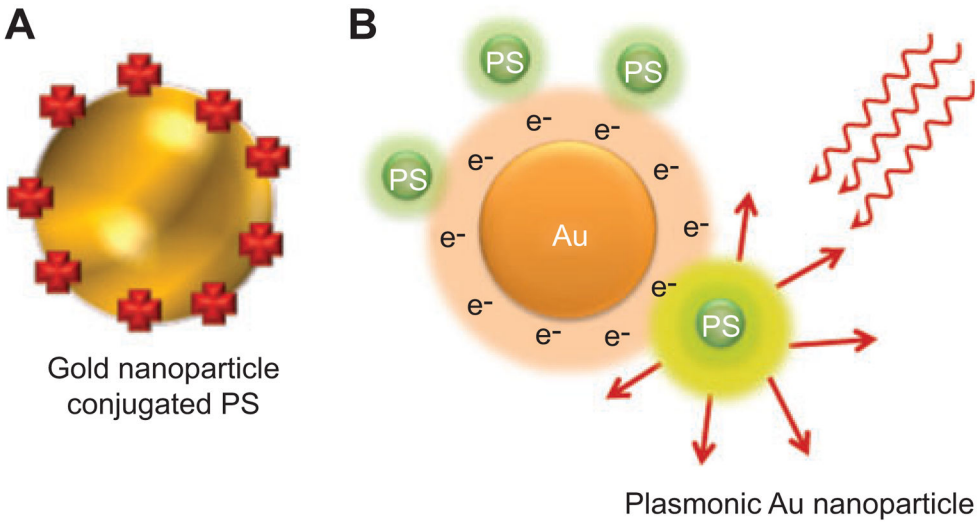

Figure 9.
AuNPs.
(A) Gold nanoshell encapsulating a PS. (B) Plasmonic AuNP. The local electric field caused by conductance electrons potentiates the optical field close to the surface and increases the fluorescence or photoactivity of an attached PS.

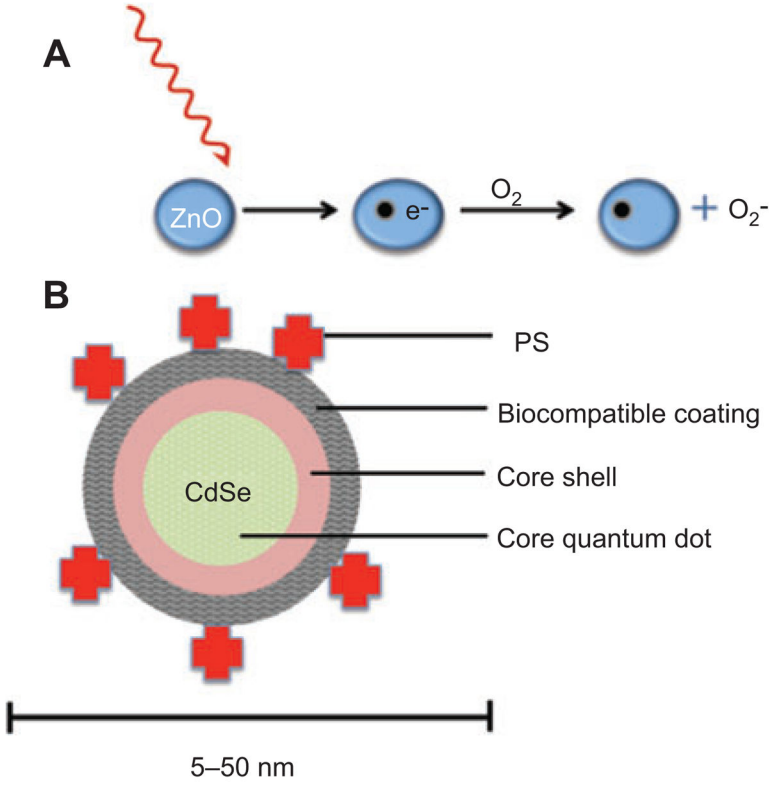

Figure 10.

Semiconductor nanoparticles.

(A) Semiconductors such as ZnO will form electron-hole pairs upon absorption of UVA or blue photons, and these electrons can be transferred to oxygen-forming superoxide that leads to further ROS. (B) Typical QD with CdSe core, followed by a zinc sulfide capping passivation layer covered by a biologically compatible layer made of thiol containing compounds. PS are covalently attached to the QD that can take part in FRET with the emission of the QD being used to excite the PS.

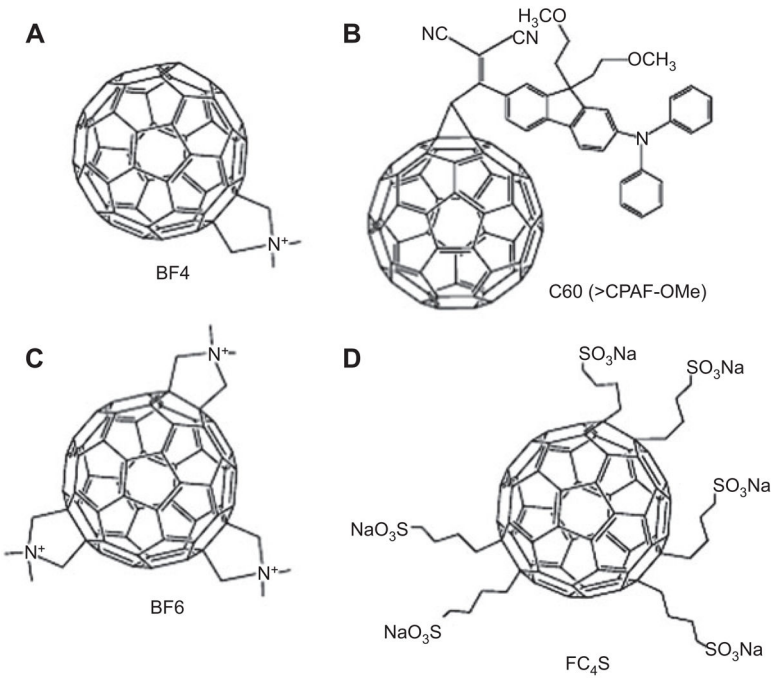

Figure 11.

Chemical structures of fullerenes used for PDT.

(A) Mono-(dimethylpyrolidinium) fullerene (BF4) [118, 173]. (B) Dicyano diphenylaminofluorene functionalized fullerene (C60, >CPAF-OMe) [174]. (C) Tris-(dimethylpyrolidinium) fullerene (BF6) [175, 176]. (D) Hexakis-sulfonated anionic fullerene (FC_4S) [177].

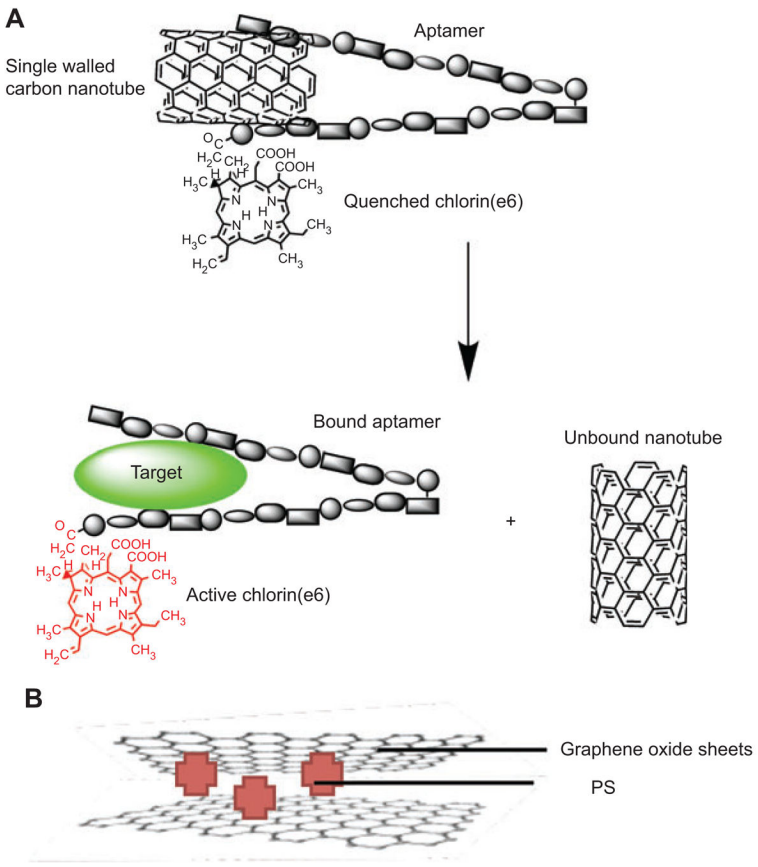

Figure 12.

SWCNT and graphene.

(A) Zhu et al. [233] engineered a novel molecular complex of a PS, an ssDNA aptamer, and SWCNTs that became activated upon aptamer binding to its target releasing the SWCNT that had been quenching the PS. (B) PS can be "sandwiched" between two sheets of GO, providing enhanced activity.

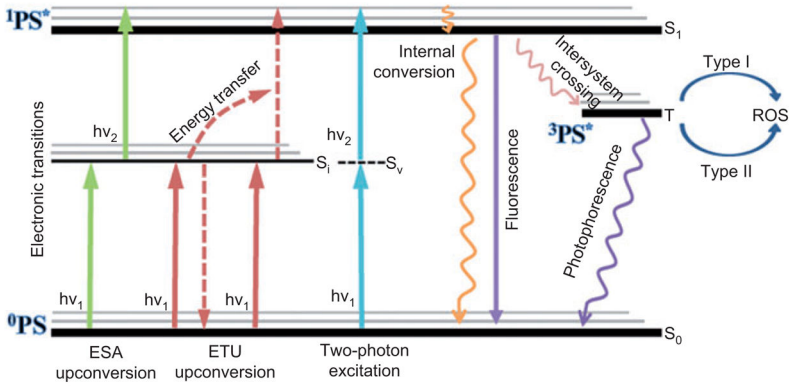

Figure 13.

UC and TPA.

Qualitative Jablonski diagrams of two possible photon UC processes and a two-photon excitation for use in PDT. ESA, excited state absorption; ETU, energy transfer UC; Si, intermediate; Sv, virtual.

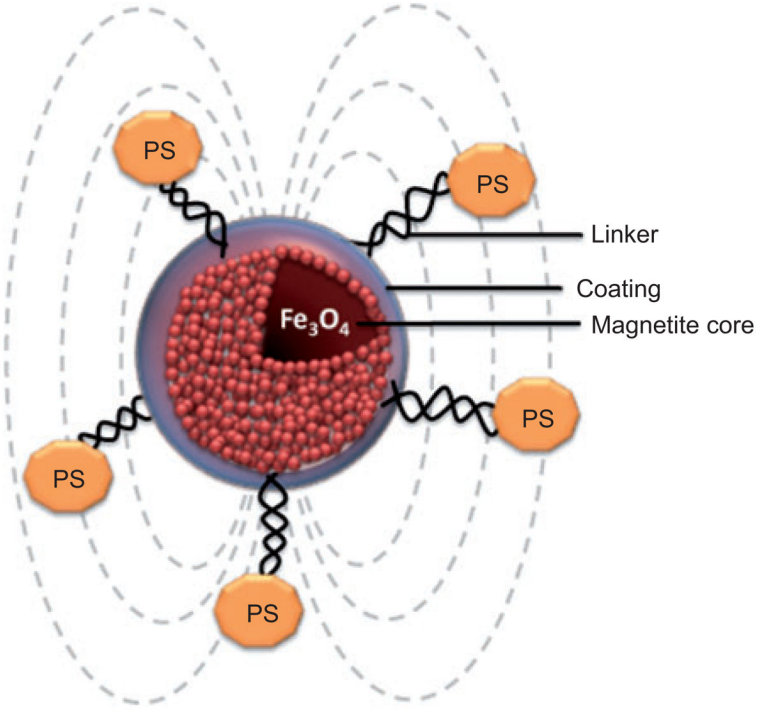

Figure 14.
MNPs.
This consists of a magnetite core (Fe_3O_4) coated by a biologically compatible layer and the PS are covalently attached by linkers.

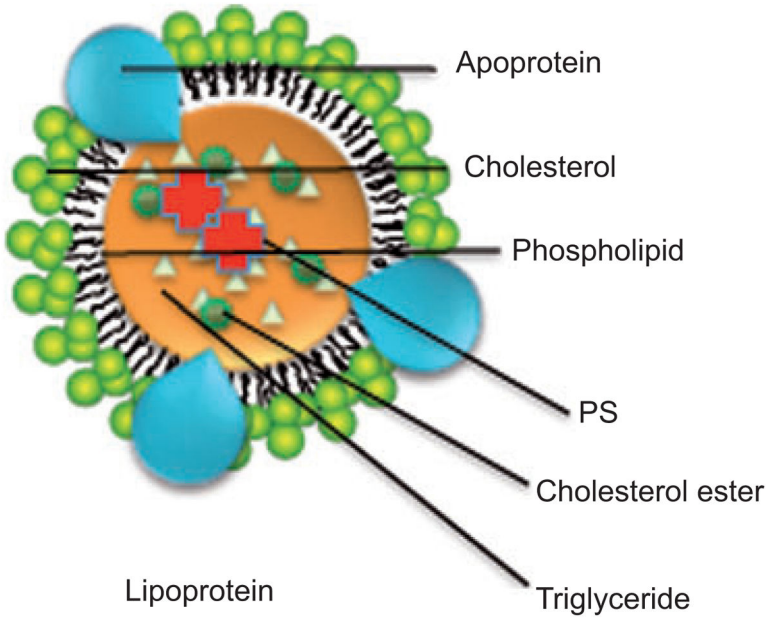

Figure 15.
Lipoprotein nanoparticles.
The reconstituted lipoprotein nanoparticle consists of the hydrophobic PS dissolved in the hydrophobic core of cholesterol esters and triglycerides surrounded by an outer layer of unesterified cholesterol and phospholipids and held together by an apoprotein chain.

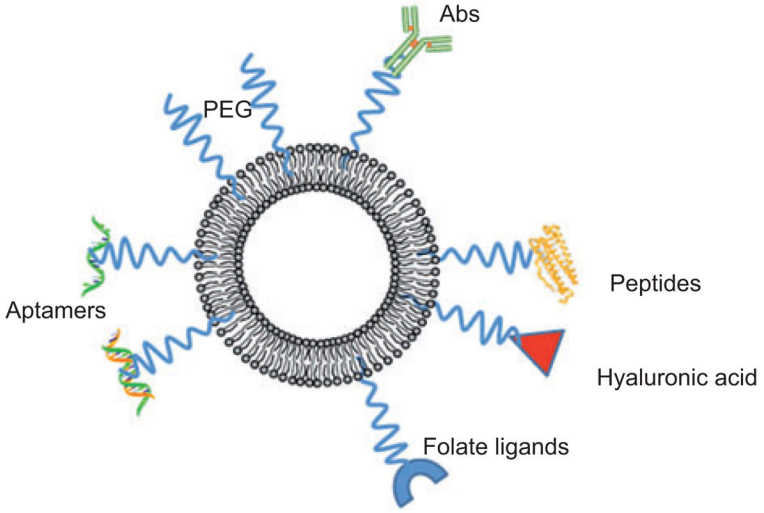

Figure 16.

Schematic illustration of active targeting of nanoparticles. Tumor targeting ligands such as antibodies, peptides, aptamers, folate, and hyaluronic can be attached to the PS-containing nanoparticle, frequently by means of linkers such as PEG.

Table 1

Examples of nanotoxicology studies from the recent literature.

Cell function damage or alteration		Samples	Reference
Cellular damage	Membrane	Cationic NP, CNT	[290, 291]
	protein	Metal oxide NP, polystyrene, dentrimer, carbon nanomaterial	[292, 293],
	DNA	AgNPs	[294]
	Mitochondria	Cationic NP, CdSe QD	[290, 295, 296]
	Liposomal	Cationic NP, CNT	[290, 295, 297, 298]
	Endoplasmic reticulum	QD	[296]
	Oxidative stress	UFP, CNT, metal oxide NP, cationic NP	[290, 295, 297–299]
Tissue and organ	Inflammation	Metal oxide NP, CNT	[298, 299]
	Fibrogenesis	CNT	[298, 300],
	Blood	SiO_2, AuNP, TiO_2	[301–303]
	Lung	UFP, AgNP, SiO_2, TiO_2, QD, AuNP	[304–307]
	Brain	UFP, TiO_2	[308, 309]
	Bone marrow	QD, metallo-fullerene, polylactic acid NP	[310]
	Liver, kidney	UFP, AgNP, AuNP	[304, 311, 312]
	Immune system	ZnO	[313]

Largely based on a table in the review by Meng et al. [314].

CNT, carbon nanotube; NP, nanoparticle; QD, quantum dot; UFP, ultrafine particle.